TRANSIENT ANALYSIS AND PERFORMANCE PREDICTION OF PASSIVE COOLING OF BUILDINGS USING LONG WAVE NOCTURNAL RADIATION IN OWERRI, NIGERIA

BY
ENGR. NWAIGWE, KEVIN NNANYE
B.ENG (FUTO), M.ENG (UPH), MNSE, MNIAE
20074734968

A PhD THESIS
SUBMITTED TO THE POSTGRADUATE SCHOOL,
FEDERAL UNIVERSITY OF TECHNOLOGY, OWERRI

IN PARTIAL FULFILMENT OF THE REQUIREMENT FOR THE AWARD OF DOCTOR OF PHILOSOPHY (PhD) DEGREE IN MECHANICAL ENGINEERING, ENERGY AND POWER ENGINEERING OPTION

JULY, 2011

CERTIFICATION

This is to certify that this project work, "TRANSIENT ANALYSIS AND PERFORMANCE PREDICTION OF PASSIVE COOLING OF BUILDINGS USING LONG WAVE NOCTURNAL RADIATION IN OWERRI, NIGERIA" is a research work carried out by Engr. Kevin Nnanye Nwaigwe, a postgraduate student in the Department of Mechanical Engineering, Federal University of Technology, Owerri.

Engr. Prof. E. E. Anyanwu, FNSE ----------
Principal Supervisor Signature/Date

Engr. Prof. D. C. Onyejekwe ----------
Supervisor Signature/Date

Engr. Dr. N. V. Ogueke ----------
Supervisor Signature/Date

Engr. Dr. A. C. Uzorh ----------
Head of Department Signature/Date

Engr. Prof. ----------
External Examiner

DEDICATION

This work is dedicated to my children:
Master Ahamba Chimbuzo Chukwudi Madu-Nwaigwe
and
Miss Ugonwanyi Chioma Adaoma Madu-Nwaigwe
For the joy and fulfillment they have brought to my life. I love you all.

ACKNOWLEDGEMENT

It is a special privilege I have to thank all those who contributed to the end of another successful academic pursuit.

I am most humbly indebted to my principal supervisor- Engr. Prof. E. E. Anyanwu who mentored this programme to a successful end. You urged me as though you were the direct beneficiary of my success. May God reward you abundantly. I am also indebted to my co-supervisors- Engr. Prof Onyejekwe and Engr. Dr. N. V. Ogueke for your painstaking efforts towards the success of this work. God bless you immensely. I am also grateful to all other academics that identified with me during the course of this programme.

Also worthy of thanks are members of my immediate family-my wife, son and daughter- who bore my absence and busy schedules. God took care of you while I toiled. Thank you for your patience, love and understanding. I am also grateful to my parents – Elder & Mrs S. M. Nwaigwe for believing in me and urging to the end of the academic ladder. You started it from my first degree and continued till this glorious end. God bless and keep you to benefit from my future successes. I am also grateful to my siblings for all the encouragement, prayers and support. God will surely reward you to your fill.

Worthy of mention also include members of my spiritual family. God has answered your prayers in my behalf. Thank you for your watch. Also to members of the Youth department of the Seventh Day Adventist Church in Anambra-Imo Conference, I thank you for you gave me the opportunity to derive joy from my fellowship with you while I bore this academic burden. May your aspirations come to fruition.

Similarly, I am indebted to my friends, colleagues and associates who urged me to success in various ways. Your words of encouragement,

advise, etc made me endure to this end. May you experience a success worthy of celebration in your lifetime. Worthy of mention is Mr. Eze Chinda who without knowing it kept me inspired throughout the duration of this programme by just a simple text message I still have saved in my mobile phone.

To my project colleague, I say thank you for the opportunity to work with you. And to my department, thank you for your support in various ways. To my employers, I say thank you for supporting me in this programme even with a fellowship that excused my fees. I will in turn be my best as long as I work here and beyond.

To God almighty, I accept the things you allowed pass me by while struggling to attain this height. I am deeply humbled by your care and protection. I run to you for further guidance. Thank you Lord for standing by me.

Engr. K. N. Nwaigwe (2011)

TABLE OF CONTENT

LIST OF FIGURES

LIST OF TABLES

NOMENCLATURE

A = Area, m^2

c = specific heat, J/kgK

D = diameter, m

G = Solar radiation, W/m^2

Gr = Grashof number

g = gravitational constant, 9.81 m/s^2

h = heat transfer coefficient, W/m^2K

k = thermal conductivity, W/mK

L = length, m

m = mass, kg

$\dot{m}$ = mass flow rate, kg/s

Pr =Prandt number

Q = energy, J

$\dot{Q}$= heat transfer rate, W

R = thermal resistance, K/W

Re = Reynolds number

t = time, s

T = temperature, °C

V = volume, m^3

v = velocity, m/s

x = Measured data

$\bar{x}$=Predicted data

Greek symbols

α=absorptivity

β = coefficient of thermal expansion

Δ= difference

ε = emissivity

θ = angle, °

ρ = density, reflectivity

μ = viscosity, m/kgs

σ = Stefan-Boltzmann constant = $5.67 \times 10^{-8} W/m^2K^4$

τ =transmissivity

η = efficiency

Subscripts

a= air = ambient

c= convector

dp= dew point

gen =internal heat generation

H =height

i = inside

infil =room air infiltration

L =length

o =outside

p =constant pressure

r =cooled room space

s= radiator panel surface

sky= sky

solar= solar

t =water storage tank

trans= wall heat transmission

W =width

w =water

wind= wind

fin= fin

Abbreviations

ACPD air room volume changes per day

ABSTRACT

Transient analysis and performance prediction of passive cooling of buildings using long wave nocturnal radiation in Owerri, Nigeria are presented. Owerri is a typical urban area in southeastern Nigeria lying between latitude 5° 4' and 6° 3' N and longitude 6° 15'and 7° 34' E. The system modeled consists of the room of a building with a radiator panel attached to its roof, water storage tank located inside the room, pump to circulate water through the radiator panel at night and through a heat exchanger in the room during the day. The mathematical model is based on the radiative properties of the local atmosphere, the heat exchange equations of the radiator panel with the sky during the night, and the equations incorporating the relevant heat transfers within the space to be cooled during the day. The resulting equations were transformed into explicit finite difference forms for easy implementation on a personal computer in Matlab language. This numerical model permits the evaluation of the rate of heat removal from the water storage tank through the radiator panel surface area between 11pm – 7am,$Q_{t,out}$, temperature depression between ambient and the room, and total heat gained from the room space through the action of the room convector into the storage tank during the day (8am – 6pm) $Q_{t,in}$. The resulting numerical solutions of the model were validated by comparison with actual field performance data taken from Okoronkwo's work [Experimental study of passive cooling of a building using long wave night sky radiation in Owerri, Nigeria; ongoing PhD thesis, Federal University of Technology, Owerri, 2011]. The resulting rate of heat removal from the radiator, Qt,out, was predicted to within 39 – 57.6 W/m2, temperature depression was predicted to within 1 – 5 oC and the rate of heat gain by the storage water was predicted to within 45 – 60 W/m2. Based on the overall good agreement between the predicted and the measured results, a sensitivity analysis of the above parameters to ±25 % of the base case input values was carried out and the results given as a percentage variation of the above system performance paramers sulting numerical solution was validated with actual field performance data obtained from a test building located at the Federal University of Technology, Owerri. The results showed a heat removal rate of 57.6 W/m^2 and temperature depression (T_a – T_r) was between 1 – 5 ^oC. Other performance parameters such as total heat gained by the storage water during the room cooling operating period, $Q_{t,in}$ and the heat removed during the night sky cooling period' $Q_{t,out}$ were 80.2 MJ and 79.5 MJ respectively. The numerical results obtained agreed quite well with an experimental study of this modeled system. The above results show that this passive nocturnal cooling technique is a reliable solution to the cooling needs for food preservation and preservation of other agricultural produce. It is also useful in small office space cooling. This modeled system is undoubtedly an aid to reducing the huge cooling cost requirements of mechanical air conditioning system of cooling.

CHAPTER ONE
INTRODUCTION

1.1 Background

When a surface on the earth faces the night sky, it loses heat by radiation to the sky, and gains heat from the surrounding air by convection. If the surface is a relatively good emitter of radiation, it radiates more heat to the sky at night than it gains from the surrounding air. The net result is that the surface temperature drops below that of the surrounding air. Since at night the insolation is zero, the surface cooling goes on throughout the night. This night-time cooling is called radiative cooling. Figure 1.1 is a schematic diagram of radiative cooling process.

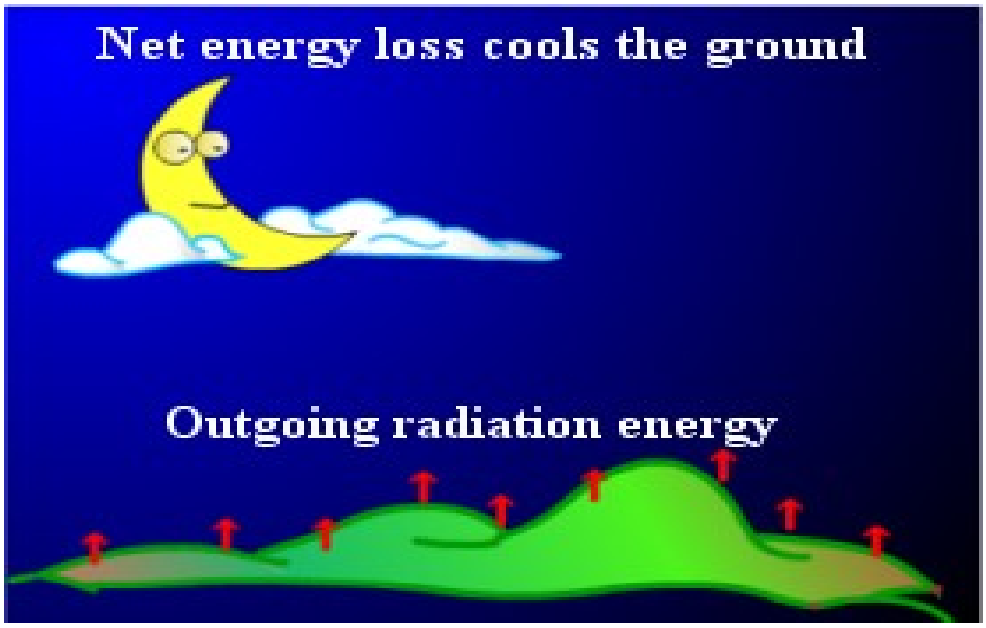

Figure 1.1: Radiation Cooling at Night (Source: Honk Kong Observatory, 2009)

Radiative cooling is one passive cooling technique utilizing the transmittance of the earth's atmosphere for thermal radiation in the wavelength interval from approximately 8 – 14 μm **(Meir, et al., 2003)**. The thermal radiation of a black body at ambient temperature on the earth's surface interacts with higher and colder atmospheric layers and may cool down below the ambient air temperature under optimal conditions. The maximal cooling power of a body at ambient temperature with high infrared emittance is of the order of 100 W/m^2 for clear night sky and low air humidity.

Radiative cooling is a very popular and well-known phenomenon and has been observed and referred to by many authors. Despite its many potential applications, including storage of food, seed and medicine, air-conditioning of buildings and water desalination, its commercial exploitation is still largely untapped **(Dobson, et al., 2003** and **Armenta-Deu, et al., 2003)**.

The energy consumption related to cooling of buildings is steadily increasing as a consequence of the world-wide industrialization and increasing living standard. **Etzion, et al. (1997)** suggests that it is often possible to harness natural energies by exploiting the local climate through adapting the architectural design of the buildings to the local climate. In this climatically adaptive approach, a variety of technologies may be integrated in the architectural design of a building, as in **Parker's (2005)** innovative residential building.

Night time cooling concept has been an age long practice .For thousands of years the sky has been recognized as the coldest available resource for passive cooling systems. However, due to the development and

improvement on compressors, this method of cooling was abandoned for the mechanical means of cooling using grid connected electricity. Today, interest in this method of cooling has been re-kindled apparently due to the growing concerns on the environment and the unpredictable cost of conventional energy sources like hydrocarbon based fuels. This is probably why research is more oriented towards improved performance through incorporation of selective coatings such as polythene films, moveable insulating panels, etc in radiative cooling concept. **(Meir, et al., 2003)**.

The amount of temperature drops at night-time is related to cloud cover, wind strength and humidity. Maximum cooling occurs under clear skies, light winds and dry conditions (see fig.1.2). Light winds tend to confine the cool air locally, preventing it from getting warm by mixing with surrounding air. Moisture in the air keeps the heat on the ground from radiating away. Hence, dry air cools off faster than moist air.

The effect of cloud on ground temperature is akin to wrapping with a blanket to keep our body warm. Thus, under cloudy conditions the overnight temperature drop is less than that under clear skies (see fig. 1.3).

Figure 1.2: Factors Affecting the Extent of Cooling at Night (Source: Honk Kong Observatory, 2009)

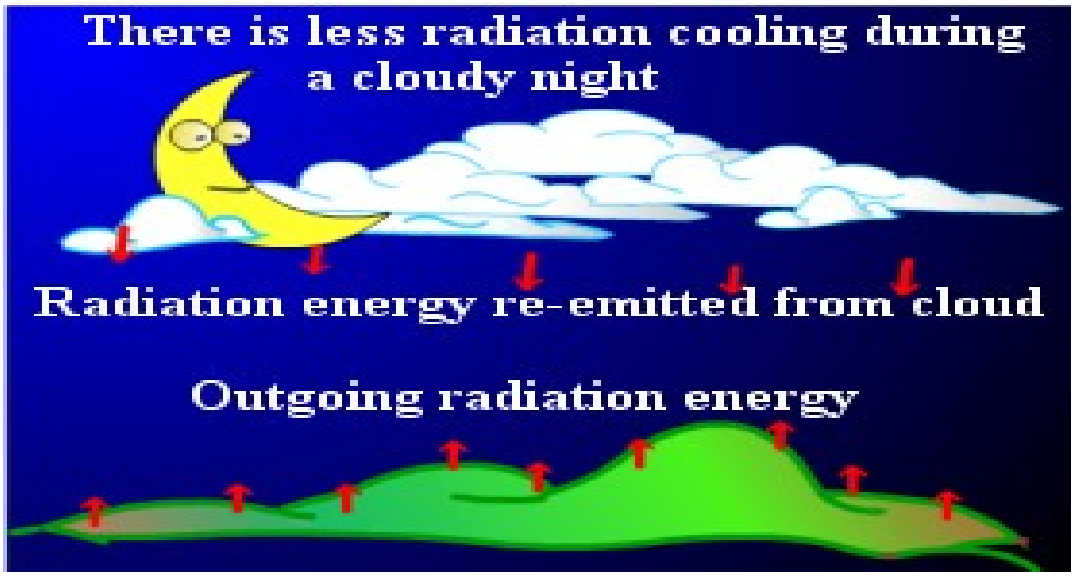

Figure 1.3: Effect of Cloud on Radiation Cooling (Source: Honk Kong Observatory, 2009)

1.2 Statement of Problem

Using a building's roof to take advantage of radiation to the night sky has long been identified as a potentially productive means to reduce energy demand for space cooling. Radiative cooling to the night sky is based on the principle of heat loss by long-wave radiation from one surface to another body at a lower temperature **(Martin and Berdahl, 1984)**. In the case of buildings, the cooled surfaces are those of the building envelope and the heat sink is the sky, since the sky temperature is lower than the temperature of most earth bound objects.

Similarly, the radiative cooling of a surface of a radiator exposed to the atmosphere at night can be used to lower the temperature of a fluid in the radiator and to condense a refrigerant used in a heat pump cooling system. Fluids, whose temperatures have been lowered in such a procedure, could then be used for cooling areas in houses and buildings, food in storage, equipment and facilities which generate heat under the ground, as well as in other situations where the application of a cooling process is necessary or desirable **(Ito and Miura, 1989)**.

The night cooling resource is large and enticing for residential energy-efficiency applications; however its potential varies from one location to another or from one season to another, depending on the location's climatic condition. For instance, on a clear desert night, according to **Parker (2005)**, a typical sky-facing surface at 80 ^{o}F (20 ^{o}C) will cool at a rate of about 75 W/m^2. In a humid climate with the greater atmospheric moisture, the rate drops to about 60 W/m^2. Night-time cloud cover is an important variable as well. With 50 % cloud cover in a humid climate, the

cooling rate drops to about 40 W/m^2 and only about 7 W/m^2 under completely overcast skies.

In urban areas, the dense population and their activities generate heat. Buildings also accumulate heat during the day. Therefore, the temperature drop in the urban areas at night-time is slower than that in rural areas, resulting in increased cooling needs in urban areas. Owerri is a typical urban area in Southeast Nigeria and presents unique night time cooling characteristics. It is situated in the south-eastern rain-forest vegetation belt of Nigeria. It lies between latitude 5° 4' and 6° 3' N and longitude 6° 15'and 7° 34' E. The area is dominated by plains 200m above sea level. It has an annual rainfall of about 1700mm to 2500mm, which is concentrated almost entirely between March and October. Average humidity is about 80%, with up to 85% occurring during the rainy season. The mean daily maximum air temperatures range from 28°C to 35°C, while the mean daily minimum ranges from 19°C to 24°C **(Okoli, 2003)**. There is, therefore need to harness the night time cooling resource to supplement the cooling needs of Owerri.

1.3 Objectives of the present study

Following the progress in harnessing nocturnal cooling resource in many countries, and the subsequent database available in such countries, there is the need to intensify work in this area in Nigeria. From extensive literature review, not much has been done in this area, particularly in numerical evaluation where there is no documented work. Thus, this work is a novel approach in the attempt to provide numerical solution to nocturnal radiative cooling in Nigeria. It is an attempt to fill a void and

contribute to the needed database requirement and solution approach in Nigeria in the area of night time cooling. The overall goal of this study will be to develop Nocturnal Cooling model for optimal cooling of a building/space requirement in Owerri. The specific objectives include:

1. To study the principle of nocturnal radiative cooling using radiative surfaces facing the night sky and integrated into cooling spaces.
2. To develop mathematical models for the integrated system for night time cooling
3. To develop a computer simulation program for design optimization of the integrated cooling system. This will take into account the various units involved in the cooling process.
4. To determine numerically the cooling rates available.
5. To propose a technical and economic optimum design for potential commercialization.

1.4 Methodology

In order to achieve the stated objectives, the study will be performed in the following sequence:

1. A thorough study of the principle of nocturnal radiative cooling using a night time facility. This will help formulate the problem of study in order to accurately describe the thermal behavior of the facility during operation. To achieve this, an extensive literature review will be carried out.

2. Discretization of the physical system into smaller control volumes of radiator panel, water storage tank, room convector, and room options for transient analysis.

3. Model Building: The abstraction of the smaller control volumes or system into mathematical-logical relationships in accordance with the problem formulation. Finite difference approximation scheme will be used. This will aim to develop energy balance equations for the component units.

4. Model Translation: This involves the generation of computer software in Matlab programming language for assembling and solving the control volumes models. This is expected to yield the numerical solution. Ambient temperature values for Owerri will be built into the translation to define the case study.

5. Validation of the numerical solution: The process of establishing that a desired accuracy or correspondence exists between the simulation model and results obtained from the real system.

6. Experimentation / Optimization of the cooling system: This involves the execution of the simulation model to obtain output values. It includes carrying out parametric tests on the various design parameters, using the computer program developed. The performance indicators include the temperature of the cooled space and the temperatures of the radiator surface and water.

7. Analysis of Results: This is the process of analyzing the simulation outputs from the optimization process to draw inferences and make recommendations for problem resolution.

8. Implementation and Documentation: Finally, the work terminates at the stage of implementing decisions resulting from the simulation and of documenting the model and its use.

1.5 Justification

The energy consumption related to cooling of buildings is steadily increasing as a consequence of the world-wide industrialization and increasing living standard. Nocturnal cooling is a renewable energy system that will adequately supplement mechanical means of cooling which utilizes compressors. Given that our thermal power generation is still unstable, night time cooling is a ready alternative. The night cooling resource is large; on a clear night, it can cool at a rate of about 75 W/m^2.

Also, the environmental hazards associated with mechanical cooling methods are taken care of as night time cooling is free from environmental pollution. Its application to residential cooling guarantees 'clean cooled air'. Its operating cost is another advantage the radiative cooling device has over other cooling methods. Its setup is simple and maintenance cost low.

1.6 Scope

To achieve the objectives of this work, focus will be on the development of model equations for the integrated radiative system. The work will be validated using raw data from an experimental shed located in Owerri. A sensitivity analysis of the achieved result will be carried out to determine degree of accuracy.

CHAPTER TWO
LITERATURE REVIEW

2.1 Nocturnal Cooling Systems

In the last three decades, special attention has been given towards the energy conservation in buildings for both heating and cooling purposes. Especially for the latter, a very important issue for countries with hot climate, several techniques have been developed one of which exploits radiative cooling **(Dimoudi and Androutsopoulos, 2006)**. Different approaches have been made to design applicable radiative cooling systems and investigate their performance. Studies were carried out both for air and water radiators. Water radiators are either water pond systems (**Hay and Yellot, 1969; Martin, 1989; Givoni, 1994; Goswami, et al., 2000)** or flat plate radiator systems.

According to **Hardy (2008),** night time cooling is feasible if any or a combination of the following occurs:

- Peak indoor zone temperature exceeds 23^{o}C
- Average zone indoor temperature exceeds 22^{o}C
- Average afternoon outdoor temperature is higher than 20^{o}C

Similarly, night time cooling should continue to be used if all of the following criteria occur:

- The indoor zone temperature is higher than the outside air temperature by +2^{o}C
- The indoor zone temperature is higher than indoor heating set point
- The outside air temperature is higher than 12^{o}C

2.1.1 Air Cooling Systems

The design and construction of the roof of a building plays an important role at the heating and cooling needs of a building. The roof is needed to protect the building from the outdoor climatic conditions (mainly by application of thermal insulation) and on the other hand can be used as an integrated component of the building that exploits the environmental sinks. In hot climates, roof may be used as an integrated building cooling component, for cooling with either evaporation or with radiation.

Using a building's roof to take advantage of long-wave radiation to the night sky has long been identified as a potentially productive means to reduce space cooling in buildings (**Givoni, 1982; Santamouris and Asimakopoulos, 1996).** The night cooling resource is large and enticing for residential energy-efficiency applications. On a clear desert night, a typical sky-facing surface at 27^{o}C will cool at a rate of about 75 W/m^{2}. In a humid climate with greater atmospheric moisture, the rate drops to about 60 W/m^{2} **(Martin and Berdahl, 1984)**.

A large problem with previous night sky radiation cooling concepts have been that they have typically exotic building configurations (such as by **Hay, 1978; Fairey, et al., 1990).** These have included very expensive roof ponds, desiccant cycles or, at the very least, movable roof insulation with massive roofs so that heat is gained during daytime hours. These systems have often proved very expensive, unreliable or too complex in application.

Parker (2005) developed an innovative night sky building cooling system to overcome these setbacks (Figure 2.1). A key element in this system is that rather than use movable insulation with a massive roof or

roof ponds, the insulation was installed conventionally on the ceiling using structurally insulated panels of 5.3 m^2. The system utilized a highly conductive metal roof on metal battens over a sealed, unventilated attic with an integrated dehumidification system.

According to Parker (2005), building surfaces radiate to the night sky primarily in the 'sky window' between 8 and 13 nanometers. Thus surfaces which have their highest emittance in this range will perform best. Also, to reduce daytime heat gain, materials which are highly reflective in the short wave range (solar spectrum) will also perform best. This will promote radiant cooling during daytime hours, as well as reflect incoming atmospheric radiation. Best performing are white paints or other light colours with strong reflectivity in the short wave range. Fortunately, most common building materials, other than foils or metallic paints have relatively high long-wave emissivities. These are generally in the range of 0.85 – 0.90. There are, however, some special coatings such as anodized aluminium surfaces which provide slightly greater performance.

Figure 2.1: Innovative Residential Nocturnal Radiation Cooling Concept

In another work **(Simonetti, et al., 2008)**, night cooling strategy was applied to school buildings in Italy. A three-storey building under construction was used as a case study. The building has a central atrium, enclosing the staircase, designed also to foster natural ventilation. Rooms were connected to the atrium by a ventilation grille and on the top of the atrium some exhaust vents were provided. Rooms have all-year mechanical air-conditioning, with radiant heating/cooling and ventilation. Free cooling was provided through earth-air heat exchangers. A night cooling system with natural ventilation was designed to reduce daily thermal load. Air inlets consist of mechanically operated tilting windows. Using computational fluid analysis (CFD) transient analysis, results obtained predicted cooling energy saving up to 50% and were compared

with experimental results obtained from the monitoring of the building, which showed close patterns.

Golaka and Exell (2007) studied the effect of obstacles that hinder the airflow and minimize the convective heat flux by CFD calculations and by wind tunnel experiments under conditions appropriate for the climate under study. The test unit was a rectangular plate 312 mm by 250 mm, with vertical metal strips for the wind shield having heights up to 100 mm along the edges of the plate. It was found that a wind shield of height 25 mm slightly increased the convective heat transfer due to increased turbulence over the surface, but wind shields of height 50 mm and 100 mm reduced the convection due to a separation of the main airflow from the surface. Radiative cooling was reduced by the wind shields. The net cooling of the surface was best with no wind shield at wind velocities less than about 1 ms^{-1}, and with the wind shield of height 100 mm at wind velocities greater than about 2 ms^{-1}.

In a similar vain, authors in the **National Institute for Rural Engineering (2008)**, identified the cooling effects when fresh vegetables are cooled by exposing them to an environment in which nocturnal radiative cooling is active, in order to save cooling energy by applying the passive use of natural cold thermal energy without using electric coolers. Net radiation flux density of about 40 to 60 W/m^2 was obtained during the clear sky night in autumn, and by the following morning, lettuces exposed to the atmosphere were cooled down to a temperature almost the same as that achieved by ordinary precooling. They further discovered that in a simple facility that provides shelter from wind or sunlight, this nocturnal radiative cooling effect was enhanced.

2.1.2 Water Cooling Systems

Water cooling systems utilize water as a medium to achieve the desired cooling. It serves as both the in situ cooling mechanism and as a cooling storage device. **Meir, et al (2003)** studied a radiative cooling system consisting of unglazed flat plate radiators with water as heat carriers and a reservoir. A typical flat-plate radiator consists of tubes through which the heat carrier is transported, an absorber plate that absorbs incoming radiation and a cover plate that prevents outgoing thermal radiation and convective losses as shown in Figure 2.2 below. The tubes can lie beneath or on top of the absorber plate, or be integrated in it. The importance is that there is good thermal contact between the tubes and the plate.

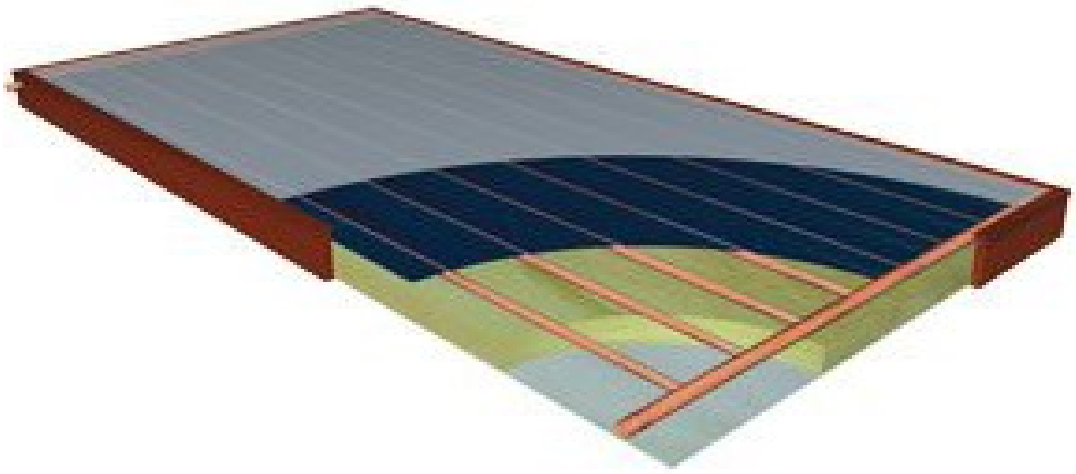

Fig 2.2: A Typical Flat Plate sky radiator

Results and the parameterization obtained from their small scale system were used to design a radiative cooling system for a single-family house. It was shown that even under unfavourable conditions; the system had the capacity to cover a significant fraction of the cooling demand. Generally, the simulations indicated that sufficient radiative cooling was obtained in

periods with modest air humidity and ambient night temperatures, with the cooling down to below 20^{o}C.

Ali (2007) investigated experimentally and analytically the natural cooling of water at night in an uninsulated open tank by evaporation, convection and sky radiation in hot arid areas. He utilized two tanks; one covered and the other uncovered. The covered tank was used to clarify the evaporative and mass transfer convective cooling contribution of the water to the total net cooling obtained from the open tank. The two tanks during experimental measurements were filled with water until they flooded. In addition, the feasibility of using the obtained cooled water for human thermal comfort inside buildings was studied. The experimental results showed that for a tank having an open surface area of 1 m^2 and a depth of 0.5 m, by the ends of nights, the water temperature values were reduced to 17.2 - 18.9 ^{o}C from an initial value of 23.8 - 27.1^{o}C at the beginning of the night. The evaporative and convective mass transfer cooling portions ranged from 38.7% - 57.4% of the total net cooling. The percentage of water loss from the tank, including the evaporated convective mass transfer cooling portions at different nights ranged from 2.5% - 4.13%. Results obtained from the model developed were validated with the measured values and good agreement prevailed. The analytical results showed that as the water depth in the open tank varied from 0.2 - 0.6 m, the net cooling of the water ranged from 10.53 - 19.7 MJ/m^2 with temperature values ranging from 14.3 - 18.7 ^{o}C. The results indicated that the naturally cooled water final temperature and cooling energy results were feasible for human thermal comfort inside buildings through radiant ceiling cooling panels systems in hot arid areas.

In their previous works, **Etzion and Erell (1991); Erell and Etzion (1992)** demonstrated that the key to improving radiative cooling systems for buildings lay in the recognition that sustaining a high cooling rate was possible only if the radiating surface remained relatively warm. This required a means of extracting the energy absorbed in the thermal mass of the building during the daytime to a radiator, where it might be dissipated to the environment at night. The cooling system proposed consisted of a shallow roof pond insulated from the environment, and flat plate collectors exposed to the sky, through which the water was circulated at night to be cooled by long wave radiation and convection.

Building on this, **Erell and Etzion (1999)** conducted a systematic analysis of the characteristics of a radiator designed specifically for the nocturnal, long wave radiative cooling of buildings. The objective was to maximize the cooling output per unit area of radiator, neglecting further improvements in the integration of the cooling system in the test building. They concluded that the following specifications were needed for the design of a radiator specifically for nocturnal cooling by long wave radiation:

- The distance between the pipes in the radiator should be kept to a minimum
- A turbulent flow regime within the pipes is required for a slightly better heat exchange between the fluid and the pipe walls
- If needed, the length of the radiator may be adapted to the geometry of the roof on which it is installed.

Also, since the cooling power produced by a flat plate radiator depended on its surface temperature, the cooling system as a whole should be designed to control the following factors:

- The radiator inlet temperature should ideally be as warm as the warmest part of the building to be cooled.
- The mass flow rate should be controlled so as to achieve a fairly flat longitudinal temperature profile, so that the average surface temperature of the radiator is high.

The mean nightly cooling output of the radiator achieved – due to the combined effect of radiation and convection – was over 90 W/m^2 under typical desert meteorological conditions.

Ali, et al (1996) studied nocturnal cooling of water flowing through a night sky radiator. They used two parallel plates night sky radiator with the top plate made from aluminium and painted black. The radiator plate was covered by a polyethylene windscreen cover. The performance of such unit was studied by the water temperature difference, the cooling power and the overall efficiency. They discovered that for typical hot dry summer nights, and for open flow systems (gravity flow) having water mass flow rate ranging from 4.8 - 20.2 kg/h, the value of the optimum water mass flow rate for maximum cooling power was about 17 kg/h. However, the lowest water temperature of 16.3^{o}C was obtained at lowest mass flow rate of 4.8 kg/h, as expected. Also, evaporation produces a slight enhancement in performance of the whole system. However, cooling power and efficiency of the radiator were lower for uncovered supply tank than those of covered supply tank. The thermal capacitance of the radiator components was observed to have has large effect on the overall performance of the system and therefore should be minimized for improved performance.

In regions with hot climates such as southern Algeria, excessive heat is the major problem that causes human discomfort. Space cooling is

therefore the most desirable factor for the inhabitants. Previous works aimed at providing solutions used a solar chimney for cooling ventilation **(Bouchair, 1989; Bouchair, 1994; Bouchair, et al, 1989)**. More recently, **Cheikh and Bouchair (2004)** used evapo-reflective roof for cooling in hot dry climates. This approach was aimed at improving the performance of roofs. The proposed roof design was composed of a concrete ceiling over which lay a bed of rocks in a water pool. The results showed that cooling inside buildings could be improved by the application of such a cooling design. It was also seen that combining evapo-reflective roof with night ventilation increased such cooling more significantly.

In another work, **Berdahl and Fromberg (1984)** presented experimental results for the global sky radiation during clear sky conditions and found an equation for predicting the sky emissivity from the dew point. Similarly**, McCathren and Akridge (1982)** developed a practical cooling system for evaluating nocturnal radiant cooling potential. The temperatures measured by a horizontal test square were used for predicting the performance of the cooling system, but it was found that actual cooling was not predicted by the simple test square model. Figures 2.3 and 2.4 below are typical nocturnal radiative cooling systems.

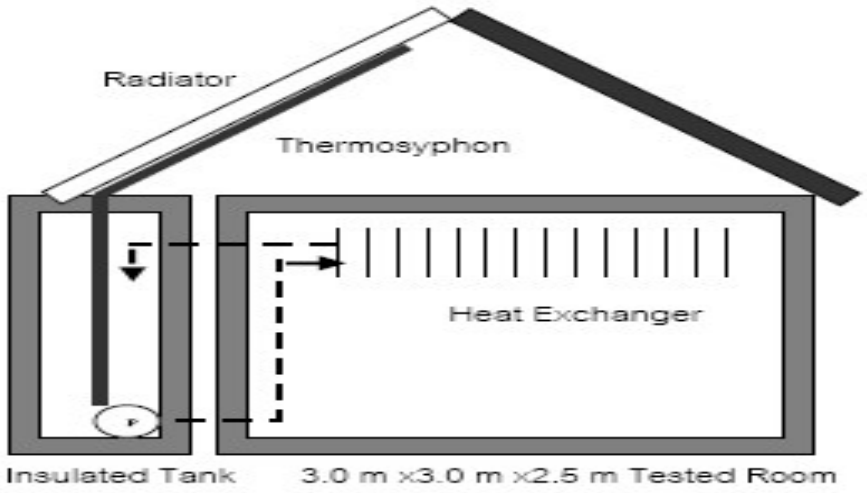

Figure 2.3: Typical nocturnal radiative space cooling application

Figure 2.4: An Experimental Facility for Nocturnal Cooling

2.2 Nocturnal Cooling in Nigeria

In a work on radiative cooling, **Ezekwe (1986)** carried out a nocturnal radiation measurement in Nigeria by measuring the net thermal radiation from a flat plate at ambient temperature to the night sky in Nsukka, Nigeria. The experimental radiator consisted of a flat mild steel plate coated with high emissivity black enamel paint. Data were obtained for the months of February through May, being a seasonal period in Nigeria free from the harmattan haze which characterizes part of the dry season (late November to early February). The effective sky temperatures obtained were on the average 12.2^{o}C less than the surface air temperatures.

There is need to further study the potentials of nocturnal cooling in Nigeria as a means of energy savings. This is particularly so because of the different climatic regions prevalent in the country and the fact that Nigeria is yet to meet her energy demand. This work is thus aimed at studying the nocturnal cooling load availability in Owerri, South East Nigeria. This is important as daytime temperatures in Owerri can be very high for home thermal comfort. Harnessing the night time coolness will unarguably improve the cooling energy requirement both at night and in the daytime.

2.3 Theory of Radiative Heat Transfer

Heat loss of an uncovered night-sky radiator is caused mainly by radiation and convection. The heat loss due to conductive heat transfer between radiator and surrounding can therefore be neglected. Thus,

$$P_c = P_{rad} + P_{conv} \quad (2.1)$$

where P_c = total cooling power (W)

P_{conv} = convective cooling power (W)

The long-wave radiative cooling power, P_{rad}, of a radiator with aperture area, A and an emittance, ε_r is given as **(Meir, et al., 2003)**:

$$P_{rad} = A.\ \varepsilon_r\ (\sigma T^4_{rad} - R) \quad (2.2)$$

R is the long-wave radiation incident on the radiator's surface.

For a horizontal surface, the long wave radiation originates mainly from a few hundred metres thick atmospheric layer near the ground. Therefore, $R = R_A$ **(Meir, et al., 2003).**

The air temperature near the ground, T_a, is fairly representative for this layer. In order to describe the radiant heat transfer of the atmosphere, R_A the term 'sky temperature', T_{sky} is introduced. **Meir, et al (2003)** defines it as the temperature of a black body radiator emitting the same amount of radiative power as the sky. Thus,

$$R_A = \sigma T^4_{sky} = \sigma \varepsilon_{sky}\ T^4_a \quad (2.3)$$

where the sky emittance, ε_{sky} is independent of wavelength.

Hence,

$$T^4_{sky} = \varepsilon_{sky} T^4_a \quad (2.4)$$

Substituting equation (2.3) for R in equation (2.2) gives:

$$P_{rad} = A\varepsilon_r \sigma (T^4_{rad} - \varepsilon_{sky} T^4_a) \quad (2.5)$$

2.3.1 Cloudless Sky

For a cloudless sky, in which $\varepsilon_{sky} = \varepsilon_o$, **Berdahl and Martin (1984)** expresses sky emissivity as a function of the dew point temperature and the relative humidity of air.

$$\varepsilon_{sky} = \varepsilon_o = 0.711 + 0.056\, T_{dp} + 0.000073\, T^2_{dp} + 0.013 \cos(2\pi t_m/24) \quad (2.6)$$

While T_{dp} is the dew point temperature defined as **(Dimoudi and Androutsopoulos, 2006):**

$$T_{dp} = \{C3\,[In\,(RH) + C1\,]\ /\ C2 - [In\,(RH) + C1]\} \quad (2.7)$$

Where,

t_m = number of hours from midnight in solar time

RH = relative humidity, $0 \leq RH \leq 1$

C1 = (C2 Ta) / (C3 + Ta)

C2 = 17.08085

C3 = 234.175

Equation (2.5) can therefore be rewritten in a more general form as:

$$P_{rad} = A\varepsilon_r\sigma (T^4_{rad} - C_a\varepsilon_{sky} T^4) \quad (2.8)$$

Where C_a is cloudiness coefficient, and

$C_a\varepsilon_{sky}T^4 = \varepsilon_o$,

The cloudiness coefficient is given as **(Dimoudi and Androutsopoulos, 2006)**:

$$Ca = 1 + 0.0224n - 0.0035n^2 + 0.00028n^3 \quad (2.9)$$

Where n = total opaque cloud amount

n = 0 for clear sky

n = 10 for overcast sky

2.3.2 Overcast Sky

For an overcast and partly overcast sky, the presence of clouds increases the atmospheric absorbance and hence the emmittance. **Martin and Berdahl (1984)** described ε_{sky} as an empirical adjustment of the cloudless models in equations (2.6) and (2.7) above.

For overcast conditions, ε_{sky} is a function of the fractional cloud cover, the cloud emittance and the temperature difference between surface and cloud base. That is,

$$\varepsilon_{sky} = \varepsilon_o + (1 - \varepsilon_o)\,\varepsilon_c\, n \exp(-z_c/z_*),\ 0 \leq n \leq 1 \quad (2.10)$$

where z_c = cloud base height (km)

z_* = a constant = 8.2 km

The hemispherical emittance ε_c is assumed to be ≈ 1 for low and medium high clouds. For cirrus clouds,

$\varepsilon_c = 0.74 - 0.084\,(z_c - 4)$ for $11 > z_c > 4$ km

and $\varepsilon_c = 0.15$ for $z_c > 11$ km

2.3.3 Inclined Radiator Surfaces

The long-wave radiation incident upon an inclined surface is given by the sum of the atmospheric radiant heat transfer, R_A and ground radiant heat transfer, R_G components.

In a model by Unsworth and Monteith **(Meir, et al., 2003),** the ground component has an isotropic angular distribution while the atmospheric radiance has an additional anisotropic term:

$$R(\alpha) = R_A(\alpha) + R_G(\alpha) \quad (2.11)$$

and,

$$R_A(\alpha) = R_A \cos^2(\alpha/2) + bI_7 \sigma T_a^4 \quad (2.12)$$

while,

$$R_G(\alpha) = \mathrm{Sin}^2(\alpha/2)(\varepsilon_g \sigma T_g^4 + \rho_g R_A) \quad (2.13)$$

Where;

$b = 0.07 – 0.14$; with a mean value of 0.09

I_7 = function of the tilt angle α

$I_7 (\alpha = 39^o) \approx 0.2$

T_g = ground surface temperature

ε_g = emittance of the ground

ρ_g = reflectance of the ground

2.3.4 Influence of Sheltering Objects

Considering the influence of sheltering objects, such as buildings or landscape topography, on the effective outgoing long-wave radiation from the radiator, where an experimental setup is surrounded by buildings of non-negligible elevation, a mean elevation angle β is introduced. This is the angle under which the buildings and sheltering objects occur to the tilted radiator surface.

In modeling the above, the tilt angle α is replaced with an effective tilt angle ά.

$$\alpha \rightarrow \acute{\alpha} \; ; \; \acute{\alpha} = \alpha + \beta \qquad (2.14)$$

Equation (2.14) may be applied to cases where the thermal behavior of the ground is similar to that of the sheltering objects.

2.4 Convective Heat Transfer

The convective heat transfer can be described by:

$$P_{conv} = h_{conv} A (T_s - T_a) \qquad (2.15)$$

For surfaces without wind screen, the coefficient for convection, h_{conv}, is in the first order a linear function of the wind speed ν which has the form:

$$h_{conv} = a + b.\nu \qquad (2.16)$$

Previous studies show a large variety in assigning values to a and b. **Molineaux, et al. (1994)** obtained the best fit with ν in (m/s):

$$h_{conv} = 3.1 + 4.1 \; .\nu \; (Wm^{-2}K^{-1}) \qquad (2.17)$$

CHAPTER THREE
METHODOLOGY

The fundamental approach to numerical analysis of a transient problem lies in the replacement of the differential equation, which represents a continuous temperature distribution in both space and time, with a finite-difference equation, which can yield results only at discrete locations and at specified times within the body.

A finite difference method typically involves the following steps:

1. Generate a grid, for example, $(x_i,t^{(k)})$, of points or locations at which approximate solutions are desired.
2. Transform the derivatives in the ordinary differential equation (ODE)/partial differential equation (PDE) forms into the finite difference schemes. The resulting equation is a linear/non-linear system of algebraic equations.
3. Generate a computer algorithm using the system of algebraic equations from where the numerical solution is obtained.
4. Solve the system of algebraic equations
5. Validate the numerical solution.
6. Do the error analysis.

Whereas there are other methods that can be used to solve ODE/PDEs such as Finite Element Methods, Spectral Methods, Finite Volume Methods, etc; Finite difference methods are simple to use for problems defined on regular geometries, such as an interval in one dimension (1D), a rectangular domain in two space dimensions, and a cubic in three dimensions.

For the partial derivatives of $T(\xi,\tau)$ at the point (ξ,τ), these being independent variables, either the forward finite-difference or the

backward difference finite-difference approximations as given in eqns 3.1 - 3.2 and eqns 3.3 – 3.4 respectively are utilized.

$$(\delta T/\delta \xi)_{\xi,\tau,fwd} \approx 1/\delta\xi \, [T(\xi + \delta\xi,\tau) - T(\xi,\tau)] \qquad 3.1$$

$$(\delta T/\delta \tau)_{\xi,\tau,fwd} \approx 1/\delta\tau \, [T(\xi,\tau + \delta\tau) - T(\xi,\tau)] \qquad 3.2$$

$$(\delta T/\delta \xi)_{\xi,\tau,bkwd} \approx 1/\delta\xi \, [T(\xi,\tau) - T(\xi - \delta\xi,\tau)] \qquad 3.3$$

$$(\delta T/\delta \tau)_{\xi,\tau,bkwd} \approx 1/\delta\tau \, [T(\xi,\tau) - T(\xi,\tau - \delta\tau)] \qquad 3.4$$

By definition of the derivative, these approximations become exact as $\delta\xi$ and $\delta\tau$ approach zero.

Second partial derivatives are usually replaced by their central finite-difference approximation:

$$(\delta^2 T/\delta \xi^2)_{\xi,\tau,cent} \approx 1/(\delta\xi)^2 \, [T(\xi + \delta\xi,\tau) - 2T(\xi,\tau) + T(\xi - \delta\xi,\tau)] \qquad 3.5$$

Also, the approximation becomes exact as $\delta\xi \rightarrow 0$.

This finite difference approach will be used in analyzing the nocturnal cooling system being studied.

3.1 System Configuration/Mode of Operation

Fig. 3.1 shows the configuration of an integrated nocturnal cooling system examined in this work. Fig. 3.2 shows the process line diagram of the cooling system being modeled.

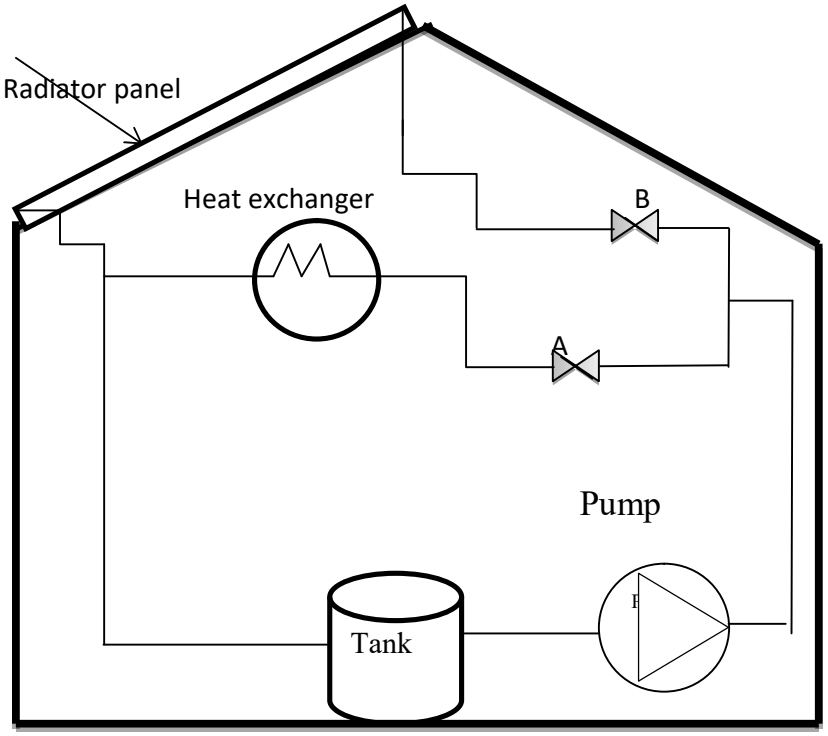

Fig. 3.1: Configuration of an Integrated Nocturnal Cooling System

The building configuration has an integrated radiator which forms part of the roof as shown above.

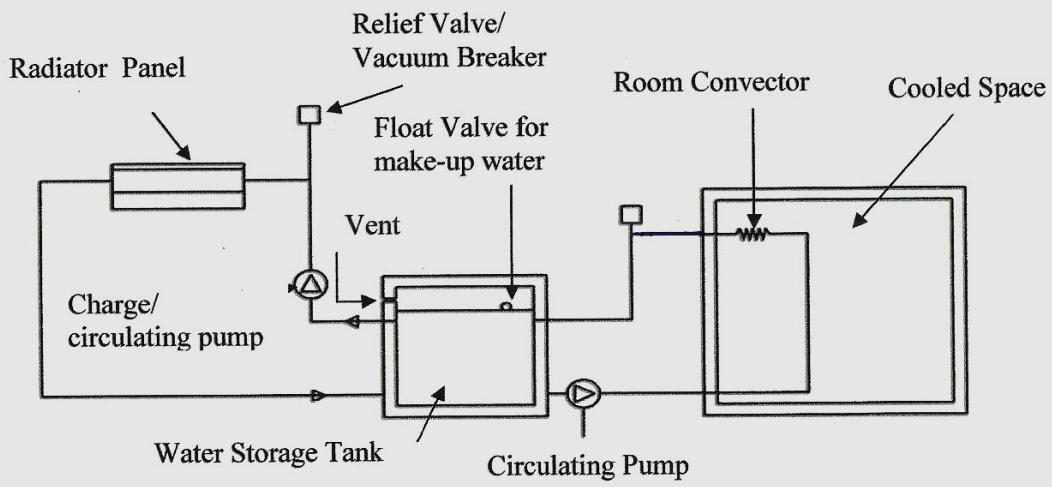

Fig. 3.2: Process Line Diagram of the Cooling System

The line diagram consists of the radiator panel, radiator panel-circulating pump, cold water storage tank, room-convector heat exchanger, convector-circulating pump, interconnecting pipe work, temperature sensors and control system. Water from the storage tank is circulated through the radiator panel at night where it is cooled by the night sky radiation. The cooled water is stored in the tank and subsequently used to cool the air in the room during the day by natural convection. This is achieved by circulating the cold water through the convector in the room.

3.2 Radiator panel

In analyzing the heat transfer modes crossing the boundary of the radiator panel, the following assumptions are made:

1. The radiator panel is made of a thin Aluminium plate with high thermal conductivity, thus the resistance to conduction across the plate thickness is negligible. This is typically true for solids of large thermal conductivity with surface areas that are large in proportion to their volume such as plates and thin metallic wires.

2. The lumped parameter analysis which assumes that there is no temperature distribution as a single temperature is assigned to the whole object, is used on the panel so that at any given interval of time, the radiator has a specific temperature.

3. Axial heat conduction and viscous dissipation for the working fluid (water) are neglected.

4. The internal heat generation in the system is negligible. Following assumption 1 above, the internal resistance of the radiator panel (L/kA) can be assumed to be small or negligible in comparison with the convective resistance (1/hA) at the surface.

5. The thermal resistance between the water and the radiating surface is relatively small, so that the temperature of the water in the panel will thus be more or less equal to the radiating surface temperature.

6. The radiator panel circulation pump is turned on before mid-night by 11pm to utilize the heat lost by the radiator panel to the sky to cool the water in the storage tank, and then switched off by 7am the next day.

Fig. 3.3 below shows a control volume indicating all the heat flow directions for the radiator panel.

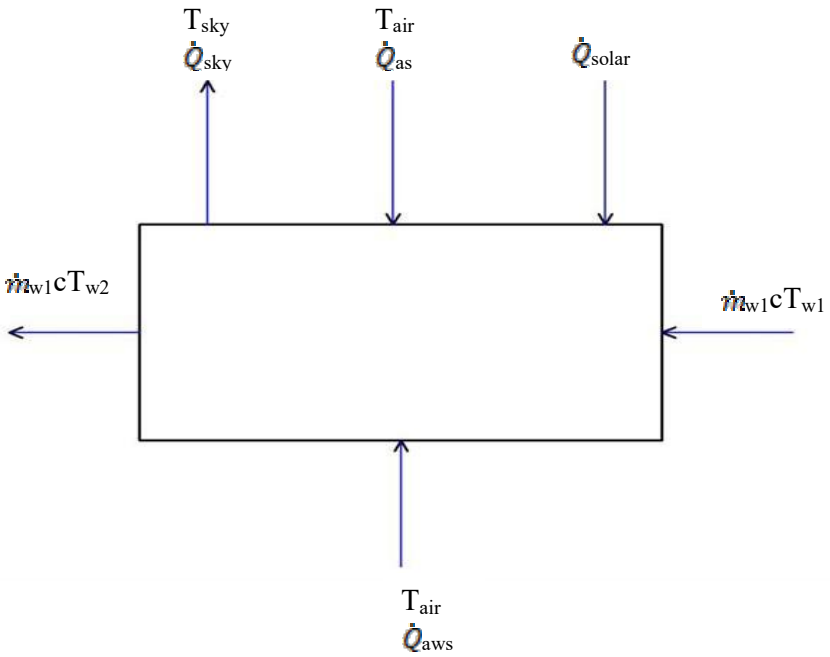

Fig. 3.3: Control volume for the radiator panel

3.2.1 Energy Balance for the Radiator Control Volume

Energy balance for this control volume requires that:

Energy flow into the control volume, $\dot{Q}_{in}$ + energy generated internally in the control volume, $\dot{Q}_{ixn}$ = Energy loss from the control volume, $\dot{Q}_{out}$ + change in internal energy of the control volume, H.

i.e $\dot{Q}_{in} + \dot{Q}_{ixn} = \dot{Q}_{out} + H$ 3.6

Following assumption 4 above, the internal energy generation is negligible and is eliminated from the equation.

Thus, eqn. 3.6 reduces to:

$\dot{Q}_{in} = \dot{Q}_{out} + H$ 3.7

From the control volume of Fig. 3.3, the energy balance equation for the parameters of eqn. 3.7 becomes:

$$\dot{Q}_{in} = \dot{Q}_{as} + \dot{Q}_{solar} + \dot{Q}_{aws} + \dot{m}_{w1}cT_{w1} \quad 3.8$$

$$\dot{Q}_{out} = \dot{Q}_{sky} + \dot{m}_{w1}cT_{w2} \quad 3.9$$

Using the finite difference method earlier explained in section 3.0, the change in internal energy, H of the control volume is:

$$H = mc\,(\delta T/\delta t) \quad 3.10$$

$$H = (m_t c_w/\Delta t)\,(T^{t+1} - T^t) \quad 3.11$$

Energy flow into the control volume consists of the convective heat transfer between the air and the panel, $\dot{Q}_{as}$; the overall solar radiation absorbed by the panel, $\dot{Q}_{solar}$; the back insulation heat transfer from the ambient air to the panel through the back insulation, $\dot{Q}_{aws}$ and energy due to water from the storage tank . The radiator surface losses heat to the night sky, $\dot{Q}_{ssky}$; and from water returning to the storage tank; while there is no internal energy generation in the radiator panel as earlier explained.

Substituting equations 3.8, 3.9 and 3.11 into equation 3.7, we have:

$$\dot{Q}_{as} + \dot{Q}_{solar} + \dot{Q}_{aws} + \dot{m}_{w1}cT_{w1} = \dot{Q}_{ssky} + \dot{m}_{w1}cT_{w2} + (m_t c_w/\Delta t)(T^{t+1} - T^t) \quad 3.12$$

Simplifying further, we have:

$$\dot{Q}_{as} + \dot{Q}_{solar} + \dot{Q}_{aws} + \dot{m}_{w1}cT_{w1} - \dot{m}_{w1}cT_{w2} - \dot{Q}_{ssky} = (m_t c_w/\Delta t)(T^{t+1} - T^t) \quad 3.13$$

And rearranging further still, eqn. 3.13 becomes:

$$\dot{Q}_{as} + \dot{Q}_{solar} + \dot{Q}_{aws} + \dot{m}_{w1}c\,(T_{w1} - T_{w2}) - \dot{Q}_{ssky} = (m_t c_w/\Delta t)\,(T^{t+1} - T^t) \qquad 3.14$$

From the assumptions that the thermal capacity of the panel is small, and that the thermal resistance between the water and the radiating surface is relatively small, it follows that the temperature of the water flowing through the panel is approximately equal to the temperature of the radiating surface.

It is also assumed that the water temperature varies linearly along its flow path since the flow rate is assumed to be steady:

Therefore,

$$T_s \approx T_w \approx (T_{w1} + T_{w2})/2 \qquad 3.15$$

The underside of the radiator panel is insulated to reduce convective heat transfer from the ambient air to the colder panel. The equivalent thermal resistance of the panels' underside is:

$$R_{th} = L_s / K_s.A_s \qquad 3.16$$

The radiator panels' efficiency is dependent on the contact with water. When water is in complete contact with the surface area of the radiator, its efficiency is unity. When water is channeled through pipes beneath the absorber, as in this case, the radiator fin efficiency value is 0.9 (**Mills, 2000**).

To solve the energy balance equation of 3.14, recall from heat transfer principles that heat transfer rate between two points is given as:

$$\dot{Q} = (T_1 - T_2)/ (R_{th}) \qquad 3.17$$

Eqn. 3.17 will be used in the subsequent sections to analyze the heat transfer modes.

3.2.2 Heat Transfer between Panel and Sky

Heat transfer rate from the radiating surface to the sky is:

$$\dot{Q}_{ssky} = (T_s - T_{sky}) / R_{ssky} \qquad 3.18$$

Where:

$$R_{ssky} = (1/h_{ssky} A_s) \qquad 3.19$$

and h_{ssky} is given as (**Dobson, 2005**)

$$h_{ssky} = \varepsilon_s \sigma \{(T_s + 273.15)^2 + (T_{sky} + 273.15)^2\} \{(T_s + 273.15) + (T_{sky} + 273.15)\} \qquad 3.20$$

The sky temperature T_{sky} is obtained as (**Dobson, 2005**):

$$T_{sky} = \{ \varepsilon_{sky} (T_a + 273.15)^4 \}^{¼} - 273.15 \qquad 3.21$$

where,

$$\varepsilon_{sky} = 0.741 + 0.00162\ T_{dp} \text{ at midnight} \qquad 3.22$$

and,

$$\varepsilon_{sky} = 0.727 + 0.00160\ T_{dp} \text{ during the day} \qquad 3.23$$

3.2.3 Heat Transfer between Ambient Air and Panel

The convective heat transfer between the air and the panel surface exposed to the air is:

$$\dot{Q}_{as} = (T_a - T_s)/R_{as} \qquad 3.24$$

Where:

$$R_{as} = (1/h_{as}\ A_s) \qquad 3.25$$

The convective heat transfer coefficient is:

$$h_{as} = a + bV_{wind} \qquad 3.26$$

The values of the constants a and b are given by **Erell and Etzion (2000)** as shown in Table 3.1below:

Table 3.1: Values of a and b for different Radiator Orientations

Orientation	Boundary Layer Surface Type	V_{wind}	a	b
Radiator Surface facing upwards and colder than the air	Laminar Flow	< 0.076 m/s (free convection takes place)	0.8	0
Radiator Surface facing upwards and warmer than the ambient air	Laminar Flow	< 0.45 m/s	3.5	0
Radiator Surface facing upwards and colder than the ambient	Laminar Flow	$1.35 < V_{wind} < 4.5$ m/s	1.8	3.8

The constants a and b depend on the panel's boundary layer surface type (laminar/turbulent) and its surface orientation.

3.2.4 The Solar Radiation to the Panel

Solar radiation absorbed by the panel surface area is:

$$\dot{Q}_{solar} = \theta\alpha\rho G A_s \qquad 3.27$$

The term [θαρ] represents a function relating the solar irradiance G onto a horizontal surface to the radiation actually absorbed by the surface. It depends on the position of the sun relative to the radiating surface as well as the spectral properties of the radiation and optical surface properties of the radiating surface. Its value is between 0.43 – 0.9 **(Dobson, 2005).**

3.2.5 Back Insulation Heat Transfer

The back of the radiator is in contact with the roof envelope of the building. To evaluate heat transfer between the ambient air and the backside of the radiator, it is assumed that the roof envelope temperature is the same as the prevailing ambient temperature. Hence, the heat transfer from the ambient air to the panel through the back insulation is:

$$\dot{Q}_{aws} = (T_a - T_s)/R_{aws} \qquad 3.28$$

Where:

$$R_{aws} = (1/h_{aws}\, A_s) + (L_s/K_s A_s) \qquad 3.29$$

Substituting equations 3.18, 3.24, 3.27 and 3.28 into equation 3.14, the energy balance equation now becomes:

$$(m_t c_w/\Delta t)\ (T^{t+1} - T^t) = \{[(T_a - T_s)/R_{aws}] + [(T_a - T_s)/R_{as}] - [(T_s - T_{sky})/R_{ssky}]$$
$$+ [(\theta\alpha\rho G A_s)] + [\dot{m}c(T_{w1} - T_{w2})]\} \quad 3.30$$

$$T^{t+1} = T^t + (\Delta t/m_t c_w)\{[(T_a - T_s)/R_{aws}] + [(T_a - T_s)/R_{as}] - [(T_s - T_{sky})/R_{ssky}]$$
$$+ [(\theta\alpha\rho G A_s)] + [\dot{m}c(T_{w1} - T_{w2})]\} \quad 3.31$$

Equation 3.31 is the functional relationship for the lumped parameter analysis of the radiator panel.

3.3 Water Storage Tank

The water storage tank is well insulated on both sides and water flow in and out of the tank is uniform. The water storage tank, considered as a control volume, has an average temperature T_t. The tank has a layer of insulation of thickness L_t and thermal conductivity K_t. The tank dimensions are chosen so that its height equals its diameter, therefore it is possible to express its surface area and volume in terms of only one variable, its diameter D_t. In this analysis, the interest is to evaluate the inlet and exit temperatures of the storage tank, however Duffie and Beckman (1991) and others have done some work to develop models for thermal stratification in storage tanks, classifying them into multi-node models and plug flow models. A control volume of the tank is shown in Fig. 3.4 below.

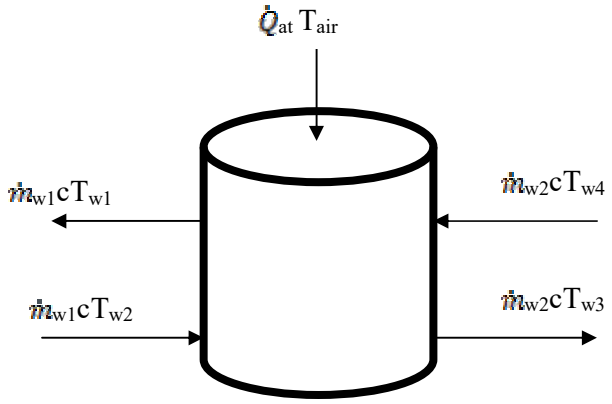

Fig. 3.4: Water storage tank control volume

3.3.1 Energy Balance of Water Storage Tank Control Volume

From the above diagram of fig. 3.4, the energy balance for this control volume is:

$$\dot{Q}_{at} + \dot{m}_{w2}cT_{w4} + \dot{m}_{w1}cT_{w2} - \dot{m}_{w2}cT_{w3} - \dot{m}_{w1}cT_{w1} = H \qquad 3.32$$

where H = change in internal energy of the control volume.

3.3.2 Net Energy Flow from Sides into Control Volume, $\dot{Q}_{rt}$

From fig. 3.4 above, and from equation 3.32, the net energy flow into the control volume from the sides is:

$$\dot{Q}_{rt} = \dot{Q}_{in} - \dot{Q}_{out} = \dot{m}_{w1}cT_{w1} - \dot{m}_{w1}cT_{w2} + \dot{m}_{w2}cT_{w4} - \dot{m}_{w2}cT_{w3} \qquad 3.33$$

Simplifying further:

$$\dot{Q}_{rt} = \dot{m}_{w1}c\,(T_{w1} - T_{w2}) + \dot{m}_{w2}c\,(T_{w4} - T_{w3}) \qquad 3.34$$

3.3.3 Heat Transfer between the Water and Ambient Air

The heat transfer rate between the water in the tank and the ambient air is:

$$\dot{Q}_{at} = (T_a - T_t)/R_{at} \qquad 3.35$$

Where:

$$R_{at} = (1/h_{at}\, A_t) + (L_t/K_{at}\, A_t) \qquad 3.36$$

$$h_{at} = a + bV_{wind} \qquad 3.37$$

$$A_t = (\pi D^2_t/4) + \pi D^2_t \qquad 3.38$$

Substituting equations 3.34 and 3.35 into equation 3.32 gives:

$$(T_a - T_t)/R_{at} + \dot{m}_{w1} c\, (T_{w1} - T_{w2}) + \dot{m}_{w2} c\, (T_{w4} - T_{w3}) = H \qquad 3.39$$

Recall from eqn. 3.11;

$$H = mc\, (\delta T/\delta t) \quad = (m_t c_w/\Delta t)\, (T^{t+1} - T^t)$$

Hence,

$$(T_a - T_t)/R_{at} + \dot{m}_{w1} c\, (T_{w1} - T_{w2}) + \dot{m}_{w2} c\, (T_{w4} - T_{w3}) = (m_t c_w/\Delta t)\, (T^{t+1} - T^t) \qquad 3.40$$

Simplifying further, we obtain eqns 3.41 and 3.42:

$$T^{t+1} - T^t = (\Delta t/m_t c_w)\{(T_a - T_t)/R_{at} + \dot{m}_{w1} c\, (T_{w1} - T_{w2}) + \dot{m}_{w2} c\, (T_{w4} - T_{w3})\} \qquad 3.41$$

$$T^{t+1} = T^t + (\Delta t/m_t c_w)\{(T_a - T_t)/R_{at} + \dot{m}_{w1} c\, (T_{w1} - T_{w2}) + \dot{m}_{w2} c\, (T_{w4} - T_{w3})\} \qquad 3.42$$

Eqn 3.42 represents the new temperature of the water in a finite time Δt.

Conversely,

$$T^{new} = T^{old} + (\Delta_t/m_t c_w)[\dot{m}_{w1} c(T_{w1} - T_{w2}) + \dot{m}_{w2} c(T_{w4} - T_{w3}) + \dot{Q}_{at}] \quad 3.43$$

3.4 Room Convector Heat Exchanger

Heat is transferred from the air in the room to the cold water circulating in the convector. The convector is made of copper tubes with aluminium fins. The fin spacing is large enough to allow for natural convection. For a typical room convector, **Dobson (2005)** states that waterside heat transfer coefficient in the order of 4000 W/m^2 K results in airside heat transfer coefficient in the order of 10 W/m^2K. This implies that the cold water pipes in the convector have to be finned on the airside so as to reduce the overall thermal resistance.

In analyzing the room convector, it is assumed that the temperature of the water circulating through the convector is a linear approximation between the inlet and outlet water temperatures. The convector pump is turned on in the morning hours (8am) to use the heat lost by the room convector through cool water from the water tank to cool the room; before it is turned off in the evening hours (6pm).The room convector is assumed to operate at steady state; its function is mainly to balance heat exchange between the room and the storage tank.

Other assumptions in analyzing the room convector include (**Rajput, 2005)**:

a. No heat generation within the convector fins.
b. Uniform heat transfer coefficient over the entire surface of the fin
c. Homogenous and isotropic fin material of aluminium with constant thermal conductivity.
d. Negligible contact thermal resistance.
e. One dimensional heat conduction and negligible radiation.

Fig. 3.5 below is a control volume of the room convector.

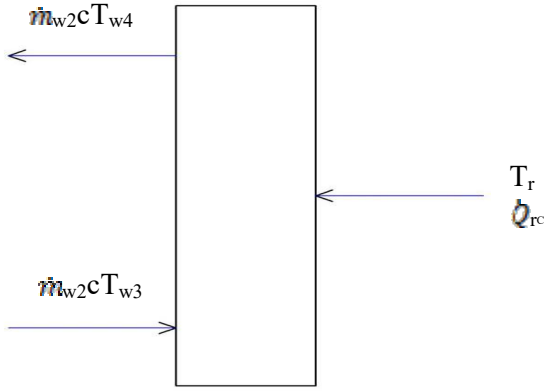

Fig. 3.5: Room convector control volume

3.4.1 Energy Balance for the Room Convector Control Volume

Energy balance for the convector is:

$$\dot{Q}_{rc} - \dot{m}_{w2}c\,(T_{w4} - T_{w3}) = 0 \qquad 3.44$$

The resultant energy present in the convector is energy due to the heat transfer from the air in the room to the water convector and energy due to water flowing from the cold tank to the room.

3.4.2 Heat Transfer between Air in the Room and the Water Convector

The heat transferred from the air in the room to the water in the convector is:

$$\dot{Q}_{rc} = (T_r - T_c)/R_{rc} \qquad 3.45$$

From the earlier assumption that $T_w \approx T_c$, it is further deduced that the water temperature varies linearly along its flow path, and the temperature of the water circulating through the convector is therefore given as:

$$T_w \approx T_c \approx (T_{w3} + T_{w4})/2 \qquad 3.46$$

The thermal resistance of the convector is given, in terms of the inside water and the outside air thermal resistances, as:

$$R_{rc} = (1/h_{rc}A_{rc}) + (1/\eta_{fin}h_{fin}A_{fin}) \qquad 3.47$$

3.4.2.1 Waterside Heat Transfer

The heat transfer coefficient on the waterside is obtained from the correlation given by **Mills (2000)** as:

$$h_{rc} = (K_s/D_{rc})\, Re^{0.8}Pr^{0.15} \qquad 3.48$$

Where:

$$Re = (4m_w/\pi D_{rc}\mu_w) \qquad 3.49$$

And,

$$Pr = (c_w \mu_w / K_w) \quad 3.50$$

3.4.2.2 Airside Heat Transfer

The heat transfer coefficient on the airside is obtained from the correlation given by **Mills (2000)** as:

$$h_{fin} = 1.07(\Delta T / L_{fin})^{1/4} \text{ , for } 10^4 < Gr < 10^9 \quad 3.51$$

$$h_{fin} = 1.3(\Delta T)^{1/3} \text{ , for } 10^9 < Gr < 10^{12} \quad 3.52$$

3.4.3 Heat Lost to Water, $\dot{Q}_{tr}$

Heat due to the water flowing from the cold tank to the room is:

$$\dot{Q}_{tr} = \dot{m}_{w2} c (T_{w4} - T_{w3}) \quad 3.53$$

Substituting eqns 3.43 and 3.51 into eqn 3.42, the steady state energy balance for the convector becomes:

$$0 = \dot{Q}_{rc} - \dot{Q}_{tr} \quad 3.54$$

$$0 = (T_r - T_c)/R_{rc} - \dot{m}_{w2} c (T_{w4} - T_{w3}) \quad 3.55$$

3.5 Room Options

An approach to the design of an enclosure situated in a tropical region (eg Owerri, South East Nigeria) environment comfortable enough for people to work in is to insulate the room walls, first of all, and then to cool the inside air and the interior wall surfaces.

A control volume for a typical enclosure showing all possible heat sources within the room enclosure is given in Fig. 3.6.

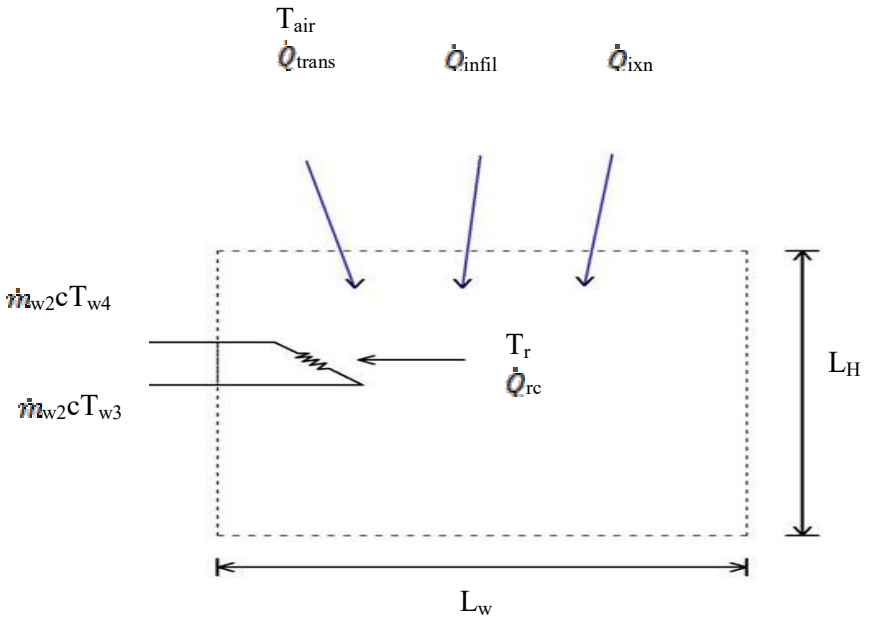

Fig. 3.6: A Control Volume for Room Options

3.5.1 Energy Balance for the Room Options Control Volume

The sources of heat gain into the conditioned space which may be external or internal include (Ibe, 2003):

i. Transmission heat gain through building fabrics such as walls, doors, windows, roofs, floors, etc

ii. Electric lighting
iii. Outdoor air brought into space due to infiltration or for the purpose of ventilation
iv. Occupancy
v. Heat dissipated by miscellaneous equipment or sources such as motors, office equipment, cooking appliances, etc
vi. In the tropics, the sun is also a source of heat, directly through windows, doors and by heating the surfaces it strikes.

From the control volume, the room heat sources can be grouped as follows:

- Internal heat source, $\dot{Q}_{ixn}$
- Infiltration of hot outside ambient air, $\dot{Q}_{infil}$
- Heat transmission from the outside ambient air into the room, $\dot{Q}_{trans}$

Recall that energy balance relationship from eqn. 3.7 is:

$$\dot{Q}_{in} + \dot{Q}_{ixn} = \dot{Q}_{loss} + H$$

Similarly, recall that change in internal energy, H from eqn. 3.11 is:

$$H = mc\,(\delta T/\delta t) \quad = (m_t c_w/\Delta t)\,(T^{t+1} - T^t)$$

From the control volume above; heat gain sources include the infiltration load and the transmission load as shown below:

$$\dot{Q}_{in} = \dot{Q}_{infil} + \dot{Q}_{trans} \qquad 3.56$$

The heat loss from the enclosure is through the room convector into the storage tank. The circulation of water from the storage tank through the room convector extracts heat from the enclosure. Other possible sources of heat loss are assumed to be negligible in this analysis. From this statement, the heat loss from the enclosure is as shown below:

$$\dot{Q}_{loss} = \dot{Q}_{rc} \qquad 3.57$$

The energy balance equation for the room option is therefore:

$$\dot{Q}_{infil} + \dot{Q}_{trans} + \dot{Q}_{ixn} - \dot{Q}_{rc} = (m_t c_a/\Delta t)\,(T^{t+1} - T^t) \qquad 3.58$$

3.5.2 Infiltration Load

Heat may be gained into the enclosure due to infiltration of ambient air entering the conditioned space. The ambient air temperature is usually expected to be higher than the conditioned room space temperature, a condition necessary to achieving thermal comfort. The infiltration of hot air therefore will raise the room temperature and should be considered in designing a room capable of maintaining thermal comfort. Infiltration is the unavoidable outside air which enters the room through the opening of doors and windows; and cracks in doors, walls and windows. This is mostly common in commercial buildings such as banks, restaurant, departmental stores, etc with heavy human traffic for transactions.

In this work, the infiltration due to door opening and other sources could be quite substantial and therefore deserves consideration to determine its magnitude. It can be evaluated as follows (Dobson, 2005):

$$\dot{Q}_{infil} = c_{infil}\,(T_a - T_r) \qquad 3.59$$

Where:

$$C_{infil} = [(ACPD.L_W.L_H.L_L.\rho_a.c_{\rho a})/(24\times3600)] \qquad 3.60$$

3.5.3 Transmission Load

Transmission load is a heat source due to heat transmission from the outside ambient air into the room. Possible sources of infiltration include building walls, doors, windows, floors, cracks, etc. It is another significant source of heat load into the conditioned space and its magnitude is given as (Dobson, 2005):

$$\dot{Q}_{trans} = (T_a - T_r)/R_r \qquad 3.61$$

Where:

$$R_r = L_r/K_r A_r \qquad 3.62$$

And,

$$A_r = 2(L_W L_L + L_W L_H + L_H L_L) \qquad 3.63$$

Eqn. (3.63) depends on the orientation of the room, direct solar radiation through windows or fenestration, actual wall and roof construction details and inside and outside wall heat transfer coefficients and the time of the day.

3.5.4 Internal Heat Generation Load

This load, $\dot{Q}_{ixn}$, is due to the number of occupants, electrical appliances, lights, etc in the room. Its value for a typical small experimental room is between 50 W –250W (Dobson, 2005).

In the test room for this study, it is assumed that the maximum load in the room is 100 W comprising of a 50 W bulb, load due to pump action and occupants observing the experiment. Hence,

$$\dot{Q}_{ixn} = 100 \text{ W} \qquad 3.64$$

Substituting eqns 3.59, 3.61, and 3.64 into eqn 3.58, the overall energy balance equation becomes:

$$c_{infil}\,(T_a - T_r) + (T_a - T_r)/R_r + \dot{Q}_{ixn} - (T_r - T_c)/R_{rc} = (m_t c_w/\Delta t)\,(T^{t+1} - T^t) \qquad 3.65$$

Simplifying further:

$$T^{t+1} = T^t + (\Delta t/m_t c_a)\,[c_{infil}\,(T_a - T_r) + (T_a - T_r)/R_r + \dot{Q}_{ixn} - (T_r - T_c)/R_{rc}] \qquad 3.66$$

Eqn. 3.66 is the functional relationship for the cooled room space.

3.6 Inter-connecting pipe work

Air relief and vacuum breakers (either separate or combined) must be placed at any of the highest points of the system, where air could collect and interfere with the water flow. In a closed system, provision must be made for thermal expansion on the water.

Pipe work should be slightly inclined to allow for any air bubble that might find itself in the system to rise under the influence of gravity to a high point where provision must be made for it to escape. Similarly, pipe work should be slightly inclined to allow the last drop of liquid to be able to drain back to suitably positioned drain points or valves.

3.7 Sensors and controls

Temperature sensors need to be provided to ensure proper operation of the circulating pumps. Two basic control options are necessary to ensure that the room temperature does not exceed a specified maximum temperature;

(i) If $T_{w2} < T_{w1}$ and $T_{w2} < T_{room}$ maximum then switch the radiator panel-circulating pump on, otherwise switch it off.

(ii) If $T_r \geq T_{room}$ maximum and $T_{w3} < T_{room}$ maximum then switch the room-circulation pump on, otherwise switch if off.

CHAPTER FOUR
RESULTS AND DISCUSSION

In this chapter, the computer program written in MATLAB programming language and used to solve the model equations developed for the nocturnal cooling system is discussed. The program simulation results are presented and discussed. The program code is as shown in the appendix.

4.1 The Programming Language

MATLAB® is a high-performance language for technical computing. It integrates computation, visualization, and programming in an easy-to-use environment where problems and solutions are expressed in familiar mathematical notation. Typical uses include Mathematics and computation Algorithm development Data acquisition Modeling, simulation, and prototyping Data analysis, exploration, and visualization Scientific and engineering graphics Application development, including graphical user interface building MATLAB is an interactive system whose basic data element is an array that does not require dimensioning. This allows us to solve many technical computing problems, especially those with matrix and vector formulations, in a fraction of the time it would have taken to write a program in a scalar noninteractive language such as C or Fortran.

The name MATLAB stands for matrix laboratory. MATLAB was originally written to provide easy access to matrix software developed by the LINPACK and EISPACK projects. Today, MATLAB engines incorporate the LAPACK and BLAS libraries, embedding the state of the art in software for matrix computation. MATLAB has evolved over a period of years with input from many users. In university environments, it is the standard instructional tool for introductory and advanced courses in

mathematics, engineering, and science. In industry, MATLAB is the tool of choice for high-productivity research, development, and analysis.

There are many other programming languages currently in use. They include FORTRAN, C++, VISUAL BASIC, etc. The programming language chosen by a programmer depends on the applicability of the programme (whether business or scientific oriented) and the programmers capability of a particular programming language. MATLAB was chosen in this work because it is robust enough to handle the models developed for the nocturnal cooling system. Thus, the results of the numerical solution presented in this chapter were obtained from computer program written in MATLAB 7 and implemented on a personal computer.

4.2 The Program

The computer program developed here has three main sections: the input section, the processing section and the output section.

4.2.1 Input Section

In this section, parameters supplied with values include dimensions and properties of the radiator panel; dimensions and properties of the water tank; dimensions and properties of the room convector; dimensions and properties of the cooled space or room; and properties of air.

4.2.2 Processing Section

The actual calculating operations of the program are handled here. The processing section is divided into sub directories, each handling the specific computation corresponding to the various components of the system. The sub directories are linked to the main directory using the 'EDIT and CLOSE' commands and results from the sub directories are

transferred to the main directory for overall processing of the system program.

4.2.3 Output Section

The results of all the computations are displayed in this section. They are viewed directly on the screen and also stored in a database for subsequent analysis. The output format is both tabulated data and graphical display. The 'RUN' command is used to generate the output. Results displayed include air temperature, radiator temperature, tank temperature and room temperature in intervals of one hour for a 24 hour period.

4.3 Numerical Solution Stability

The stability of a finite difference scheme can be investigated using the Von Neumann method (Fletcher, 1990). In this method, the errors distributed along grid lines at one time level are expanded as a finite Fourier series. If the separate Fourier components of the error distribution amplify in progressing to the next time level, then the scheme is unstable.

The error equation is given as:

$$\varsigma_{i+1,j+1} = A(\varsigma_{i+1,j} + \varsigma_{i,j+1}) - \varsigma_{i,j} \qquad \ldots(4.1)$$

where $\varsigma_{i,j}$ is the error at the (i,j) grid point. We write $\varsigma_{i,j}$ as $\lambda^j e^{\sqrt{-1}\theta_m i}$ where λ is the amplification factor for the mth Fourier mode of the error distribution as it propagates one step forward in time and $\theta_m = m\pi h$. For linear schemes it is sufficient to consider the propagation of the error due

to just a single term of the Fourier series representation i.e. the subscript m can be dropped.

Substituting $\varsigma_{i,j} = \lambda^j e^{\sqrt{-1}\theta i}$ into equation (4.1) gives:

$$\lambda^{j+1} e^{\sqrt{-1}\theta(i+1)} = A\left(\lambda^j e^{\sqrt{-1}\ \theta(i+1)} + \lambda^{(j+1)} e^{\sqrt{-1}\theta i}\right)$$

$$= -\lambda^j e^{\sqrt{-1}\theta i}$$

$$\lambda = \frac{Ae^{\sqrt{-1}\theta} - 1}{e^{\sqrt{-1}\theta} - A}$$

…(4.2)

For stability it is required that $|\lambda| \le 1 \forall \theta$ i.e. $\left|\frac{Ae^{\sqrt{-1}\theta} - 1}{e^{\sqrt{-1}\theta} - A}\right| \le 1 \forall \theta$ which implies $\left|e^{\sqrt{-1}\theta} - A\right| \ge \left|Ae^{\sqrt{-1}\theta} - 1\right|$

Squaring both sides and further simplifying, it is obtained that for $|\lambda| \le 1 \forall \theta, A$ must satisfy $A^2 \ge 1$. Since $A = \frac{1+r}{1-r}$ and $r > 0$, it is obtained that the scheme is stable $\forall r$ (except r = 1). Hence, any time step Δt could be used. Time step is selected such that Δt = PΔt is satisfied (Bass and Ott, 1980), where Δt is the acquisition interval for measured data. For this work, Δt = 3600 sec (1 hour). P=1 gives Δt = Δt while P<1 yeilds smaller time interval. When P>1, the solution is generated using fewer time steps. In this work, P=1 is used. Thus, Δt = 3600s.

4.4 Numerical Solution Consistency

To test for consistency, the exact solution of the partial differential equation is substituted into the finite difference scheme and values at grid points expanded as a Taylor series. For consistency, the expression obtained should tend to the partial differential equation as the grid size tends to zero (Twizell, 1984).

Substituting the exact solution into a partial differential equation scheme of the form:

$$\frac{u_{i+1,j+1} + u_{i,j} - u_{i+1,j} - u_{i,j+1}}{h^2} = \frac{1}{4}\left(u_{i+1,j+1} + u_{i,j} + u_{i+1,j} + u_{i,j+1}\right) \qquad \ldots(4.3)$$

leads to:

$$\frac{1}{h^2}\left\{\begin{matrix} u(x_{i+1}, y_{j+1}) + u(x_i, y_j) - \\ u(x_{i+1}, y_j) - u(x_i, y_{j+1}) \end{matrix}\right\} = \frac{1}{4}\left\{\begin{matrix} u(x_{i+1}, y_{j+1}) + u(x_i, y_j) \\ + u(x_{i+1}, y_j) + u(x_i, y_{j+1}) \end{matrix}\right\} \qquad \ldots(4.4)$$

Expanding as a Taylor series about (x_i, y_j) gives:

$$\frac{1}{h^2}\left\{\begin{matrix} u + hu_x + hu_y \\ + \frac{1}{2}(h^2 u_{xx} + 2h^2 u_{xy} + h^2 u_{yy}) + \ldots \\ + u - (u + hu_x + \frac{h^2}{2} u_{xx} + \ldots) \\ - (u + hu_y + \frac{h^2}{2} u_{yy} + \ldots) \end{matrix}\right\} = \frac{1}{4}\left\{\begin{matrix} u + hu_x + hu_y \\ + \frac{1}{2}\left(h^2 u_{xx} + 2h^2 u_{xy} + h^2 u_{yy}\right) + \ldots \end{matrix}\right\}$$

$$+\frac{1}{4}\left\{u + hu_x + \frac{h^2}{2}u_{xx} + \ldots\right\}$$
$$+\frac{1}{4}\left\{u + hu_y + \frac{h^2}{2}u_{yy} + \ldots\right\} + \frac{1}{4}u$$

…(4.5)

[Note: All terms involving *u* in equation (4.5) are evaluated at (x_i, y_j)]

As $h \to 0$, equation (4.5) becomes $u_{xy} = u.$ Thus the condition for consistency is satisfied.

4.5 Numerical Solution Convergence

A solution of the algebraic equations which approximate a given partial differential equation is said to be convergent if the approximate solution approaches the exact solution for each value of the independent variables as the grid spacing tends to zero. The Lax Equivalence Theorem (Richtmyer and Morton, 1967) states that given a properly (well) posed linear initial value problem and a finite difference equation that satisfies the consistency condition, stability is the necessary and sufficient condition for convergence.

The nocturnal cooling finite difference models are well posed as it can be transformed into linear equations and solved by Matlab. They are both stable and consistent. Thus from the Lax Equivalence Theorem we can conclude it is convergent.

4.6 Simulation Results and Discussion

Test runs were carried out for four different weather seasons – early (March/April) and late (July/ September) rainy seasons; and early (November/December) and late (January/February) harmattan seasons. The input variables include the ambient weather conditions for the

various seasons as shown in Figs. 4.1 – 4.4 below, the solar irradiation as shown in Figure 4.4b, and the wind speeds as shown in Figure 4.4c. According to Anyanwu and Iwuagwu (1994), the average wind speed for Owerri is 2.80 m/s ± 0.81; annual mean wind power density is 12.91 ± 0.26 W/m^2.

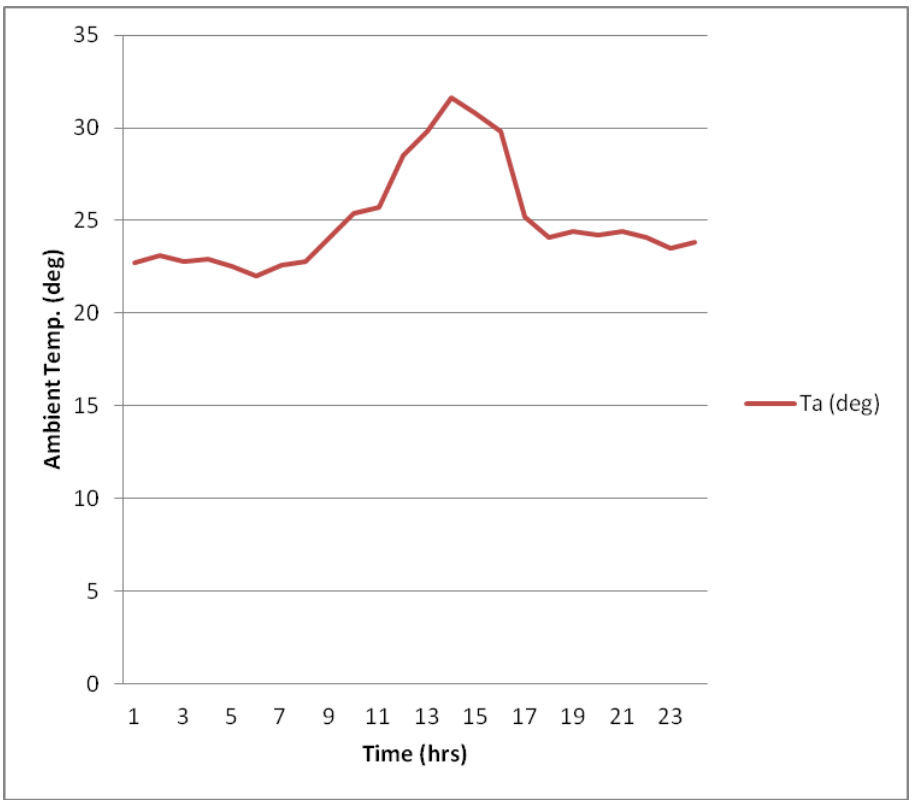

Fig. 4.1: Average Input Ambient Temperatures for Early Rainy Season (March/April)

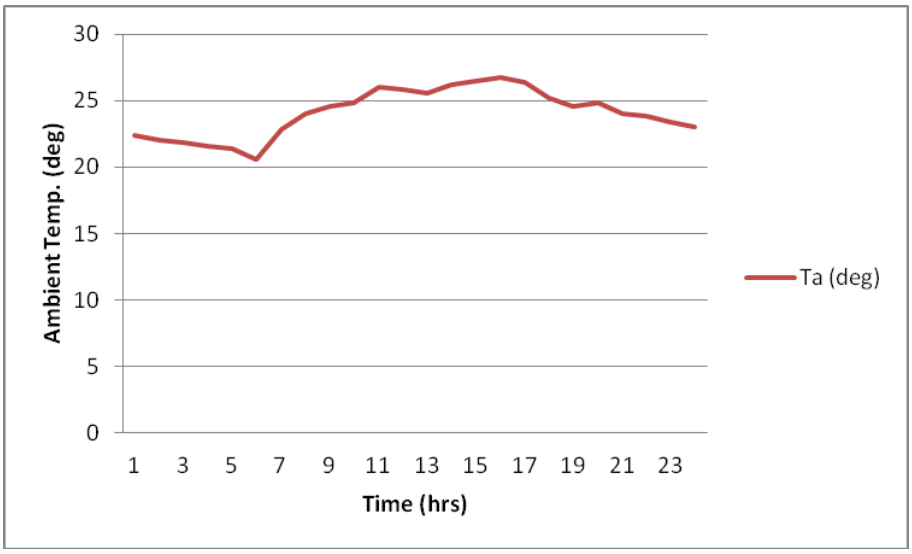

Fig. 4.2: Average Input Ambient Temperatures for Late Rainy Season (July/September)

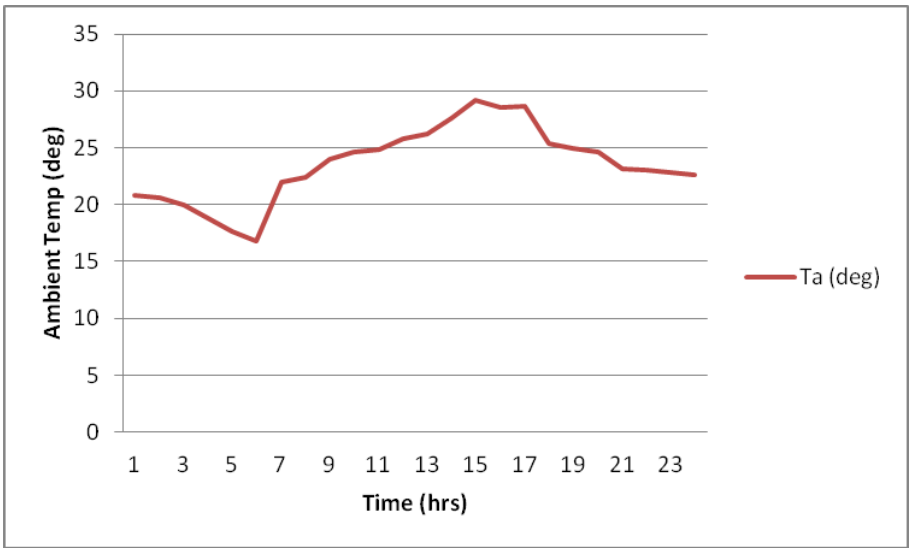

Fig. 4.3: Average Input Ambient Temperatures for Early Harmattan Season (November/December)

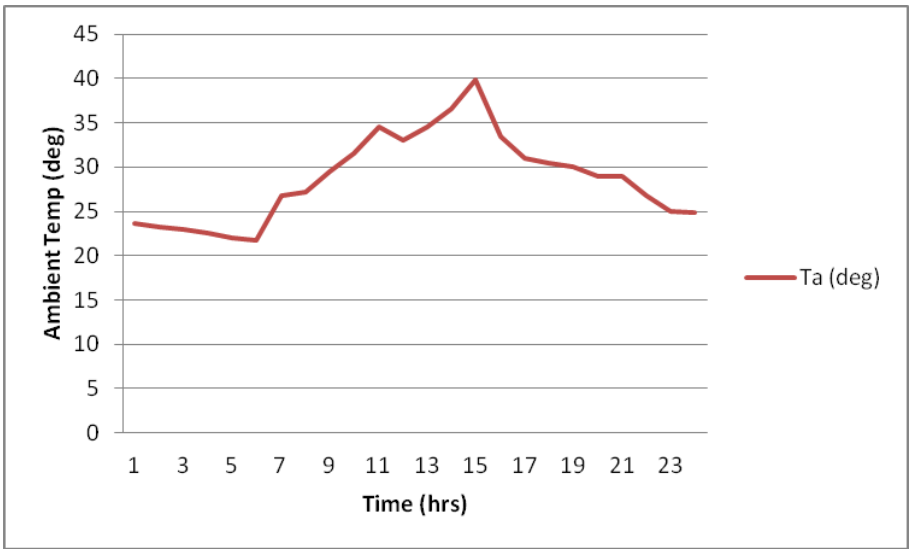

Fig. 4.4: Average Input Ambient Temperatures for Late Harmattan Season (January/February)

In developing the simulation program, actual ambient values are used to achieve a true temperature profile.

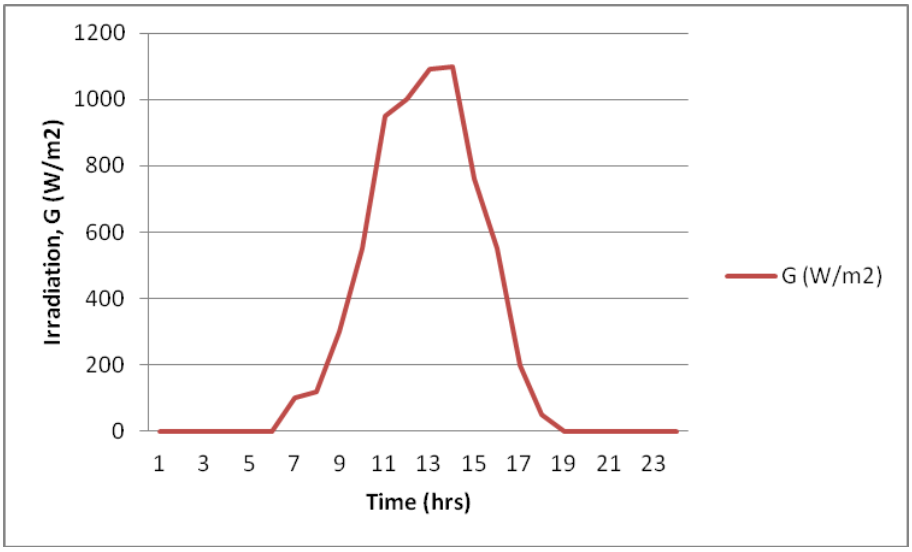

Fig. 4.5: Average Irradiation Input Values for Owerri

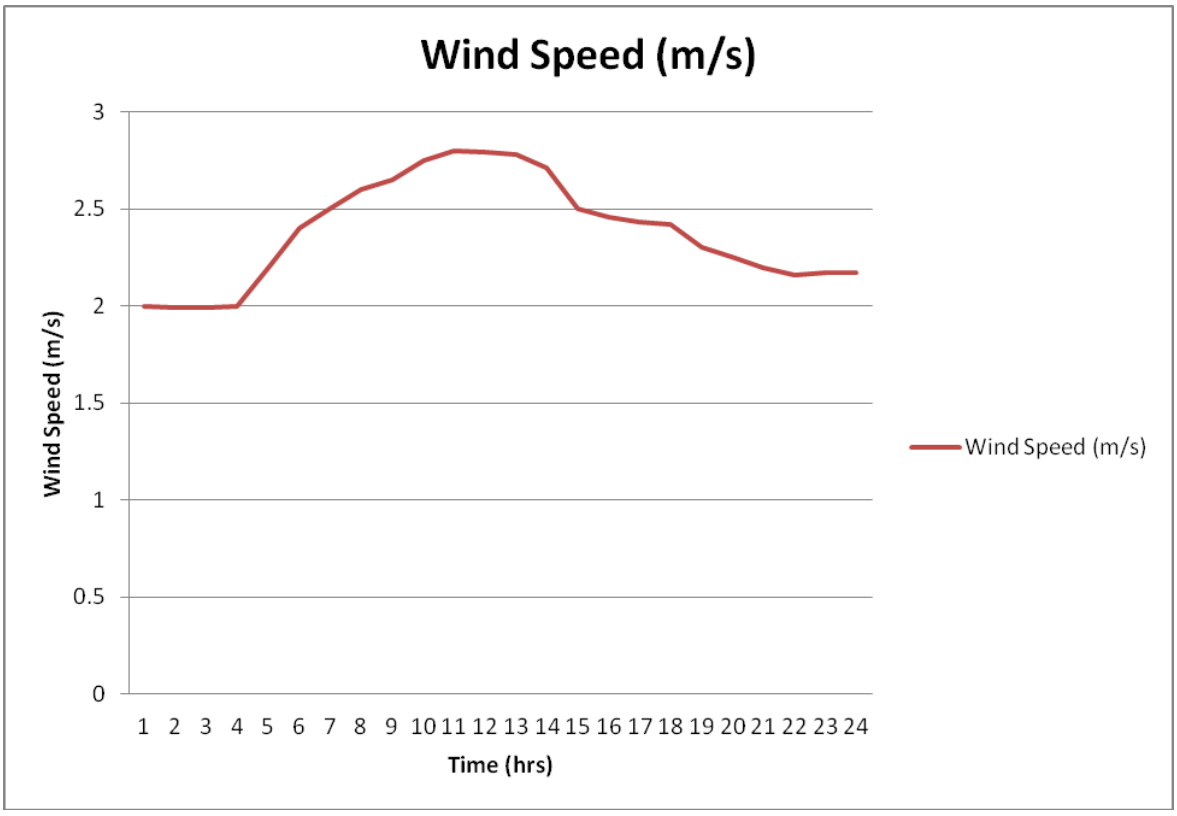

Fig. 4.6: Average Wind Speeds for Owerri

Other input variables and parameters are as shown in the program code (see appendix). The solution algorithm flow chart is shown below and results from the numerical analysis for the four seasons are also shown below.

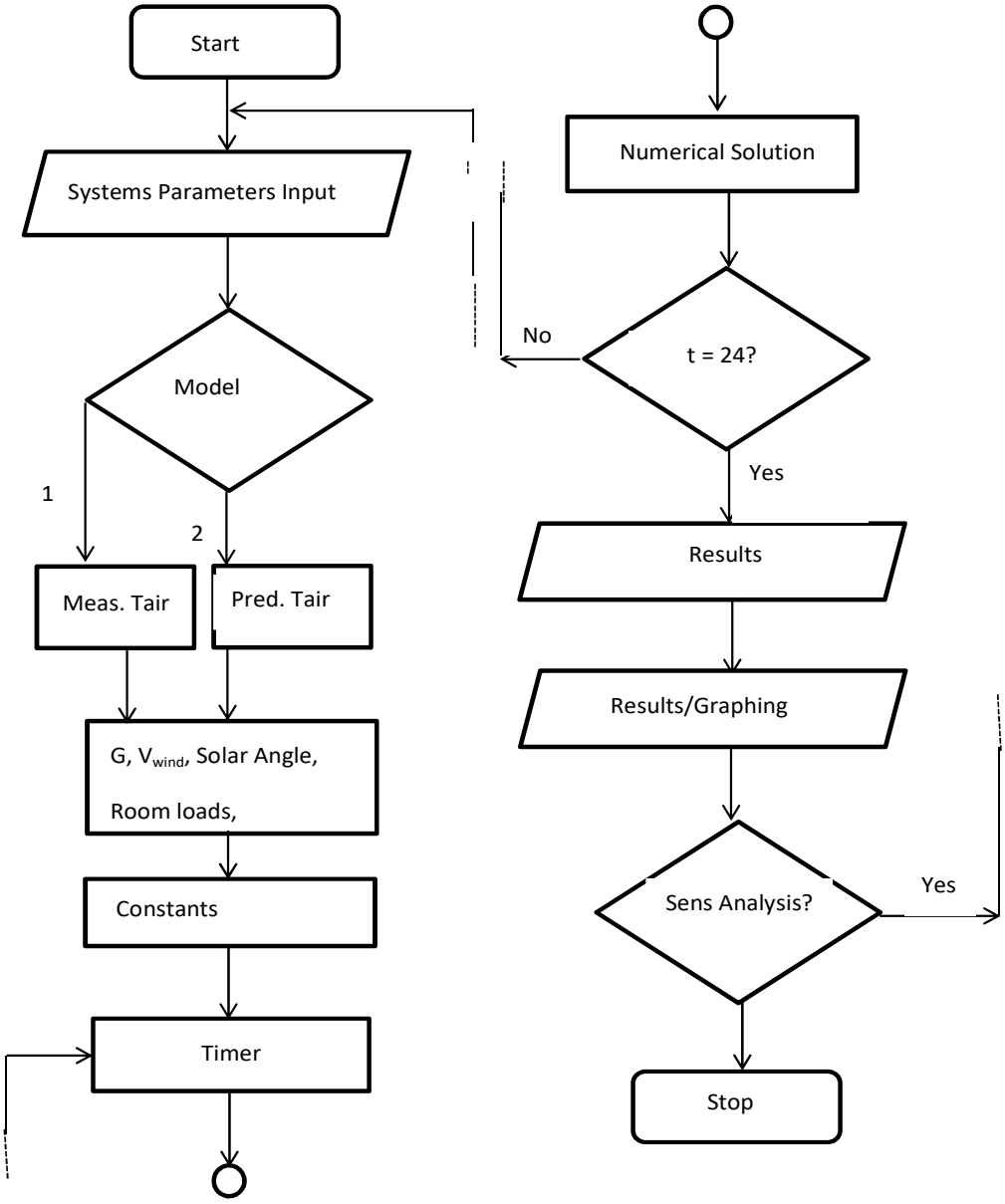

Fig. 4.7: Solution Algorithm Flow Chart showing Inputs, Processes and Outputs

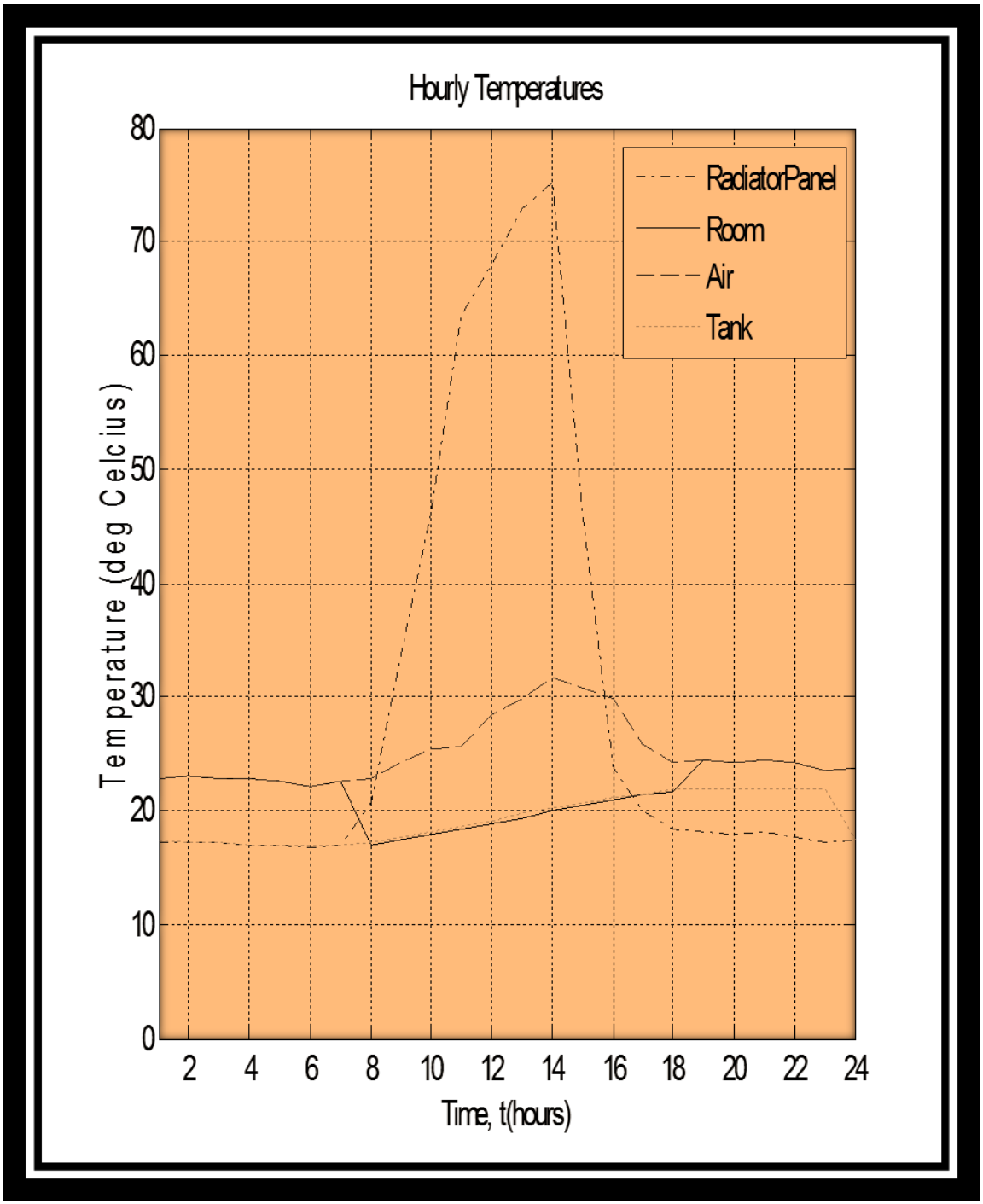

Fig. 4.8: Plots of Temperatures of Radiator panel, cooled room space, ambient air and storage tank against hourly time interval for early rainy season

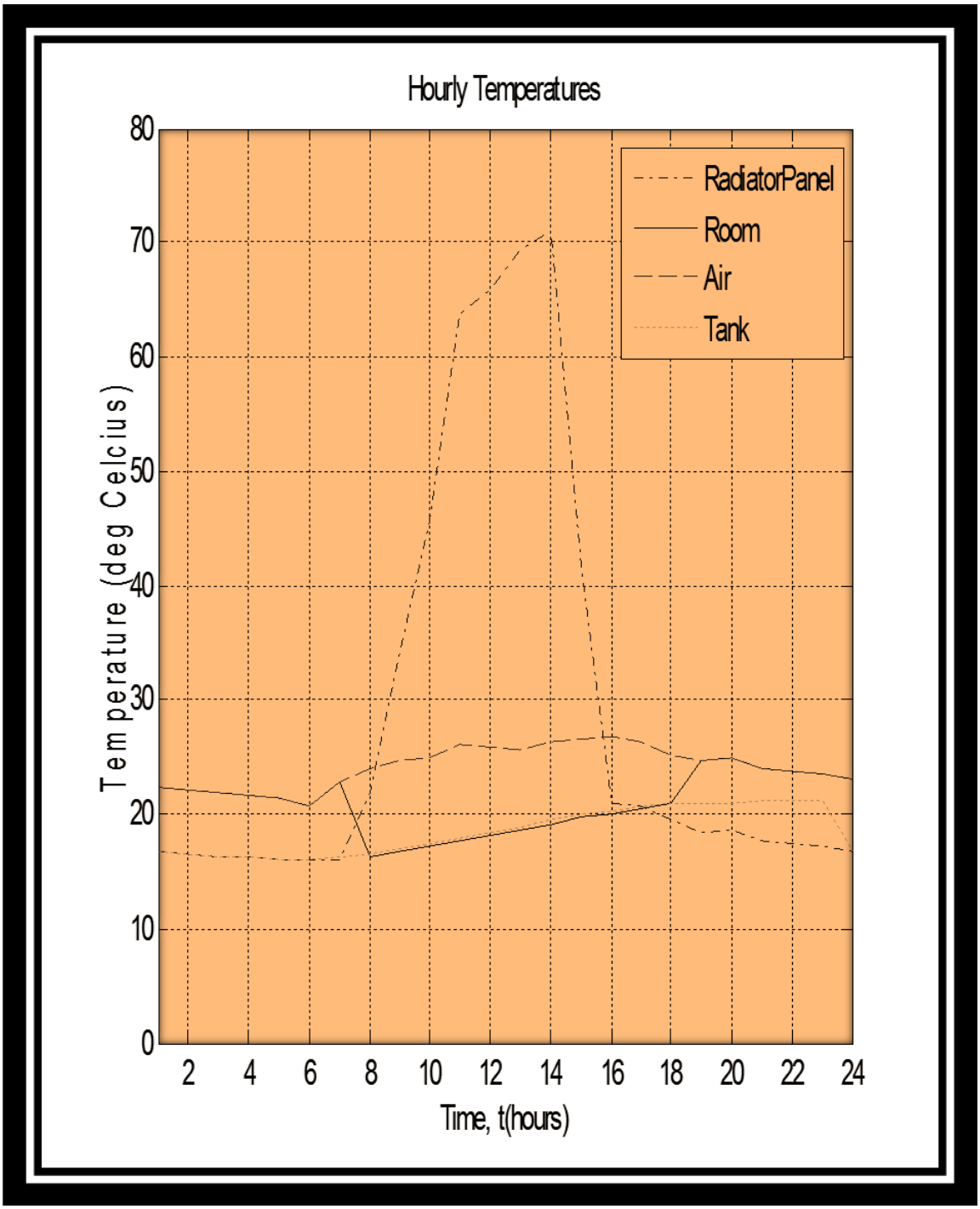

Fig. 4.9: Plots of Temperatures of Radiator panel, cooled room space, ambient air and storage tank against hourly time intervals for late rainy season

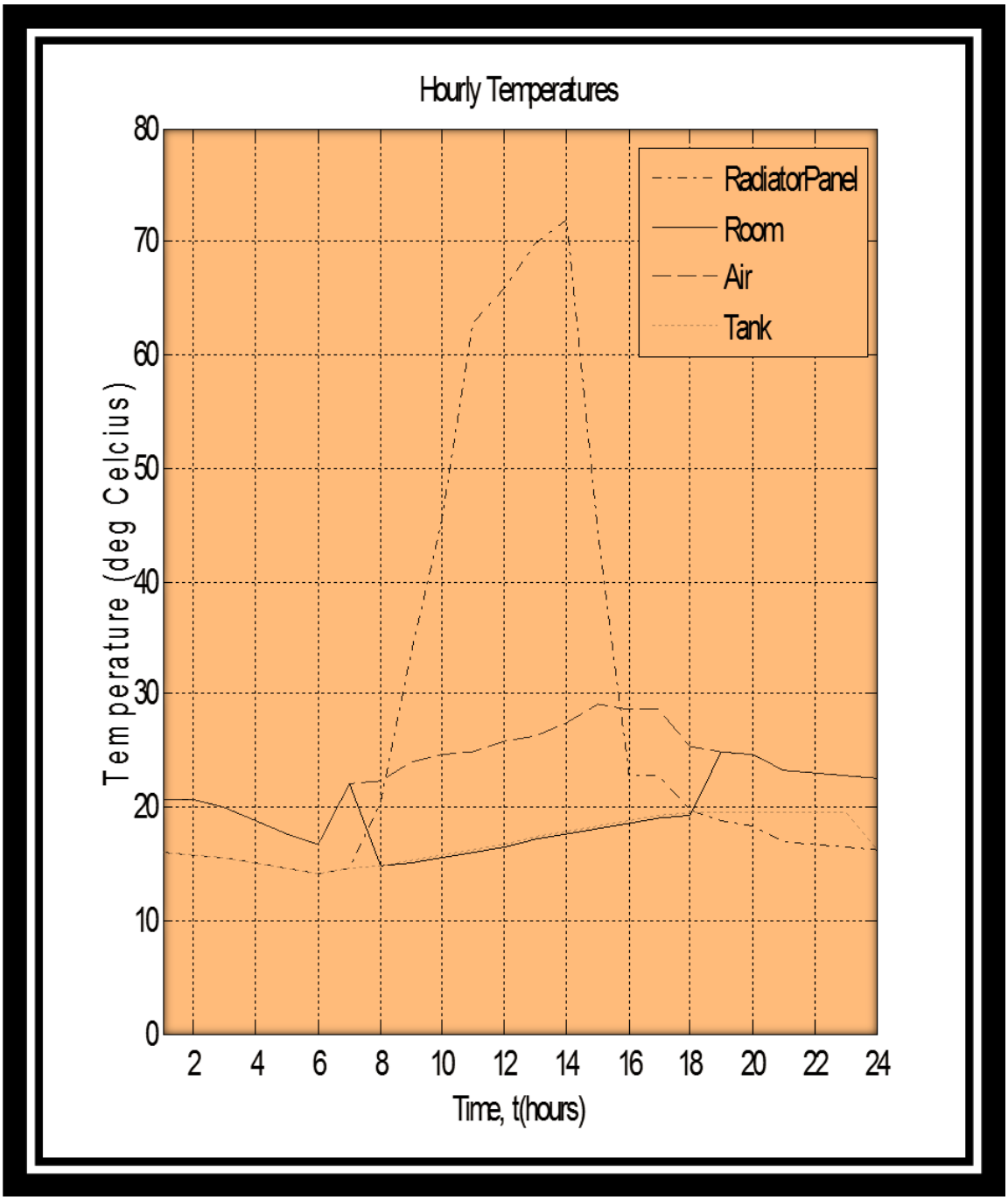

Fig. 4.10: Plots of Temperatures of Radiator panel, cooled room space, ambient air and storage water tank against hourly time intervals for early harmattan season

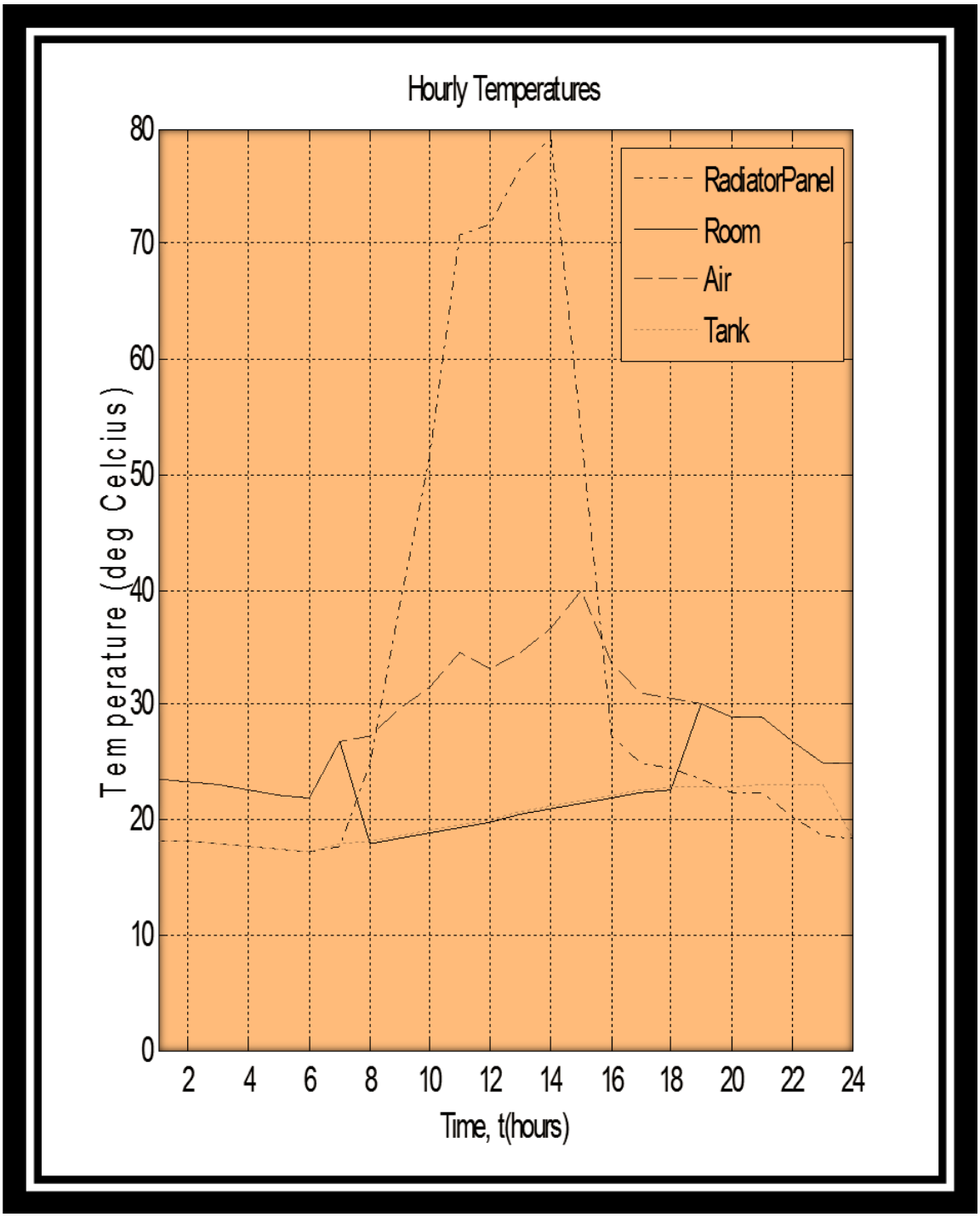

Fig. 4.11: Plots of Temperatures of Radiator panel, cooled room space, ambient air and storage water tank against hourly time intervals for late harmattan season

Figs. 4.8 – 4.11 above are different temperature plots for different ambient temperature conditions representing early early rainy season, late rainy season, early harmattan season, and late harmattan season respectively.

To generate these profiles, the radiator circulation pump was turned on at 23 hours (11pm), to utilize the heat lost by the radiator panel to cool the water in the storage tank and then switched off by 7 hours (7am) the next day. Then the room convector circulation pump was turned on by 8 hours (8am), to utilize the heat lost by the room convector to cool water from the water tank, so as to cool the room. The convector pump is switched off at 18 hours (6pm).

From the figures, the room temperature, which from the night was programmed to 'mirror' the ambient temperature, begins to drop significantly from around 6am, achieving the lowest daytime cooling at about 8am when the room convector is switched on. This is expected as the room convector extracts any heat within the space, given that the ambient temperature is only gradually increasing. As the ambient temperature continues to rise during the day, the room temperature experiences a steady increment but at a rate that is insignificant due to the building configuration and the action of the room convector. This trend continues till towards evening (about 5pm) when the room temperature has built up nearly equaling the ambient temperature which is steadily decreasing towards the evening into the night.

Another reason for the rise in room temperature towards evening is the build-up of heat in the water storage tank due to repeated extraction of heat through the action of the room convector. Even though the storage

tank is properly insulated, the water flowing through the convector is getting 'hotter' after each successive pumping through the room convector loop. The ability of the water to further extract heat from the cooled space is steadily decreasing as the water temperature is gradually rising. At this point, the convector pump is turned off and the radiator pump is switched on to expel the accumulated heat in the water storage tank. More so, the radiator temperature which was hitherto high, has now decreased significantly even below the ambient temperature. The relatively hot water in the storage tank is used to defrost the radiator panel surface by passing it through the fins of the radiator at night while still maintaining thermal comfort within the space. This continues until the morning, dropping the temperature of the water in the storage tank to about the same as that of the radiator panel surface. This equilibrium is important both to avoid freezing of the panel surface, considering the dew point temperature, and to reduce the water temperature to the possible minimum in readiness for heat extraction during the day. Cold water is needed in the storage tank to contain possible heat generation within the cooled space during the day.

From Fig. 4.8, temperature depression as much as 12^{o}C is achieved. This is a good result as the early rainy season is still considerably hot. The ambient temperature is still significantly high. From Fig. 4.9, the temperature depression is at a maximum of about 7^{o}C. This is the late rainy season characterized by reduced ambient temperatures. Room temperature is as low as 16^{o}C very early in the morning.

From Fig. 4.10, the temperature depression gets narrower. The ambient temperature is now significantly low. The room architecture is still capable of maintaining depressions of about 10^{o}C. The harmattan is set

and the season is generally cold. From Fig. 4.11, the ambient temperature has risen tremendously and a peak temperature depression of about 18^{o}C is achieved. However, the room temperature is considerably comfortable during most of the day. This period is characterized by a very hot weather and this accounts for the reduced performance of the nocturnal cooling system.

Using these models to predict nocturnal cooling during the day, room temperatures of between 17^{o}C minimum and 22^{o}C maximum are achieved. This temperature range is thermally comfortable for human habitation.

Daytime cooling, which is the major objective of nocturnal cooling systems, is significantly achieved as shown in figures 4.8 – 4.11. During the day, between 7am – 6pm, the maximum room temperature is below 25^{o}C. Considering the human body temperature average of about 37^{o}C, a temperature of 25^{o}C for a conditioned space is capable of providing significant cooling of up to 12^{o}C depression to the human body. This is obviously thermally comfortable. Considering other factors affecting thermal comfort such as the mean radiant temperature of the surroundings, the plots show that during the day, the room temperature is far less than the surrounding air temperature, i.e $T_r << T_a$. This is another significant factor in thermal comfort of occupants of a cooled space.

4.7 Validation of Model and Sensitivity Analysis

The mathematical model of a nocturnal cooling system presented in chapter 3 was used to study the cooling system behavior numerically. Results obtained were presented and discussed in the earlier part of this

chapter. In the following sections, these numerical results are compared with results obtained from the actual field test of a similar unit to ascertain their level of agreement. Also presented are the effects of various design parameters on the system's performance.

4.8 Model Validation

In order to test the accuracy and reliability of the estimated nocturnal cooling system performance data, the cooled room space temperature, water tank storage temperature, and radiator temperature values were compared with the actual field test results for common ambient temperature conditions. The ambient temperature conditions used and the measured temperature values are presented in the appendix. The validation will dwell more on temperatures between 6pm – 6am, being the temperature time period of the actual field experimentation using a similar facility located in Owerri.

The experimental facility is located at the Federal University of Technology Owerri, Imo State and is as shown in fig. 4.12 below.

Fig. 4.12: Nocturnal Cooling Experimental Facility at Owerri, Imo State

The criterion of error used for the analysis between the predicted and measured temperature values is the mean deviation. The mean deviation of a statistical data is defined as the arithmetic mean of the numerical values of the deviations of items from some average value. Mean deviation is also known as average deviation. The mean deviation is generally denoted by M.D.

Formula for mean deviation for ungrouped data or an individual series is given by

$M.D = \frac{\Sigma|x - a|}{n}$, where a is the average about which M.D is to be calculated.

If M.D is calculated about mean, then it is written as M.D ($\bar{x}$).

$$M.D(\bar{x}) = \frac{\Sigma|x - \bar{x}|}{n} \qquad \text{(For individual series)}$$

Using the above relationship, below is the resulting error analysis for radiator temperature, room space temperature and water tank temperature.

Table 4.1: Error Analysis Result of Predicted Values over Measured Values

Date	T_{rad}	T_{room}	T_{tank}
10/8/10	4.35	1.65	4.41
12/8/10	3.82	0.98	4.16
15/8/10	4.35	1.23	4.68
20/8/10	4.16	1.23	4.67
29/7/10	3.67	1.89	4.09
15/7/10	5.10	2.10	4.12
2/8/10	4.63	1.76	3.06
27/7/10	4.72	0.53	3.98
17/7/10	5.02	2.14	4.63

The above error analysis table shows that in the case of the temperature of the cooled room space, there is consistency between the measured and the predicted values. In the case of the radiator temperature and storage tank temperature where there exist significant deviations, the trend exposes possible instrumentation errors during experimental measurements. In reality, the radiator temperature is expected to be lower than both the room and tank temperatures through the time period under consideration (6pm – 6am).

4.8.1 Cooled Room Space Temperature: Predicted versus Measured

Figs. 4.13 – 4.21 below are the charts for cooled room space temperatures against time for different days with different ambient conditions.

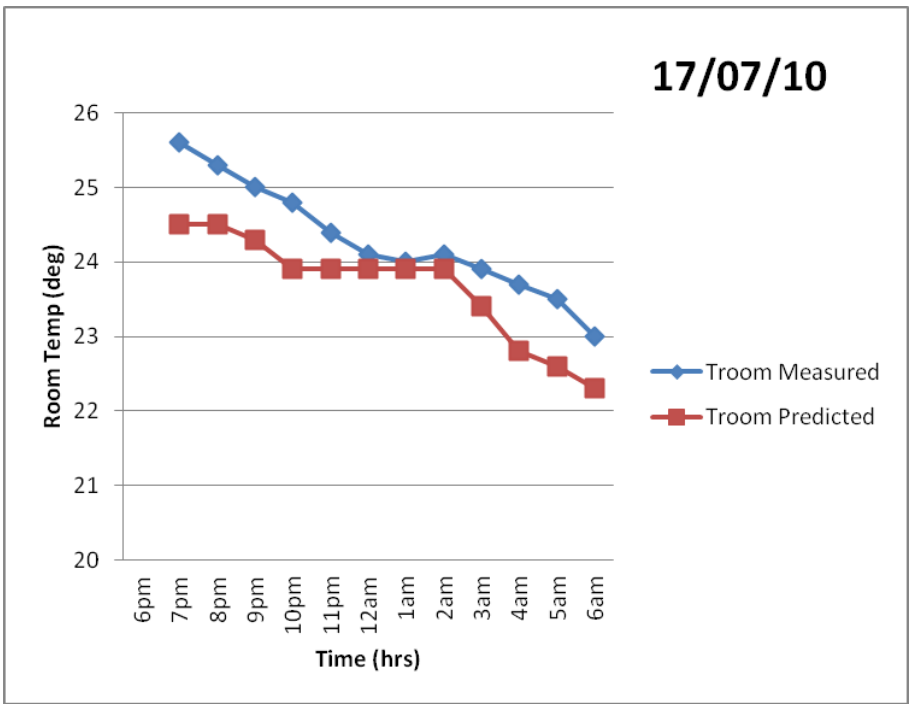

Fig. 4.13: Plots of Predicted and Measured Temperatures against Time for 17/07/10

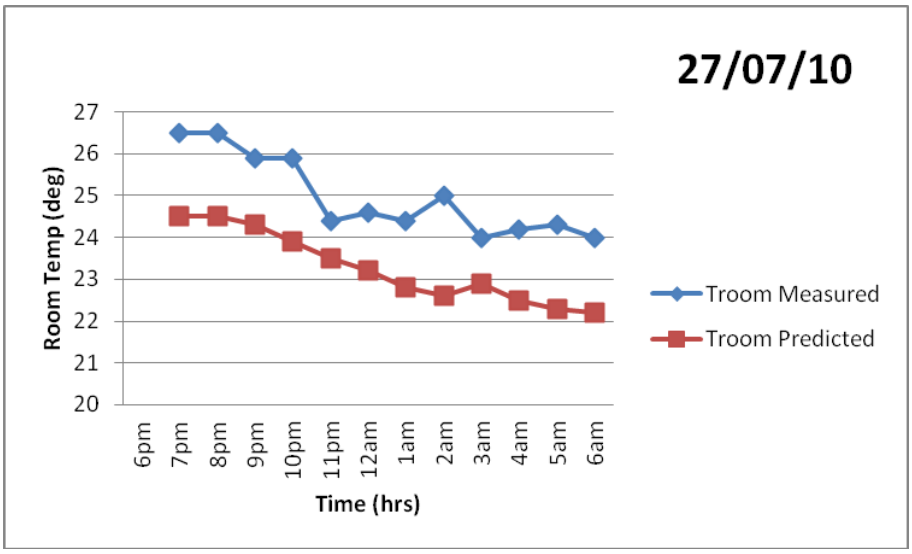

Fig. 4.14: Plots of Predicted and Measured Temperatures against Time for 27/07/10

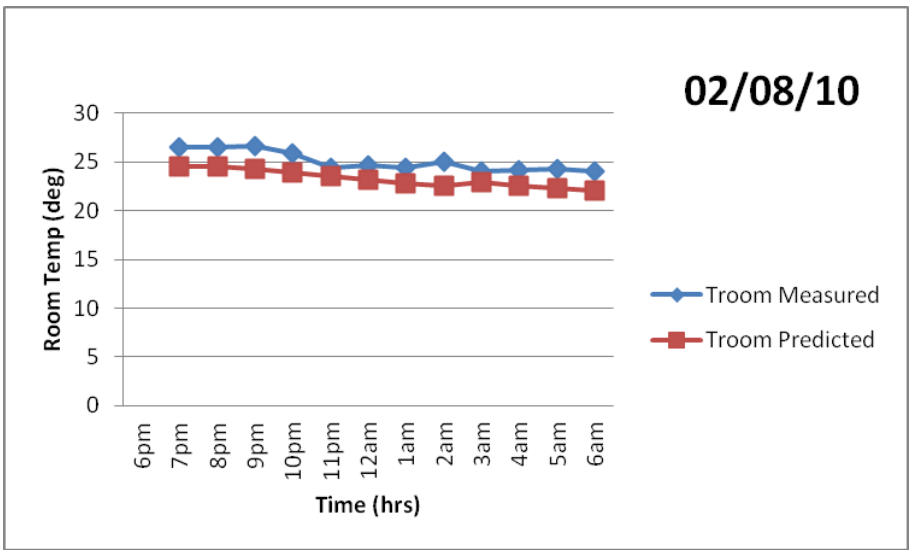

Fig. 4.15: Plots of Predicted and Measured Temperatures against Time for 2/08/10

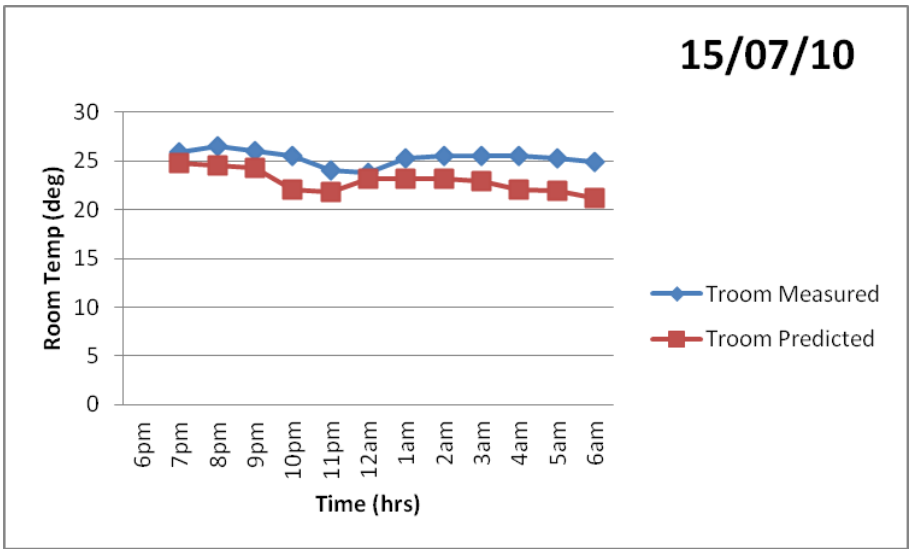

Fig. 4.16: Plots of Predicted and Measured Temperatures against Time for 15/07/10

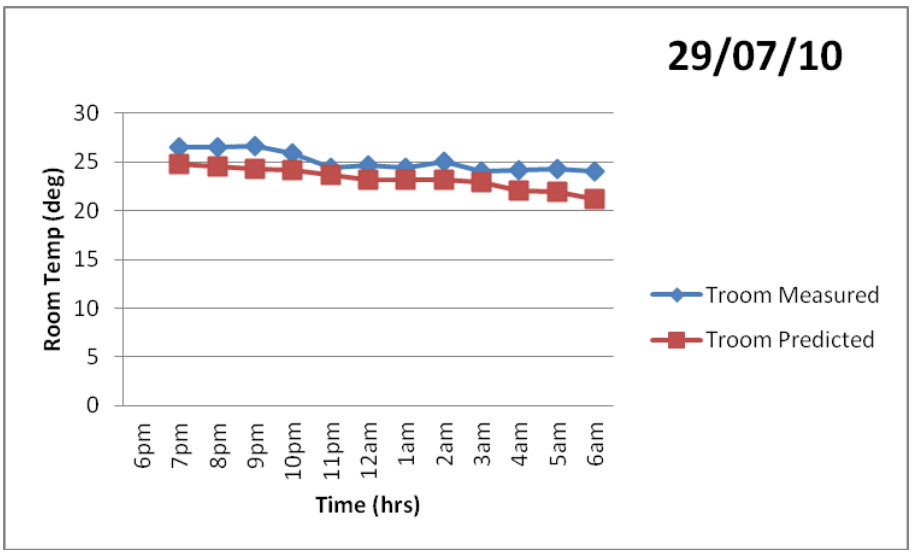

Fig. 4.17: Plots of Predicted and Measured Temperatures against Time for 29/07/10

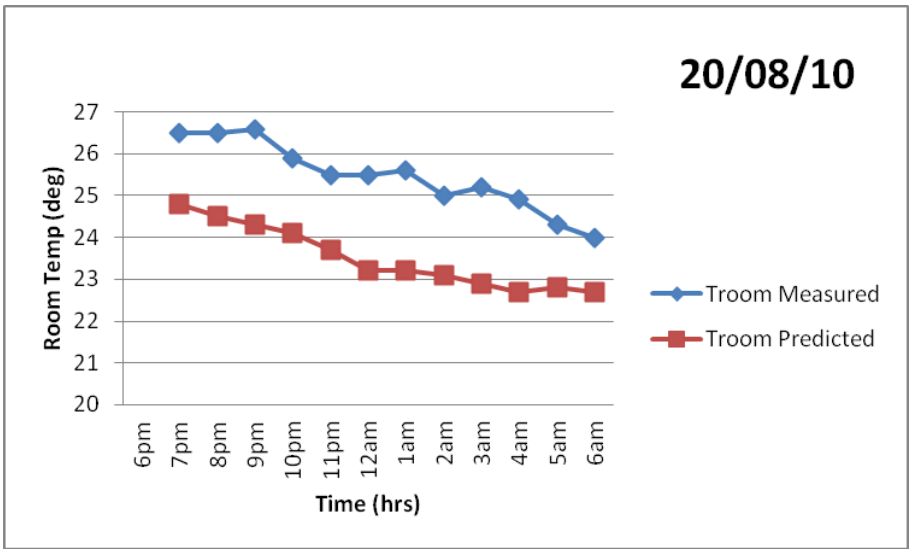

Fig. 4.18: Plots of Predicted and Measured Temperatures against Time for 20/08/10

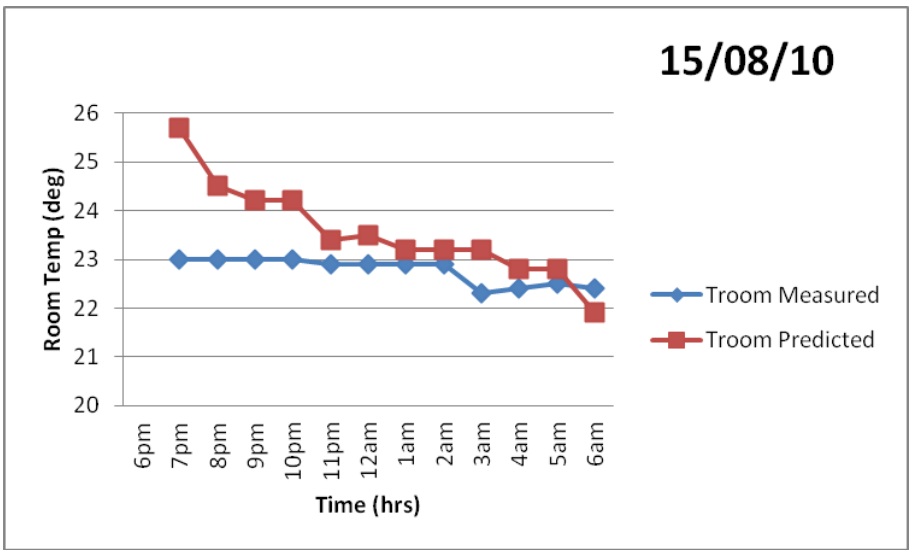

Fig. 4.19: Plots of Predicted and Measured Temperatures against Time for 15/08/10

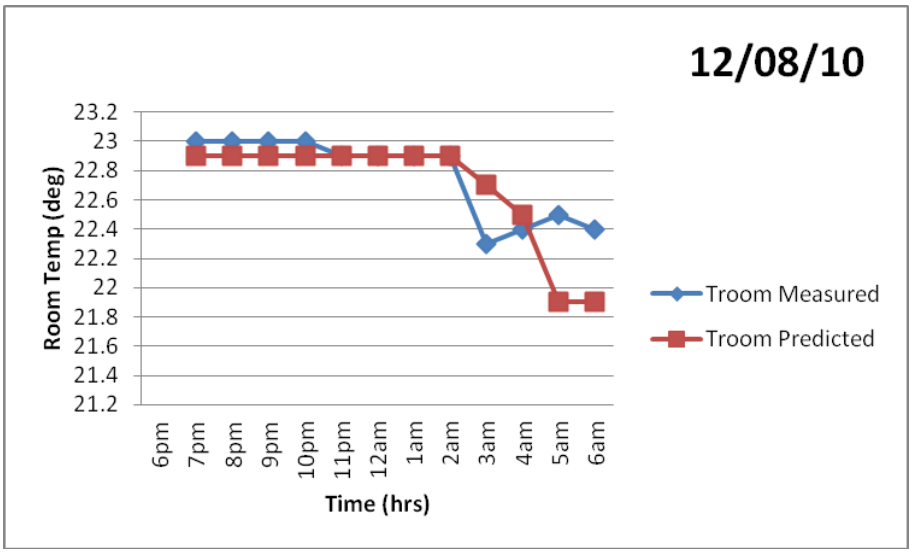

Fig. 4.20: Plots of Predicted and Measured Temperatures against Time for 12/08/10

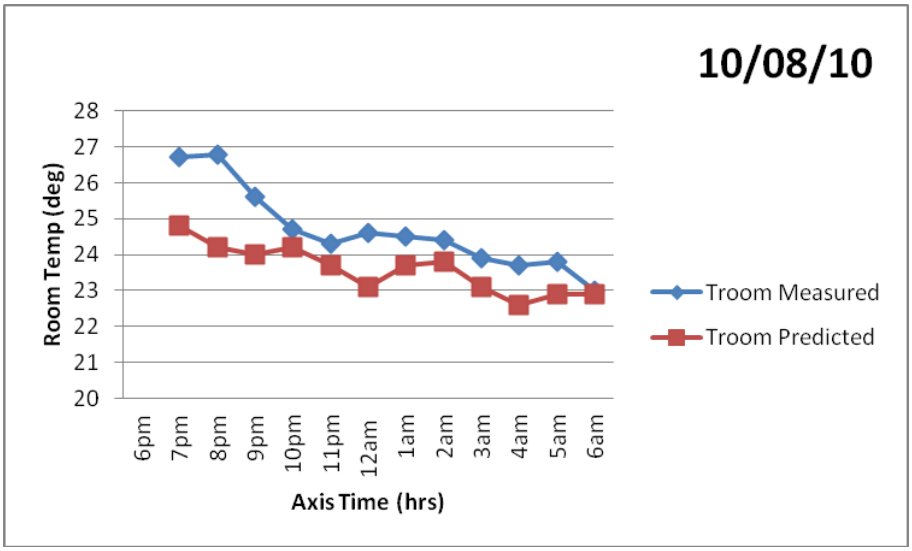

Fig. 4.21: Plots of Predicted and Measured Temperatures against Time for 10/08/10

From figs. 4.13 – 4.21, a comparison of the predicted trends against the measured trends is given. The trends show similarity/agreement in a progressive temperature drop of the room temperature throughout the night till early morning. From the mean deviation error table, the deviation between the predicted and measured room temperature values is between 0.53 at the minimum and 2.14 at the maximum. This reflects a very good agreement between measured and predicted values.

4.8.2 **Storage Water Tank Temperature: Predicted versus Measured**

Figs. 4.22 – 4.30 below are plots for different ambient conditions for both measured and predicted temperatures of the storage water tank.

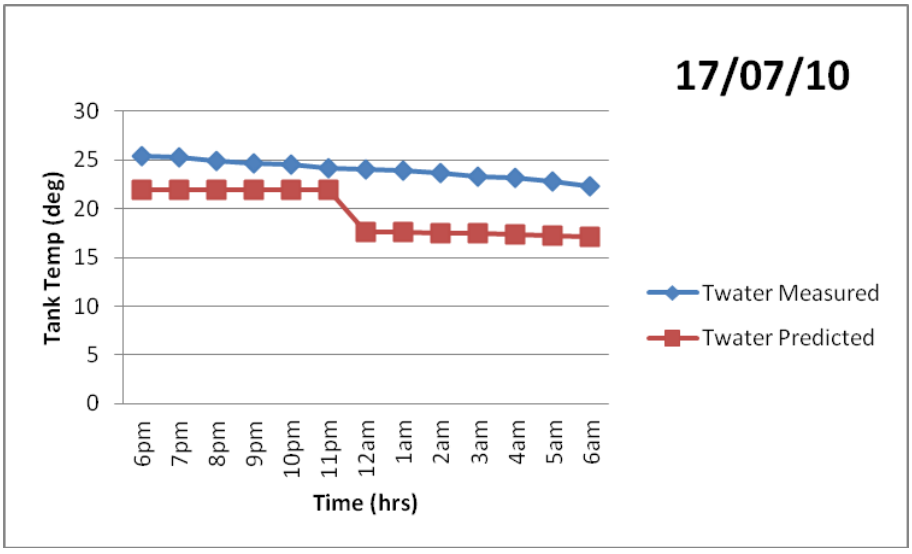

Fig. 4.22: Plots of Predicted and Measured Water Temperatures against Time for 17/07/10

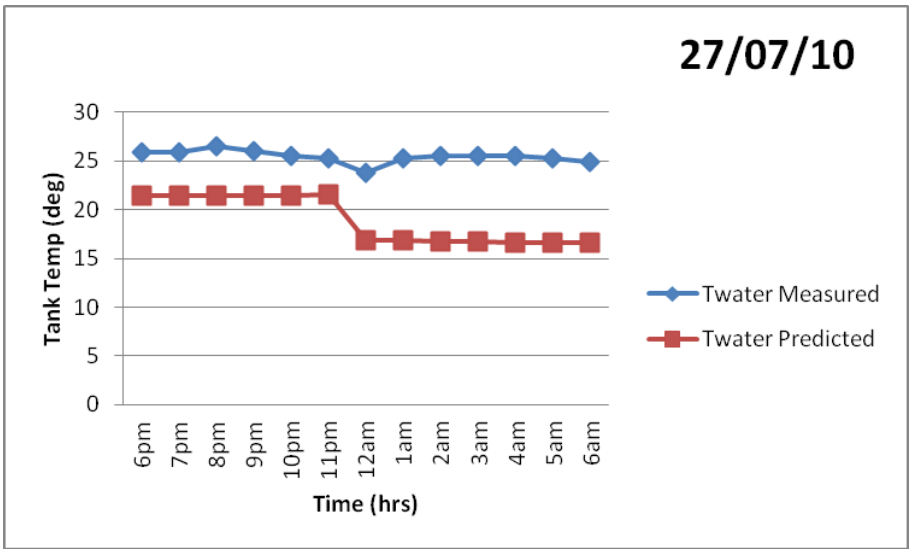

Fig. 4.23: Plots of Predicted and Measured Water Temperatures against Time for 27/07/10

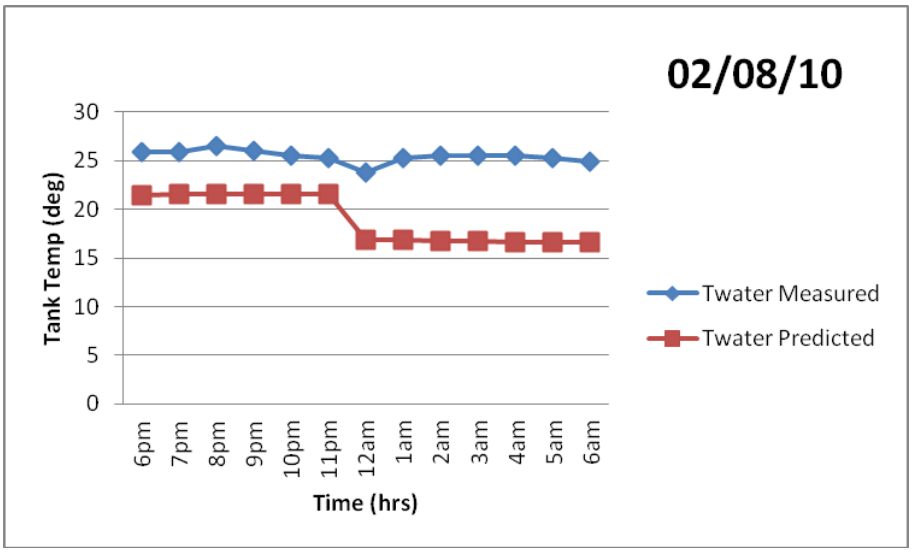

Fig. 4.24: Plots of Predicted and Measured Water Temperatures against Time for 2/08/10

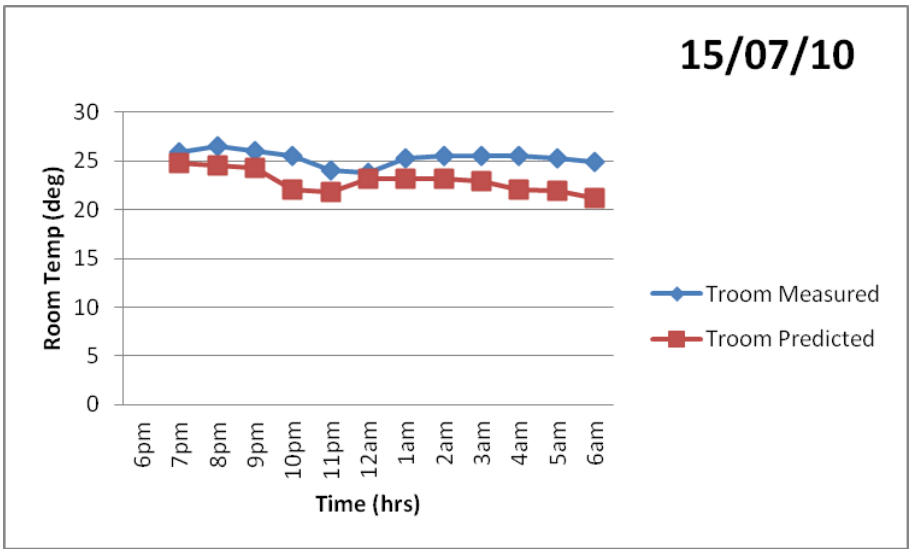

Fig. 4.25: Plots of Predicted and Measured Water Temperatures against Time for 15/07/10

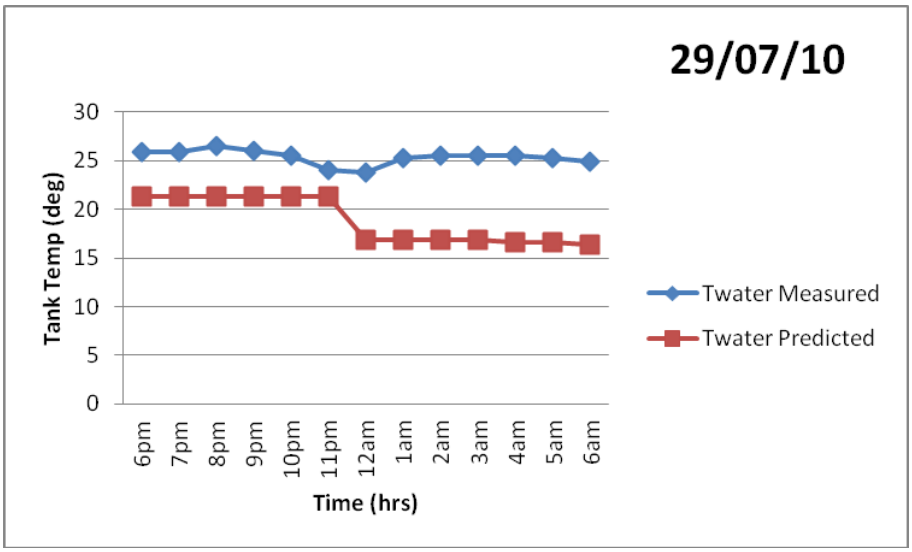

Fig. 4.26: Plots of Predicted and Measured Water Temperatures against Time for 29/07/10

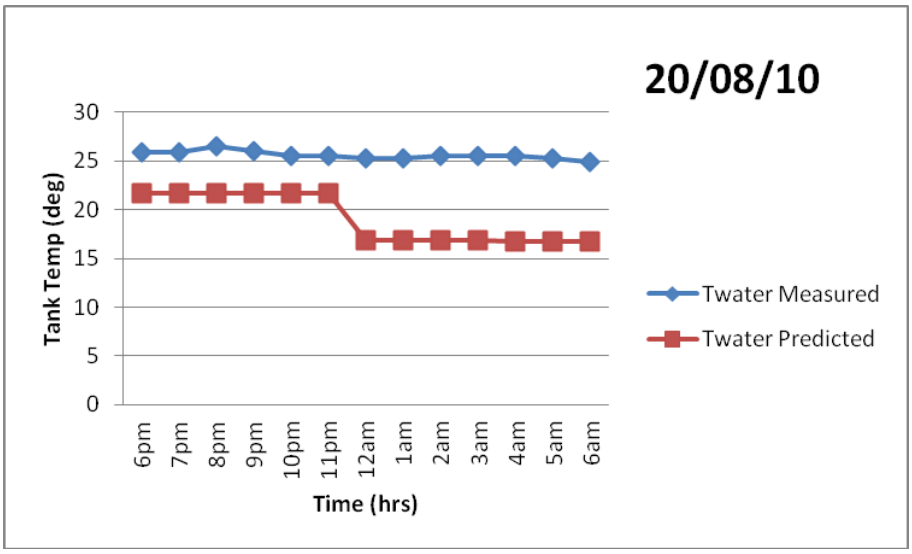

Fig. 4.27: Plots of Predicted and Measured Water Temperatures against Time for 20/08/10

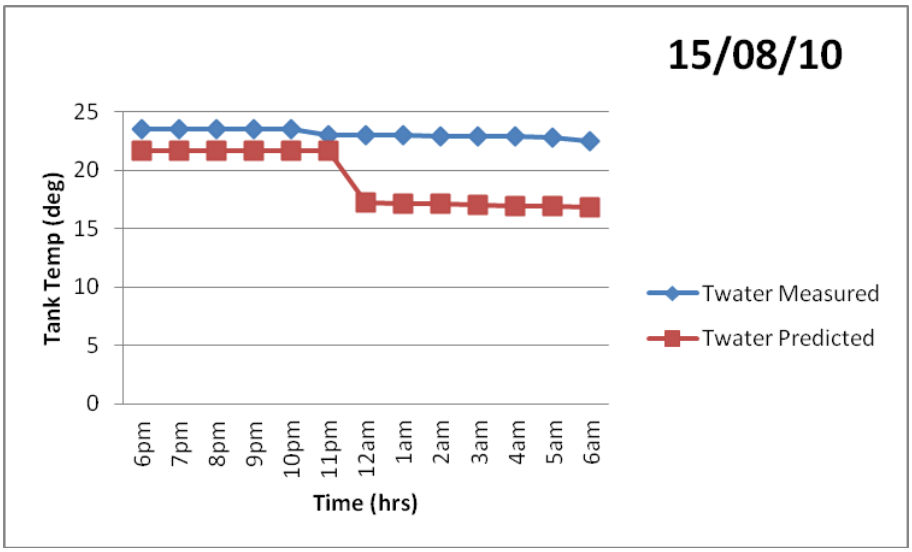

Fig. 4.28: Plots of Predicted and Measured Water Temperatures against Time for 15/08/10

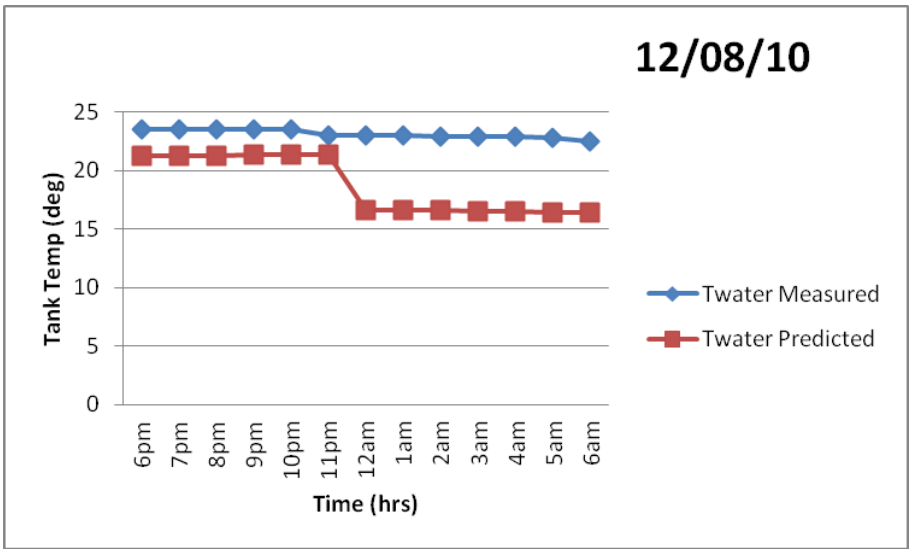

Fig. 4.29: Plots of Predicted and Measured Water Temperatures against Time for 12/08/10

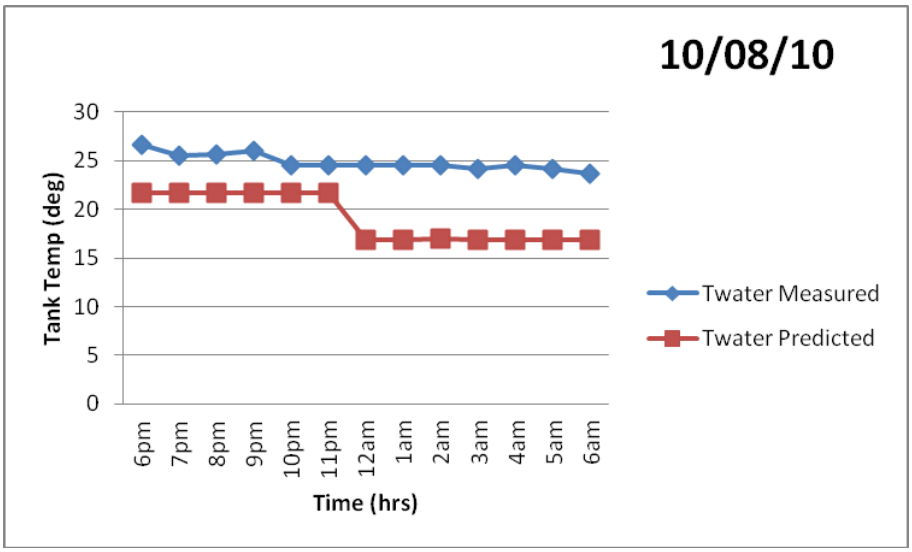

Fig. 4.30: Plots of Predicted and Measured Water Temperatures against Time for 10/08/10

From figs. 4.22 – 4.30, a comparison of measured storage water tank temperature is evaluated. In most cases, the trends showed agreement particularly between 6pm – 10pm and 12am – 6am. Due to the action of the circulating pump, there is a sharp decrease in the temperature of the predicted storage water tank of about 3.5^{o}C. This is practically true as the tank is expected to release most heat within the first hour of circulation when the temperature gradient between the storage tank and the radiator surface is most significant. Beyond this time, temperature drop continues very slowly and gradually.

The mean deviation error analysis shows good agreement as a value of 3.06 was calculated for 02/08/10. A maximum value of 4.68 (15/07/10) was calculated. The trends show the validity of the models used in the prediction. The different values of mean deviation are reflective of the unsteady nature of weather conditions, even within a particular season. Similarly, the high deviation values suggest inaccuracy in the instrumentation of the measured values. It is observed that the measured temperature values experienced a rise between 12 midnight and 1am. This is practically impossible as the tank continues to lose heat till morning.

4.8.3 **Radiator Temperature: Predicted versus Measured**

Figs. 4.31 – 4.39 below are plots of radiator temperature for both predicted and measured temperature values for different ambient temperatures.

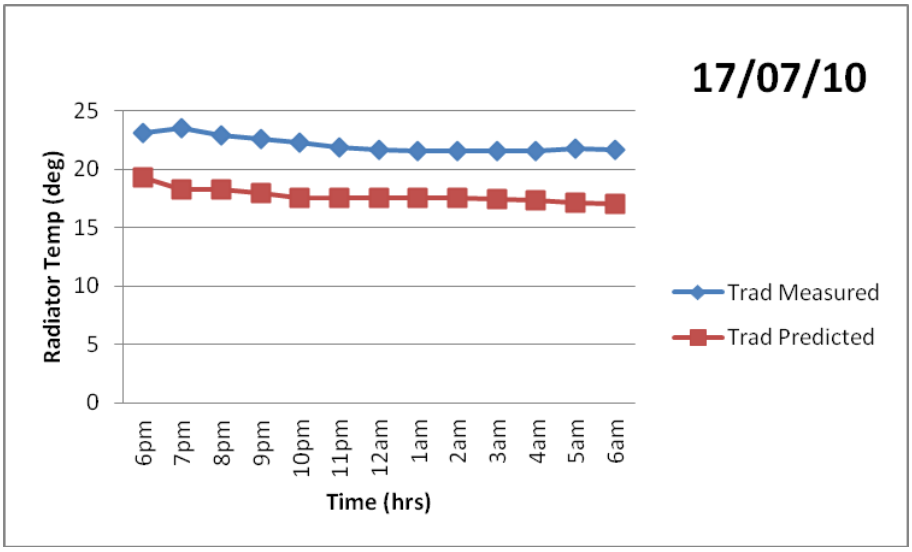

Fig. 4.31: Plots of Predicted and Measured Radiator Temperatures against Time for 17/07/10

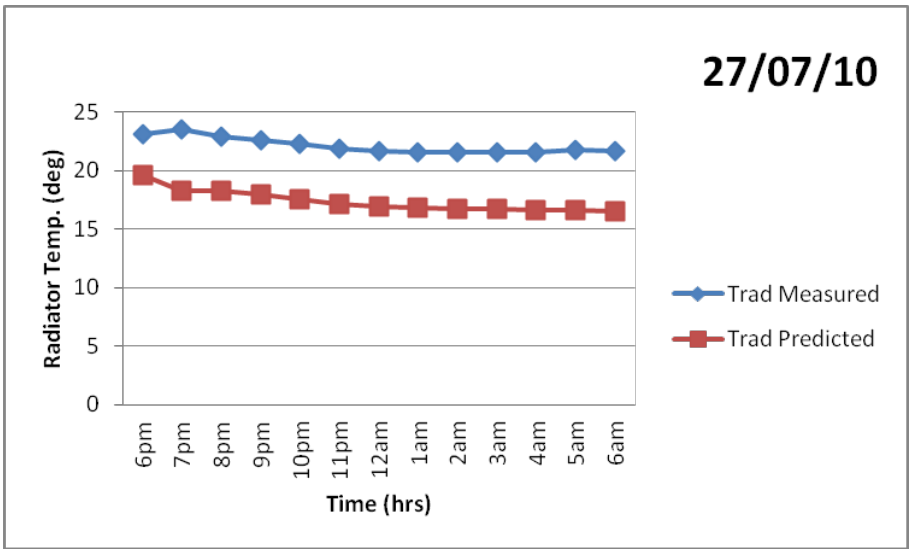

Fig. 4.32: Plots of Predicted and Measured Radiator Temperatures against Time for 27/07/10

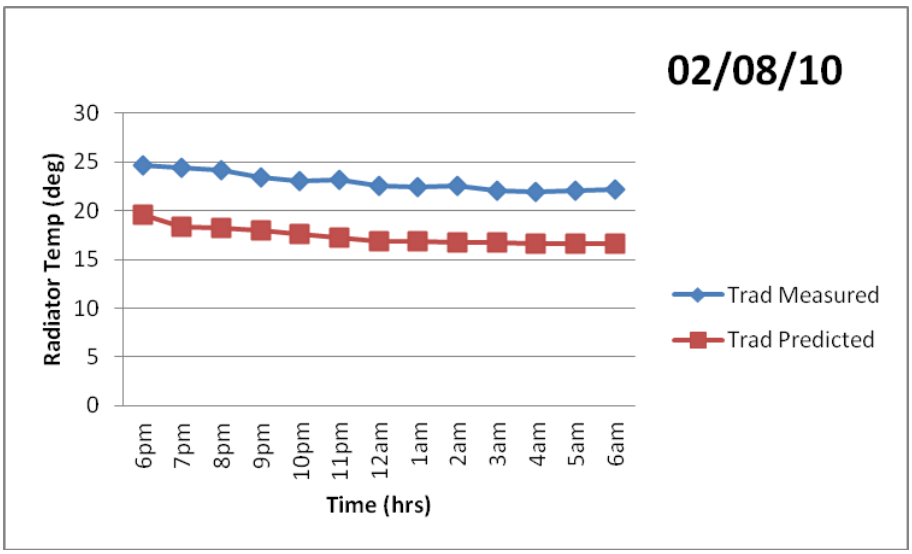

Fig. 4.33: Plots of Predicted and Measured Radiator Temperatures against Time for 2/08/10

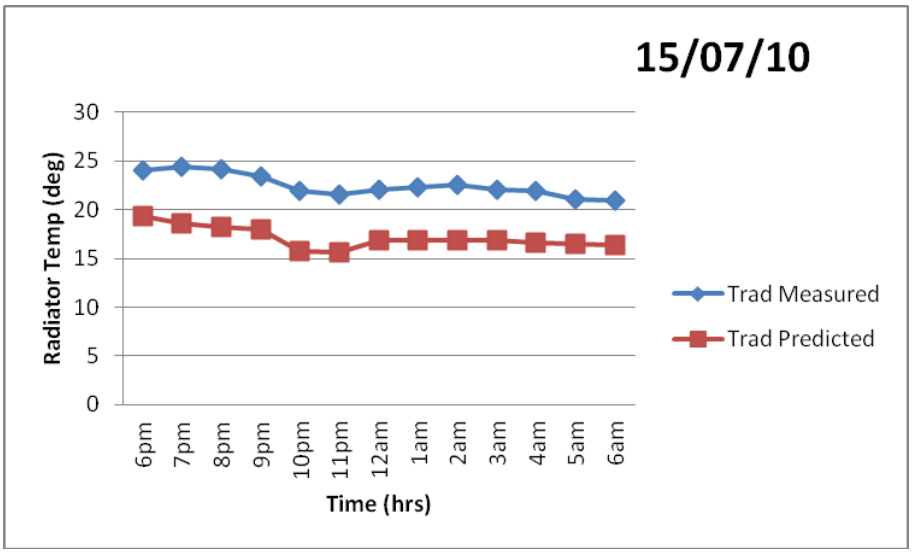

Fig. 4.34: Plots of Predicted and Measured Radiator Temperatures against Time for 15/07/10

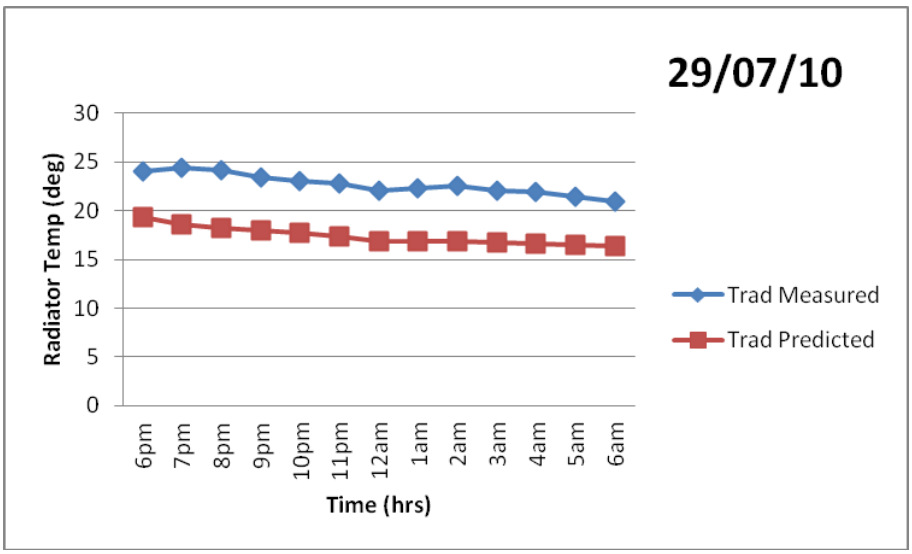

Fig. 4.35: Plots of Predicted and Measured Radiator Temperatures against Time for 29/07/10

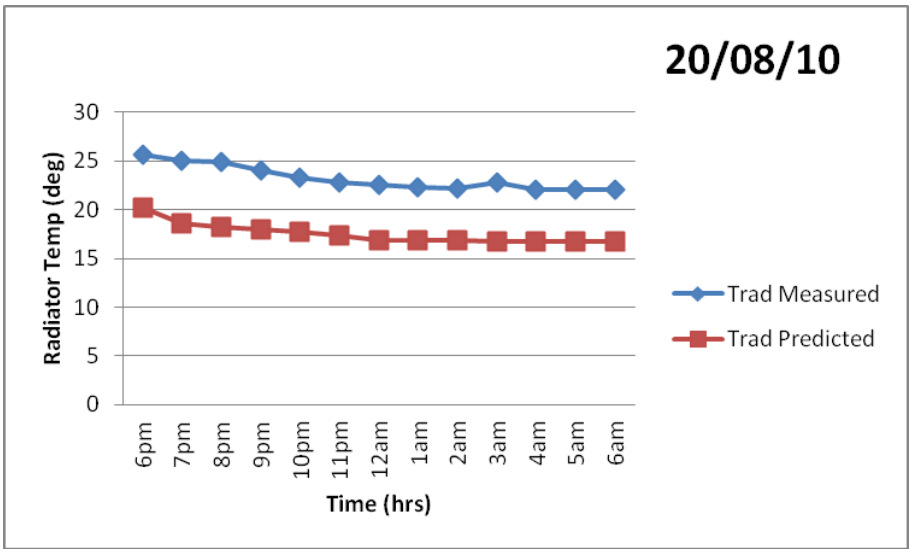

Fig. 4.36: Plots of Predicted and Measured Radiator Temperatures against Time for 20/08/10

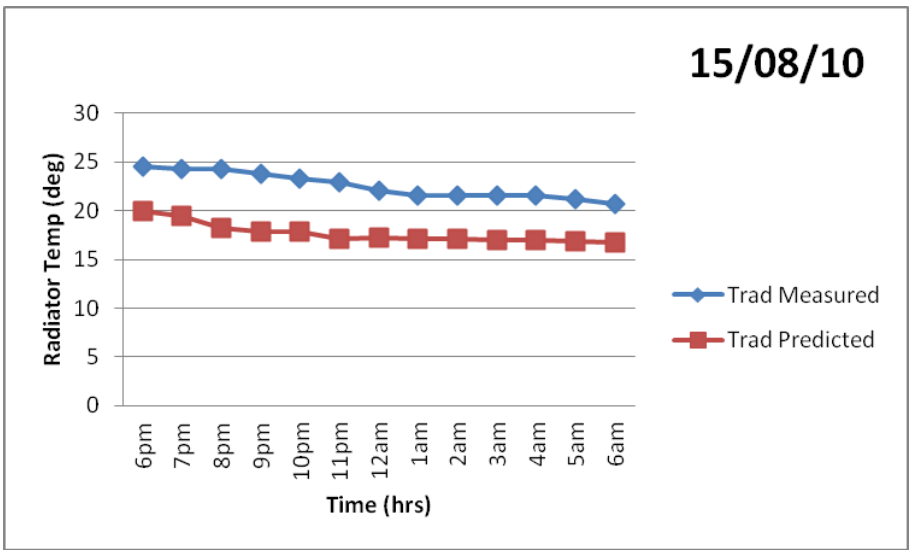

Fig. 4.37: Plots of Predicted and Measured Radiator Temperatures against Time for 15/08/10

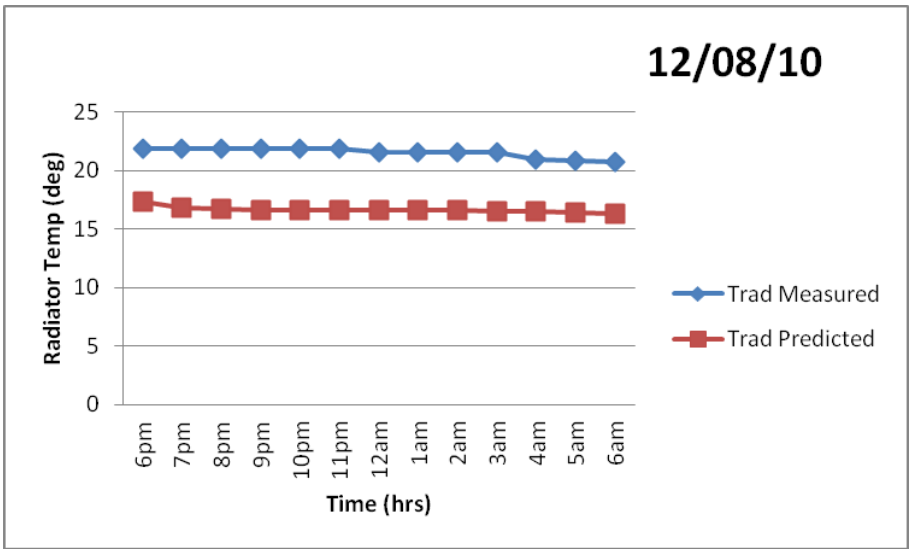

Fig. 4.38: Plots of Predicted and Measured Radiator Temperatures against Time for 12/08/10

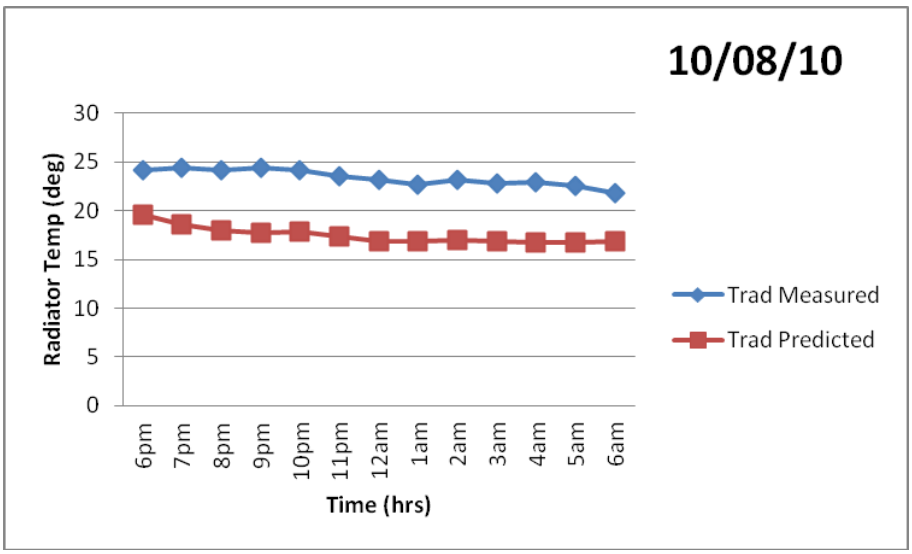

Fig. 4.39: Plots of Predicted and Measured Radiator Temperatures against Time for 10/08/10

From figs. 4.31 – 4.39, the validation of the models predicting the radiator temperature using measured values showed that the models are effective. The trends in the above plots showed good agreement between the measured and predicted values. The deviation ranged from 3.67 – 5.02. The high values of mean deviation could be from measurement errors, poor architectural design or low emissivity of radiator plate. However generally, most radiators practically attain temperatures lower than the ambient temperatures during the night till early morning hours as reflected by the predicted results.

4.9 Sensitivity Analysis

In performing a sensitivity analysis, a ±25% of the system variables including the radiator panel surface, storage tank volume, room wall thickness, convector fin surface area and the mass flow rate analyses were conducted. Below are the resultant plots for the observed variations in radiator temperature and tank temperature.

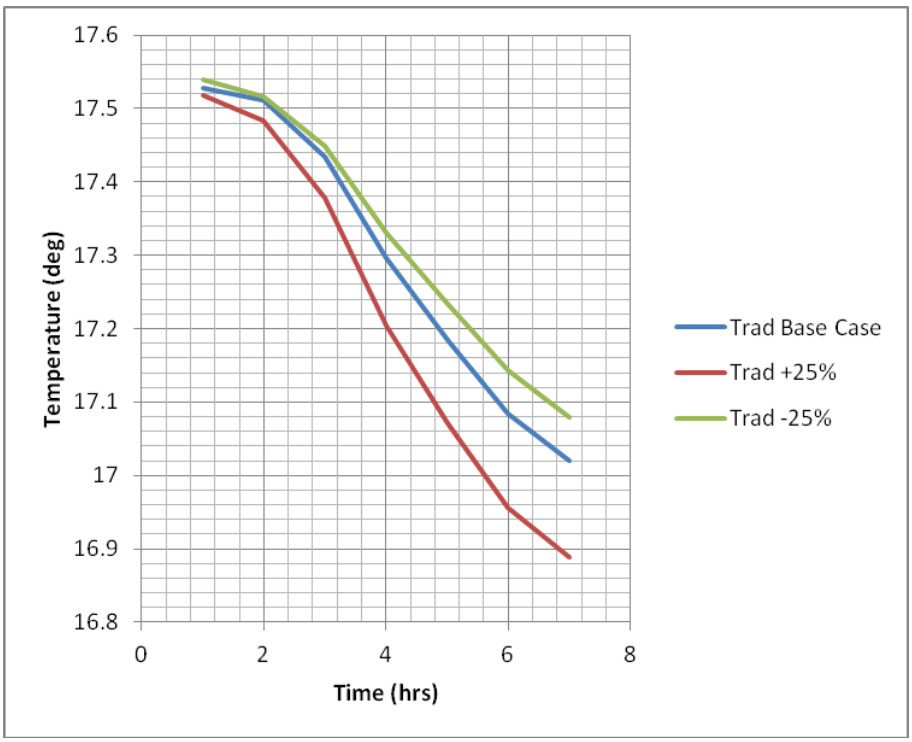

Fig. 4.40: Plots showing the values of the radiator panel temperature for the base case inputs, and ±25% of the base case inputs.

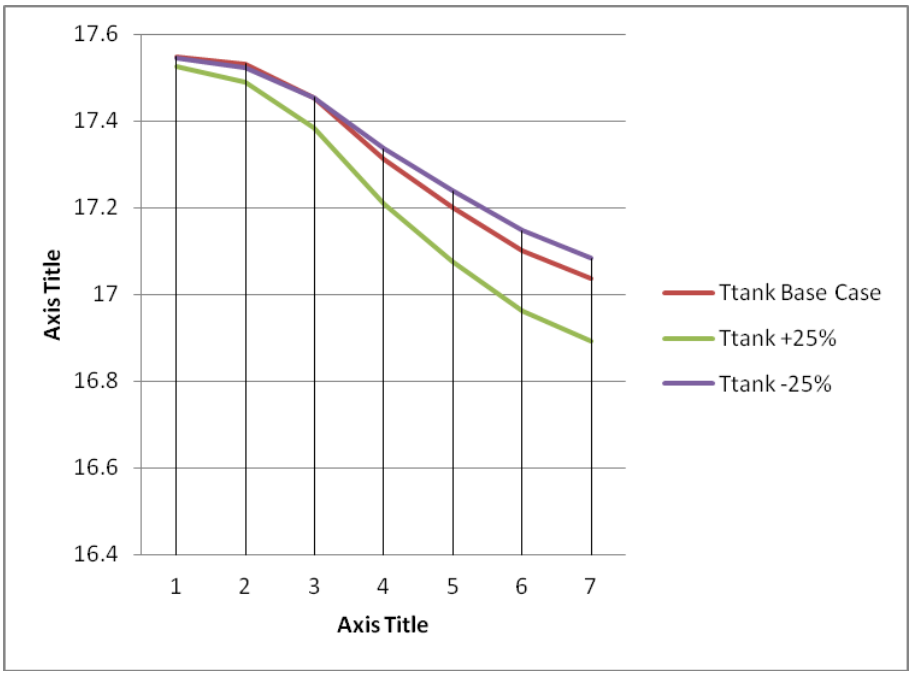

Fig. 4.41: Plots showing the values of the water storage tank temperature for the base case inputs and ±25% of the base case inputs

The results of this sensitivity analysis are given as a percentage variation of a number of the system performance parameters which include the sum of the difference between the outside ambient air temperature and the inside room air temperature multiplied by the time step for each of the hours of the nine hour period (8am – 5pm) that the room circulation pump was switched on, i.e $\sum(T_a - T_r)\Delta t$. Others are the total amount of heat gained by the storage water during the room cooling operating period, $Q_{t,in}$, and the heat removed during the night sky cooling period $Q_{t,out}$,

Table 4.2: Sensitivity analysis of performance parameters with a variation of ±25% from base case input values

Variable	$Q_{t,in}$ (MJ)	$Q_{t,out}$ (MJ)	$\sum(T_a - T_r)\Delta t$ [^oC.hour]
Base Case	80.2	79.5	38.07
0.75 A_s	77.5	70.5	30.52
1.25 A_s	84.6	87.2	44.87
0.75 V_t	78.4	68.2	36.8
1.25 V_t	81.9	88.6	38.09
0.75 L_r	80.3	79.7	29.6
1.25 L_r	77.8	79.6	41.6
0.75 A_{co}	71.9	76.4	1.26
1.25 A_{co}	84.7	79.9	46.3
0.75 mw	80.1	78.8	36.7
1.25 mw	80.2	79.3	37.5

For an 8-hour period (11pm – 7am), the radiator panel surface area was able to remove 79.5 MJ from the water storage tank as shown in the base case values. This corresponds to an average heat removal rate of 57.6 W/m^2. This heat removal rate compares favourably with the value of 80 W/m^2 as reported by Erell and Etzion (1996) and the value of 60.8 W/m^2 as reported by Dobson (2005).

The variations due to the parametric analyses show that the models are stable as an analysis tool. Variations of ±25% of the chosen variables showed significant changes in the values of the performance parameters. Similarly, the heat gained from the room space through the action of the

room convector into the storage tank during the day (8am – 6pm) shows a value of 80.2 MJ. This value is slightly more than the value of the heat lost to the ambient from the system. This is practically correct as the temperature of the water in the storage tank is never zero; there is always some amount of sensible heat in the water within the storage tank.

The values of $\sum(T_a - T_r)\Delta t$ from the above table is indicative of the functionability of the modeled system. These values are comparable to values from Dobson (2005). The depression between the values of the ambient air and the room is critical in determining the cooling power available to a system; hence the values are useful in analyzing a nocturnal system. Below is a table of the difference between the ambient air temperature and the room temperature against time between 8am – 5pm for the base case, and ±25% of the base case.

Table 4.3: $T_a - T_r$ values for the Base Case and ±25% of the base case (9am- 5pm)

Time (hrs)	$T_a - T_r$ Base Case	$T_a - T_r$ for -25%	$T_a - T_r$ for +25%
9am	2.56	3.57	1.89
10am	2.75	3.8	2.05
11am	2.93	4.02	2.21
12noon	3.12	4.24	2.37
1pm	3.3	4.46	2.52
2pm	3.48	4.68	2.67
3pm	3.66	4.9	2.83
4pm	3.83	5.11	2.98
5pm	4.01	5.33	3.13

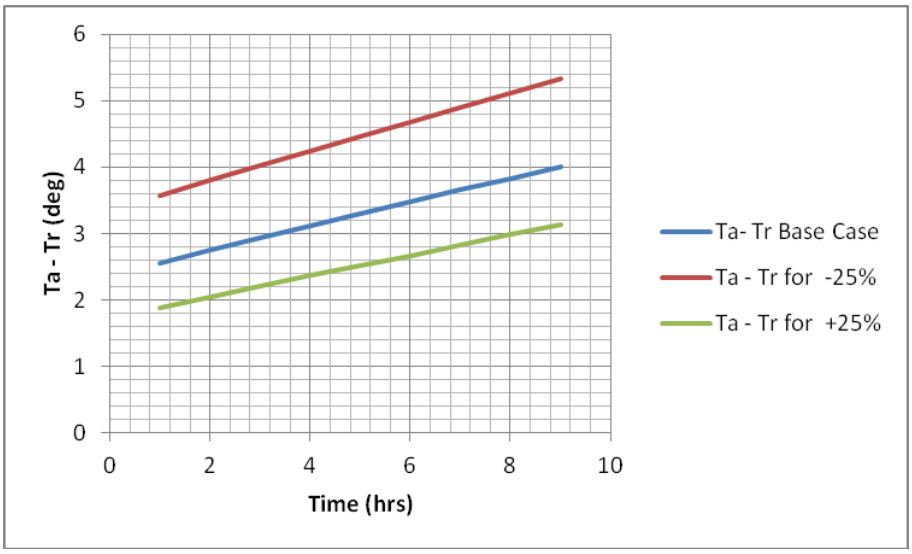

Fig. 4.42: Plots of $T_a - T_r$ for base case and ±25% of the base case values.

For the base case situation, the maximum temperature difference is 4.01, which is comparable to values in literature. This depression is indicative that nocturnal cooling is possible using this model. A very large value of $T_a - T_r$ is indicative of impossibility of nocturnal cooling. This is because it implies that much heat is added to the cooled space during the day and it could be due to poor insulation. This difference contributes the heat added to the room during the day and extracted to the water reservoir through the room convector. It is also indicative of the possible amount of heat to be removed from the cooled space at night.

During the nocturnal hours when cooling is added to the room space (9am – 7am), the temperature depression of ($T_a - T_r$) has a maximum value of -0.69. This very low temperature value makes it possible for heat to flow from the water reservoir, now at a higher temperature, to the radiator panel which is obviously at a lower temperature. Also it is important to note that the negative direction is an added impetus to cooling at night, as

some heat is also further lost due to this temperature depression. This can be viewed as natural cooling of the room space.

Similarly, a comparison of the temperature depression, as shown below, obtained in this study to the ones in literature show that the model is a robust tool for the prediction of night cooling.

Table 4.4: Temperature depression ($T_a - T_r$) comparison for different locations.

Temperature depression ($T_a - T_r$)	**Country**	**Author**
5°C	Norway	Meir, et at (2003)
3°C	Thailand	Ito and Miura (1989)
5°C	Namibia	Dobson (2005)
4.01°C	Nigeria	Present study

Following the sensitivity analysis, the optimal design parameters for the modeled 3.0 x 3.0 x 2.5 room is as given below:

Table 4.5: Optimal values of design parameters

Parameters	**Values**
Radiator surface area (m^2)	18.2
Convector area (m^2)	28.62
Tank volume (m^3)	1.57
Room volume (m^3)	22.5
Surface area of room (m^2)	48.0

CHAPTER FIVE
CONCLUSION AND RECOMMENDATIONS

5.1 Conclusion

The mathematical model of a nocturnal cooling system using an integrated system comprising a radiator panel, water storage tank, room convectors and a cooled space was developed from first principle. The model was developed for a transient system. The resulting equations were transformed into the numerical format using the finite difference scheme and subsequently used to carry out a transient analysis and performance evaluation of the nocturnal system using a computer program written in Matlab 7.0. The numerical solution was validated with data from the actual field performances of a similar system tested at a site in the Federal University of Technology, Owerri (FUTO). The predicted temperature values showed agreement with the measured values. The mean deviations between the predicted and measured temperature values varied over the ranges of 3.67 – 5.02^{o}C for the radiator temperature and 0.53 – 2.14^{o}C for the room temperature, while that between the predicted and measured water tank temperatures varied over the range of 3.06 – 4.68 ^{o}C.

On the heat removal rate, the radiator panel surface area was able to remove 79.5 MJ from the water storage tank which represents an average heat removal rate of 57.6 W/m^2 over an 8-hour period of radiator circulation pump operation (11pm – 7am). This is very comparable to other works such as Erell and Etzion (1996) with heat removal rate of 80W/m^2 and Dobson (2005) with heat removal rate of 60.8W/m^2.

From the above and in line with the objectives of this work, it is summarized as follows:

1. A thorough study on the principle of nocturnal cooling for the purposes of cooling room spaces was carried out.
2. Mathematical models governing the relationship of the various variables involved in the integrated system were developed in the transient phase.
3. A computer simulation program in Matlab 7.0 was developed to solve the objective functions of the subsystems involved in the setup.
4. The available cooling due to the design was evaluated and a heat removal rate of 57.6 W/m^2 was achieved.
5. A sensitivity analysis carried out to within ±25% showed a consistency in heat removal rate with a deviation of 0.54 representing 0.94% deviation. This further validates the model.
6. An optimal scheme for commercialization showed the following component sizes: a radiator area of 18.2 m^2, a convector area of 28.62 m^2 and a tank volume of 1.57 m^3.

It is therefore concluded that the thermal model presented in this work can be used with confidence as a design tool for the sizing of a cooling system using night sky radiation.

The overall thermal management strategies adopted in order to keep the cooled space to within the acceptable limits were as follows:

a. The room was insulated properly from heat ingress due to environmental conditions.
b. Internally generated heat was removed from the cooled room space during the day by allowing the heated air to flow over a finned

room convector heat exchanger through which cold water from the storage tank is circulated.

c. Heat extracted into the storage tank during the day is expelled during the night by passing the heated water through the finned heat exchanger of the radiator panel to the ambient. This prevents the radiator from forming frost on the surface and removes heat within the system to achieve desired cooling during the day.

5.2 Achievements of the Present Work

The following are the achievements of this work:

i. A comprehensive numerical study of an integrated nocturnal cooling system has been successfully undertaken using the finite difference method of numerical analysis. The solution algorithm is a good tool for the system performance analysis and sizing and may be easily applied to other system configurations with slight modifications. This is considered a useful contribution to the emerging body of knowledge on the performance characteristics of nocturnal systems.

ii. Previous works, as comparatively few as they are, in this area of knowledge were mainly from Asia, America and northern Africa. The only documented exception is the preliminary work of Ezekwe (1986). In this work, a further and more comprehensive approach was adopted towards studying this trend in Nigeria. It is indeed a milestone in the evaluation of nocturnal cooling available in Nigeria.

iii. This work covers the peculiar seasons in Nigeria. The work was investigated for the various seasons thus making it easier to evaluate and compare the cooling rate availability in these seasons.

iv. The sensitivity analysis carried out indicated that irrespective of the input parameters, the developed model is stable and can be confidently used as a design tool for nocturnal cooling systems.

5.3 Recommendations

The following areas or interests are recommended for further studies:

1. Using the established data bank in this work, a further analysis to establish the nocturnal pattern in all the seasons of harmattan and rain prevalent in Nigeria should be carried out. This will enable designers predict correctly the expectation in various seasons.

2. To further aid nocturnal cooling, a further study towards integrating radiator panel-cooling improvements in the computer simulation sensitivity should be considered.

3. Due to the emerging nature of this area of knowledge particularly in Nigeria, funded research as available in other areas carrying out similar work should be made available to interested researchers.

References

Ali, A.H.H. (2007) 'Passive cooling of water at night in uninsulated open tank in hot arid areas'. Energy conversion and management 48, 93 – 100.

Ali, A.H.H., Taha, I.M.S., and Ismail, I.M. (1996) 'Cooling of water through a night sky radiator'. Solar energy vol. 55 no. 4 pp 235 – 253. Elsevier science Ltd. USA.

Armenta-Deu, C., Doaire, T., and Hernando, J. (2003) 'Thermal analysis of a prototype to determine radiative cooling thermal balance'. Renewable energy, volume 28 pp 1105 – 1120.

Anyanwu, E. E. and Iwuagwu, C. J. (1995) 'Wind characteristics and energy potentials for Owerri, Nigeria'. Renewable energy, vol. 6, No. 2, pp 125 – 128. Elsevier Science Ltd, Great Britain.

Bass, B. R. and Ott, L. J. (1980) 'Application of the finite element method to the two dimensional non linear inverse heat conduction problem (In: Taylor, C.; Hinton, E. and Qwen, D. R. J. (ed.) Numerical Methods for Non Linear Problems, vol 1, Pineridge Press, Swansea, UK.

Berdahl, P., and Fromberg, R. (1984) 'The thermal radiance of clean skies'.Solar energy, volume 29, no. 4, pp 299 – 314.

Bouchair, A. (1989) 'Solar induced ventilation in the Algerian and similar climates'. PhD thesis. UK: University of Leeds.

Bouchair, A. (1994) 'Solar chimney for promoting cooling ventilation in Southern Algeria'. Building services engineering research and technology.

Bouchair, A., Fitzgerald, D., and Tinker, J.A. (1989) 'Passive solar induced ventilation'. Alternative energy sources VIII. Proceedings of the Miami International conference on alternative energy sources (1987: Maimi beach, Florida). Solar energy fundamental and applications, vol.1. New York, USA. Hemisphere Publishing Corporation.

Cheikh, H.B., and Bouchair, A. (2004) 'Passive cooling by evapo reflective roof for hot dry climates'. Renewable energy: 29, 1877 – 1886.

Dimoudi, A., and Androutsopolous, A. (2006) 'The cooling performance of a radiator based roof component. Solar energy 80, 1039 – 1047.

Dobson, K.A., Hodes, G., and Mastai, Y. (2003) 'Thin semi-conductor films for radiative cooling applications. Solar energy materials and solar cells, volume 80 pp 283 – 296.

Dobson, R. T. (2005) 'Thermal modelling of a night sky radiation cooling system'. Journal of Energy in Southern Africa, vol.16 No 2.

Duffie, J. A. and Beckman, W. A. (1991) 'Solae engineering of thermal Processes. New York. John Wiley and sons.

Erell, E. and Etzion, Y. (2000) 'Radiative cooling of buildings with flat plate solar collectors'. *Building and Environment*. Vol. 35, No. 6, pp 297-305.

Erell, E. and Etzion, Y. (1999) ' Analysis and experimental verification of an improved cooling radiator'. Renewable Energy 16, 700–703.

Erell, E., and Etzion, Y. (1992) 'A radiative cooling system using water as heat transfer medium'. Architectural Science Review 35, 35–49.

Etzion, Y., and Erell, E. (1991) 'Thermal storage mass in radiative cooling systems'. Building and Environment 26 (4), 389–394.

Etzion, Y., Pearlmutter, D., Erell, E., and Meir, I.A. (1997) 'Adaptive architecture: Integrating low-energy technologies for climate control in the desert. Automation in construction, volume 6, pp 417 – 425.

Ezekwe, C.I. (1986) 'Nocturnal radiation measurements in Nigeria'. Solar energy vol. 37, no. 1. Pergamon press, New York.

Fairey, P.W., Kerestecioglu, A., Vieira, R., Swami, M., and Chandra, S. (1990) 'An analytical assessment of the desicant enhanced radiative cooling concept'. FSEC-PF-207-90, ASME 1990 International Solar Energy conference, Miami, FL.

Fletcher, C. A. J. (1990) 'Computational Techniques for Fluid Dynamics' Vol. 1 2nd ed., Springer Verlag.

Givoni, B. (1982) 'Cooling by long wave radiation'. Passive solar journal, no. 1, 131.

Givoni, B. (1994) 'Passive and Low Energy Cooling of Buildings'. Van Nostrand Reinhold, New York.

Golaka, A., and Exell, R.H.B. (2007) 'An investigation into the use of a wind shield to reduce the convective heat flux to a nocturnal radiative cooling surface'. Renewable energy, 32. Pp 593 – 608.

Goswami, D.Y., Kreith, F., and Kreider, J. (2000) 'Principles of Solar Engineering'. Second edition. Taylor and Francis Publishers.

Hardy, M. (2008) 'A practical guide to free cooling, alternative cooling, night cooling and low energy systems for air conditioning systems. Ambthair services Ltd. http//www.ambthair.com

Hay, H.R. (1978) 'A passive heating and cooling system from concept to commercialisation'. Proceedings of the annual meeting of the international section of the Solar Energy society, pp 262 – 272.

Hay, H.R., and Yellot, J.J. (1969) 'Natural air conditioning with roof ponds and natural air conditioning'. ASHRAE Trans. 75 (1), 165–177.

Ibe, C. A. (2003) 'Principles of Tropical Airconditioning'. Spectrum Books Ltd, Ibadan. Nigeria.

Ito, S., and Miura, N. (1989) 'Studies of radiative cooling systems for storing thermal energy'. Journal of solar energy, 111, 251.

Martin, M. (1989) 'Radiative cooling'. In: Cook, J. (Ed) Passive cooling, the MIT press, Cambridge, Mass, pp. 593.

Martin, M., and Berdahl, P. (1984) 'Summary of results from the spectral and angular sky radiation measurement program'. Solar Energy 33, 241–252.

Mcathren, J.R., and Akridge, J.M. (1982) 'Radiant cooling to the night sky in hot, humid climates'. Progress in passive solar energy systems, American solar energy society, pp 877 – 882.

Meir, M.G., Rekstad, J.B., and Lovvik, O.M. (2003) 'A study of a polymer based radiative cooling system'. Solar energy volume 73, no. 6 pp 403 – 417.

Mills, A. F. (2000) 'Heat Transfer. Prentice Hall, Upper Saddle River, New Jersey. USA.

National Institute for Rural Engineering (2008) 'Effects of the passive use of nocturnal radiative cooling in fresh vegetable cooling'. Lab. of regional energy resources, department of regional resources.

Okoli, I.C. (2003) 'Incidence and modulating effects of environmental factors on trypanosomosis, peste des petit ruminants (PPR) and bronchopneumonia of West African dwarf goats in Imo state, Nigeria'. Livestock Research for Rural Development 15 (9).

Parker, D.S. (2005) 'Theoritical evaluation of the night cool nocturnal radiation cooling concept'. FSEC-CR-1502-05, Florida solar energy centre, Cocoa, FL.

Rajput, R. K. (2005) 'Heat and Mass Transfer in SI Units'. Published by S. Chand & Company Ltd. New Delhi, India.

Richtmyer, R. and Morton, K. W. (1967) 'Difference Methods for Initial Value Problems', Wiley Interscience.

Santamouris, M., and Asimakopoulos, D. (1996) 'Passive cooling of buildings'. James and James, London.

Simonetti, M., Fracastoro, G.V., and Perino, M. (2008) ‘CFD transient analysis of night cooling strategy applied to school buildings’. Department of energetic, Turin Polytechnic, Italy.

Twizell, E. H. (1984) ‘Computational Methods for Partial Differential Equations’, Ellis Horwood.

APPENDIX

I: PROGRAM CODE IN MATLAB PROGRAMMING LANGUAGE

```
% parameter description
%for the radiator panel:
Es =0.90  ; As = 48; n = 0.9;
Ao = As * n ; Ks = 0.030; Ls = 0.025;   %radiator panel underside
d = 5.67e-8; %Stefan-Boltzman constant
%water tank parameters
Kat = 0.030; At = 14.296; Lt = 0.025;
Mw = 4150; %mass of water circulated
Mt = 4150; %mass of water in the tank
Vt = 4.15;% volume of tank
c = 4186; %specific heat capacity of water
DeltaTime = 3600; %time to circulate one tank of water (1 hour)
Mdot = 4150/3600;%mass of water circulated per second
% convector parameters
Hcw = 4000; % water-side heat transfer coefficient
Hca = 10; % air-side heat transfer coefficient
Aa = 75.50; % air side area
Aw = 9.060; % water side area
Na = 0.915; % air-side efficiency
Rrc = (1/(Hcw*Aw)) + (1/(Hca*Aa*Na));% room convector thermal
resistance

a = 1.8; b = 3.8;
rho = 1000; %specific density
RadTemp = [];RoomTemp = []; AirTemp =[]; TankTemp = [];

%calculate the radiator temp & tank temp at the tank turn on time
time = 23;
SolAngle = SolarAngle(time);
G = SolarIrradiance(time);
Qsolar = SolAngle*G*As;
Tsky = SkyTemperature(time);
Ta = AirTemperature(time);
AirTemp(time) = Ta;
Vwind = WindVelocity(time);
Has = a + b*Vwind;
Haws = Has;
Raws = (1/(Haws*Ao)) + (Ls/(Ks*Ao));
%calculate panel temperature from energy balance equation when heat
%transfer due to water circulation through the panel is zero.
Ts = fzero(@(Ts) (Qsolar + Has*As*(Ta - Ts) + (Ta - Ts)/Raws - ...
    (As*Es*d*(Ts - Tsky)*((Ts + 273.15)^2 +(Tsky + 273.15)^2)*...
    ((Ts + 273.15)+(Tsky + 273.15)))), 20);
Hat = Has;
Rat = (1/(Hat*At)) + (Lt/(Kat*At));
Tt = fzero(@(Tt) ((Ta-Tt)/Rat),20); %Tank Temperature at this time
RadTemp(time) = Ts;




time = 24;
SolAngle = SolarAngle(time);
G = SolarIrradiance(time);
Qsolar = SolAngle*G*As;
Tsky = SkyTemperature(time);
```

```
Ta = AirTemperature(time);
AirTemp(time) = Ta;
Vwind = WindVelocity(time);
Haws = a + b*Vwind;
Has = Haws;
Raws = (1/(Haws*Ao)) + (Ls/(Ks*Ao));


Tw1 = Tt; %temperature of the water leaving the tank
Ts = fzero(@(Ts) ((Mdot*c*(Tw1 - Ts)/DeltaTime) + Qsolar +...
    Has*As*(Ta - Ts) + (Ta - Ts)/Raws - (As*Es*d*(Ts - Tsky)*...
    ((Ts + 273.15)^2 + (Tsky + 273.15)^2)*((Ts + 273.15)+...
    (Tsky + 273.15)))),20);
Tw2 = Ts; %Temperature of the water leaving the panel surface
% Update the temperature of the tank
Told = Tt;
Tnew = Told + ((DeltaTime/(Mt*c))*((Mw*c*(Tw2 - Tw1)/3600) + ...
    ((Ta - Tt)/Rat)));

RadTemp(time) = Ts;
TankTemp(time) = Tnew;



for time = 1:7
   SolAngle = SolarAngle(time);
G = SolarIrradiance(time);
Qsolar = SolAngle*G*As;
Tsky = SkyTemperature(time);
Ta = AirTemperature(time);
AirTemp(time) = Ta;
Vwind = WindVelocity(time);
Haws = a + b*Vwind;
Has = Haws;
Raws = (1/(Haws*Ao)) + (Ls/(Ks*Ao));
Tw1 = Tnew;
Tt= Tnew;
Ts = fzero(@(Ts) ((Mw*c*(Tw1 - Ts)/3600) + Qsolar + Has*As*(Ta -
Ts)...
    + (Ta - Ts)/Raws - (As*Es*d*(Ts - Tsky)*((Ts + 273.15)^2 + ...
    (Tsky + 273.15)^2)*((Ts + 273.15)+(Tsky + 273.15)))),20);
Told = Tt; DeltaTime = 3600; Tw2 = Ts;
Tnew = Told + ((DeltaTime/(Mt*c))*((Mw*c*(Tw2 - Tw1)/3600) +...
    ((Ta - Tt)/Rat)));
RadTemp(time) = Ts;
TankTemp(time) = Tnew;
end


SolAngle = SolarAngle(time);
G = SolarIrradiance(time);
Qsolar = SolAngle*G*As;
Tsky = SkyTemperature(time);
Ta = AirTemperature(time);
Vwind = WindVelocity(time);
Hat = a + b*Vwind;
Rat = (1/(Hat*At)) + (Lt/(Kat*At));

Tw3 = TankTemp(7);
```

```
Tt = Tw3;
Told = Tt;
for time = 8:18
Ta = AirTemperature(time);
Qtrans = HeatTrans(time); %heat transmission from outside ambient air
Qinfil = HeatInfil(time); %due to infiltration of hot outside ambient
air
Qgen = HeatGen(time);%internal heat source

Tw4 = Tw3 + ((Qinfil + Qgen + Qtrans)/(Mdot*c));
Tr = (Tw3 + Tw4)/2;
Tnew = Told + ((DeltaTime/(Mt*c))*((Mw*c*(Tw4 - Tw3)/3600) + ...
    ((Ta - Tt)/Rat)));
TankTemp(time) = Tnew;
Told = Tnew;
Tw3 = Tnew;
Tt = Tw3;
RoomTemp(time) = Tr;
end


Told = TankTemp(18);

for time = 19:23

Ta = AirTemperature(time);
Vwind = WindVelocity(time);
Hat = a + b*Vwind;
Rat = (1/(Hat*At)) + (Lt/(Kat*At));
     RoomTemp(time) = AirTemperature(time);
     Vwind = WindVelocity(time);
Hat = a + b*Vwind;
Tnew = Told + ((DeltaTime/(Mt*c))*((Ta - Told)/Rat));


TankTemp(time) = Tnew;
Told = Tnew;
 end



 for time = 8:22
    SolAngle = SolarAngle(time);
G = SolarIrradiance(time);
Qsolar = SolAngle*G*As;
Tsky = SkyTemperature(time);
Ta = AirTemperature(time);
AirTemp(time) = Ta;
Vwind = WindVelocity(time);
Haws = a + b*Vwind;
Has = Haws;
Raws = (1/(Haws*Ao)) + (Ls/(Ks*Ao));

%calculate Ts
Ts = fzero(@(Ts) (Qsolar + Has*As*(Ta - Ts) + (Ta - Ts)/Raws - ...
    (As*Es*d*(Ts - Tsky)*((Ts + 273.15)^2 +(Tsky + 273.15)^2)*...
    ((Ts + 273.15)+(Tsky + 273.15)))),20);
RadTemp(time) = Ts;
end
```

```
%Room temperatures b4 convector turn on: Qinfil + Qgen + Qtrans = 0
%therefore the room temperature mirrors the air temperature
for time = 1:7
    RoomTemp(time) = AirTemperature(time);
end

RoomTemp(24) = AirTemperature(24);
%Graphing
 Ts = RadTemp'; Ta = AirTemp'; Tt = TankTemp'; Tr = RoomTemp';
Time = 1:24;
disp(['      Time   AirTemp   RadTemp   TankTemp  RoomTemp'])
format short
[Time', AirTemp', RadTemp', TankTemp', RoomTemp']
plot(Ts,'b-.')
 hold on
 plot(Tr,'k-')
plot(Ta,'r--')
plot(Tt,'g:')
 axis([1 24 0 80])
 grid on
title('Hourly Temperatures')
xlabel('Time, t(hours)')
ylabel('Temperature (deg Celcius)')
legend('RadiatorPanel','Room','Air','Tank')



% parameter description
%for the radiator panel:
Es =0.90  ; As = 48; n = 0.9;
Ao = As * n ; Ks = 0.030; Ls = 0.025;   %radiator panel underside
d = 5.67e-8; %Stefan-Boltzman constant
%water tank parameters
Kat = 0.030; At = 14.296; Lt = 0.025;
Mw = 4150; %mass of water circulated
Mt = 4150; %mass of water in the tank
Vt = 4.15;% volume of tank
c = 4186; %specific heat capacity of water
DeltaTime = 3600; %time to circulate one tank of water (1 hour)
Mdot = 4150/3600;%mass of water circulated per second
% convector parameters
Hcw = 4000; % water-side heat transfer coefficient
Hca = 10; % air-side heat transfer coefficient
Aa = 75.50; % air side area
Aw = 9.060; % water side area
Na = 0.915; % air-side efficiency
Rrc = (1/(Hcw*Aw)) + (1/(Hca*Aa*Na));% room convector thermal
resistance

a = 1.8; b = 3.8;
rho = 1000; %specific density
RadTemp = [];RoomTemp = []; AirTemp =[]; TankTemp = [];

%calculate the radiator temp & tank temp at the tank turn on time
time = 23;
SolAngle = SolarAngle(time);
G = SolarIrradiance(time);
Qsolar = SolAngle*G*As;
Tsky = SkyTemperature(time);
```

```
Ta = AirTemperature(time);
AirTemp(time) = Ta;
Vwind = WindVelocity(time);
Has = a + b*Vwind;
Haws = Has;
Raws = (1/(Haws*Ao)) + (Ls/(Ks*Ao));
%calculate panel temperature from energy balance equation when heat
%transfer due to water circulation through the panel is zero.
Ts = fzero(@(Ts) (Qsolar + Has*As*(Ta - Ts) + (Ta - Ts)/Raws - ...
    (As*Es*d*(Ts - Tsky)*((Ts + 273.15)^2 +(Tsky + 273.15)^2)*...
    ((Ts + 273.15)+(Tsky + 273.15)))), 20);
Hat = Has;
Rat = (1/(Hat*At)) + (Lt/(Kat*At));
Tt = fzero(@(Tt) ((Ta-Tt)/Rat),20); %Tank Temperature at this time
RadTemp(time) = Ts;
```

```
time = 24;
SolAngle = SolarAngle(time);
G = SolarIrradiance(time);
Qsolar = SolAngle*G*As;
Tsky = SkyTemperature(time);
Ta = AirTemperature(time);
AirTemp(time) = Ta;
Vwind = WindVelocity(time);
Haws = a + b*Vwind;
Has = Haws;
Raws = (1/(Haws*Ao)) + (Ls/(Ks*Ao));
```

```
Tw1 = Tt; %temperature of the water leaving the tank
Ts = fzero(@(Ts) ((Mdot*c*(Tw1 - Ts)/DeltaTime) + Qsolar +...
    Has*As*(Ta - Ts) + (Ta - Ts)/Raws - (As*Es*d*(Ts - Tsky)*...
    ((Ts + 273.15)^2 + (Tsky + 273.15)^2)*((Ts + 273.15)+...
    (Tsky + 273.15)))),20);
Tw2 = Ts; %Temperature of the water leaving the panel surface
% Update the temperature of the tank
Told = Tt;
Tnew = Told + ((DeltaTime/(Mt*c))*((Mw*c*(Tw2 - Tw1)/3600) + ...
    ((Ta - Tt)/Rat)));

RadTemp(time) = Ts;
TankTemp(time) = Tnew;
```

```
for time = 1:7
   SolAngle = SolarAngle(time);
G = SolarIrradiance(time);
Qsolar = SolAngle*G*As;
Tsky = SkyTemperature(time);
Ta = AirTemperature(time);
AirTemp(time) = Ta;
Vwind = WindVelocity(time);
Haws = a + b*Vwind;
Has = Haws;
Raws = (1/(Haws*Ao)) + (Ls/(Ks*Ao));
```

```
Tw1 = Tnew;
Tt= Tnew;
Ts = fzero(@(Ts) ((Mw*c*(Tw1 - Ts)/3600) + Qsolar + Has*As*(Ta -
Ts)...
    + (Ta - Ts)/Raws - (As*Es*d*(Ts - Tsky)*((Ts + 273.15)^2 + ...
    (Tsky + 273.15)^2)*((Ts + 273.15)+(Tsky + 273.15)))),20);
Told = Tt; DeltaTime = 3600; Tw2 = Ts;
Tnew = Told + ((DeltaTime/(Mt*c))*((Mw*c*(Tw2 - Tw1)/3600) +...
    ((Ta - Tt)/Rat)));
RadTemp(time) = Ts;
TankTemp(time) = Tnew;
end


SolAngle = SolarAngle(time);
G = SolarIrradiance(time);
Qsolar = SolAngle*G*As;
Tsky = SkyTemperature(time);
Ta = AirTemperature(time);
Vwind = WindVelocity(time);
Hat = a + b*Vwind;
Rat = (1/(Hat*At)) + (Lt/(Kat*At));

Tw3 = TankTemp(7);
Tt = Tw3;
Told = Tt;
for time = 8:18
Ta = AirTemperature(time);
Qtrans = HeatTrans(time); %heat transmission from outside ambient air
Qinfil = HeatInfil(time); %due to infiltration of hot outside ambient
air
Qgen = HeatGen(time);%internal heat source

Tw4 = Tw3 + ((Qinfil + Qgen + Qtrans)/(Mdot*c));
Tr = (Tw3 + Tw4)/2;
Tnew = Told + ((DeltaTime/(Mt*c))*((Mw*c*(Tw4 - Tw3)/3600) + ...
    ((Ta - Tt)/Rat)));
TankTemp(time) = Tnew;
Told = Tnew;
Tw3 = Tnew;
Tt = Tw3;
RoomTemp(time) = Tr;
end


Told = TankTemp(18);

for time = 19:23

Ta = AirTemperature(time);
Vwind = WindVelocity(time);
Hat = a + b*Vwind;
Rat = (1/(Hat*At)) + (Lt/(Kat*At));
     RoomTemp(time) = AirTemperature(time);
     Vwind = WindVelocity(time);
Hat = a + b*Vwind;
Tnew = Told + ((DeltaTime/(Mt*c))*((Ta - Told)/Rat));
```

```
TankTemp(time) = Tnew;
Told = Tnew;
 end



 for time = 8:22
    SolAngle = SolarAngle(time);
G = SolarIrradiance(time);
Qsolar = SolAngle*G*As;
Tsky = SkyTemperature(time);
Ta = AirTemperature(time);
AirTemp(time) = Ta;
Vwind = WindVelocity(time);
Haws = a + b*Vwind;
Has = Haws;
Raws = (1/(Haws*Ao)) + (Ls/(Ks*Ao));

%calculate Ts
Ts = fzero(@(Ts) (Qsolar + Has*As*(Ta - Ts) + (Ta - Ts)/Raws - ...
    (As*Es*d*(Ts - Tsky)*((Ts + 273.15)^2 +(Tsky + 273.15)^2)*...
    ((Ts + 273.15)+(Tsky + 273.15)))),20);
RadTemp(time) = Ts;
end

%Room temperatures b4 convector turn on: Qinfil + Qgen + Qtrans = 0
%therefore the room temperature mirrors the air temperature
for time = 1:7
    RoomTemp(time) = AirTemperature(time);
end

RoomTemp(24) = AirTemperature(24);
%Graphing
 Ts = RadTemp'; Ta = AirTemp'; Tt = TankTemp'; Tr = RoomTemp';
Time = 1:24;
disp(['      Time   AirTemp   RadTemp   TankTemp  RoomTemp'])
format short
[Time', AirTemp', RadTemp', TankTemp', RoomTemp']
plot(Ts,'b-.')
 hold on
 plot(Tr,'k-')
plot(Ta,'r--')
plot(Tt,'g:')
 axis([1 24 0 80])
 grid on
title('Hourly Temperatures')
xlabel('Time, t(hours)')
ylabel('Temperature (deg Celcius)')
legend('RadiatorPanel','Room','Air','Tank')



function Qgen = HeatGen(time)
if time >= 7 & time <= 18
    Qgen = 1500;
else
    Qgen = 0;
end
```

```
function Qinfil = HeatInfil(time)
if time >= 7 & time <= 13
    Qinfil = (55*time - 385)/6;
elseif time > 13 & time <= 18
    Qinfil = -11*time + 198;
else
    Qinfil = 0;
end


Tdp = 9; Es =0.90  ; As = 48; d = 5.67e-8; Ks = 0.030; Ls = 0.025;Mw
= 4150;
time = 23;
if time >= 6 & time <= 18
    Esky = 0.741 + 0.00162*Tdp;
else
    Esky = 0.727 + 0.00160*Tdp;
end

if  time >= 0 & time <= 6
    Ta = -10/6 * time + 19;
    elseif time > 6 & time <= 13
        Ta = (23.5*time - 75)/7;
elseif time >13 & time <= 24
    Ta = (-13.5*time + 533)/11;
end

Tsky = (Esky*(Ta + 273.15)^4)^0.25 - 273.15;

WindVelocity

Has = a + b * Vwind;

Raws = 1/(Has*As*0.9) + Ls/(Ks*As*0.9) ;

SolAngle

if time >= 0 & time < 6
    G = 0;
elseif time >= 6 & time <= 18
    G = 1000*(sin((pi/12)*(time-6)));
elseif time > 18 & time <= 24
    G = 0;
end

Qsolar = SolarAngle*G*As;

Ts = fzero(@(Ts) (Qsolar + Has*As*(Ta - Ts) + (Ta - Ts)/Raws -
(As*Es*d*(Ts - Tsky)*((Ts + 273.15)^2 +(Tsky + 273.15)^2)*((Ts +
273.15)+(Tsky + 273.15)))),50);
% calculate temperature of the water in the storage tank
Dt = 1.742; rho = 1000; Mt = 4150; Vt = 4.15; c = 4186; Kat = 0.030;
At = 14.296; Lt = 0.025;
Hat = a + b*Vwind;
Rat = (1/(Hat*At) + Lt/(Kat*At));

Tt = fzero(@(Tt) ((Ta-Tt)/Rat),17);

%%%%
```

```
clear time
time = tim;

%%%%

Told = Tt; Tw1 = Tt; Tw2 = Ts;


%%%
if time > 23 & time < 24
    DeltaTime = (time - 23)*3600;
    AirTemperature
    Tdp = 9; Es =0.90  ; As = 48; d = 5.67e-8; Ks = 0.030; Ls =
0.025;Mw = 4150;
time = 23;
if time >= 6 & time <= 18
    Esky = 0.741 + 0.00162*Tdp;
else
    Esky = 0.727 + 0.00160*Tdp;
end

Tsky = (Esky*(Ta + 273.15)^4)^0.25 - 273.15;

WindVelocity

Has = a + b * Vwind;

Raws = 1/(Has*As*0.9) + Ls/(Ks*As*0.9) ;

SolAngle

if time >= 0 & time < 6
    G = 0;
elseif time >= 6 & time <= 18
    G = 1000*(sin((pi/12)*(time-6)));
elseif time > 18 & time <= 24
    G = 0;
end

Qsolar = SolarAngle*G*As;

    Tnew = Told + ((DeltaTime/(Mt*c))*((Mw*c*(Tw2 - Tw1)/3600) + ((Ta
- Tt)/Rat)));
    Ts = fzero(@(Ts) ((Mw*c*(Tw1 - Tw2)/3600) + Qsolar + Has*As*(Ta -
Ts) + (Ta - Ts)/Raws - (As*Es*d*(Ts - Tsky)*((Ts + 273.15)^2 +(Tsky +
273.15)^2)*((Ts + 273.15)+(Tsky + 273.15)))),20);
    Ta, Ts, Tnew
else, end



function Qtrans = HeatTrans(time)
if time >= 7 & time <= 13
    Qtrans = (1000*time - 7000)/6;
elseif time > 13 & time <= 18
    Qtrans = -200*time + 3600;
else
    Qtrans = 0;
```

```
end


function Tsky = SkyTemperature(time)
Tdp = 9;% dew point temperature is assumed to be 9 deg celcius
if time > 6 & time <= 18
    Esky = 0.741 + 0.00162*Tdp;
else
    Esky = 0.727 + 0.00160*Tdp;
end
Ta = AirTemperature(time);
Tsky = (Esky*(Ta + 273.15)^4)^0.25 - 273.15;


function SolAngle = SolarAngle(time)
if time >= 0 & time < 8
    SolAngle = 0;
elseif time == 8
    SolAngle = 0.5;
elseif time > 8 & time < 15
    SolAngle = 0.9;
elseif time == 15
    SolAngle = 0.5
elseif time > 15 & time <= 24
    SolAngle = 0;
end
function G = SolarIrradiance(time)
    if time < 7
        G = 0;
    elseif time == 7
        G = 100;
    elseif time == 8
        G = 120;
    elseif time == 9
        G = 300;
    elseif time == 10
        G = 550;
    elseif time == 11
        G = 950;
    elseif time == 12
        G = 1000;
    elseif time == 13
        G = 1090;
    elseif time == 14
        G = 1100;
    elseif time == 15
        G = 760;
    elseif time == 16
        G = 550;
    elseif time == 17
        G = 200;
    elseif time == 18
        G = 50;
    elseif time > 18
        G = 0;
    end


function Vwind = WindVelocity(time)
if time == 1
```

```
    Vwind = 2;
elseif time == 2
    Vwind = 1.99;
elseif time ==3
    Vwind = 1.99;
elseif time == 4
    Vwind = 2;
elseif time == 5
    Vwind = 2.2;
elseif time == 6
    Vwind = 2.4;
elseif time == 7
    Vwind = 2.5;
elseif time == 8
    Vwind = 2.6;
elseif time == 9
    Vwind = 2.65;
elseif time == 10
    Vwind = 2.75;
elseif time == 11
    Vwind = 2.8;
elseif time == 12
    Vwind = 2.79;
elseif time == 13
    Vwind = 2.78;
elseif time == 14
    Vwind = 2.71;
elseif time == 15
    Vwind = 2.5;
elseif time == 16
    Vwind = 2.46;
elseif time == 17
    Vwind = 2.43;
elseif time == 18
    Vwind = 2.42;
elseif time == 19
    Vwind = 2.3;
elseif time == 20
    Vwind = 2.25;
elseif time == 21
    Vwind = 2.2;
elseif time == 22
    Vwind = 2.16;
elseif time == 23
    Vwind = 2.17;
elseif time == 24
    Vwind = 2.17;
end
```

II: EXPERIMENTAL RESULTS FOR VARIOUS DAYS IN FUTO

10/08/2010

	T rad	T amb	T room	T water	T dewp	comment
6.00pm	24.1	25.3	27.3	26.6	21.9	Clear
6.30pm	24.4	25	27	25.9	21.8	weather
7.00pm	24.4	24.8	26.7	25.5	21.7	
7.30pm	24.3	24.5	26.9	25.2	21.7	
8.00pm	24.2	24.2	26.8	25.6	21.6	
8.30pm	24.3	24.1	24.8	26.5	21.6	
9.00pm	24.4	24	25.6	26	21.6	
9.30pm	24.3	24	24.8	26	21.6	
10.00pm	24.1	24.2	24.7	24.5	21.5	
10.30pm	23.5	24.2	24.6	24.5	21.5	
11.00pm	23.5	23.7	24.3	24.5	21.5	
11.30pm	23.8	23.7	24.3	24.5	21.5	
12	23.2	23.1	24.6	24.5	21.4	
1.00am	22.7	23.7	24.5	24.5	21.4	
1.30am	22.6	23.4	24.4	24.5	21.4	
2.00am	23.1	23.8	24.4	24.5	21.4	
2.30am	23.1	23	24	24.1	21.3	
3.00am	22.8	23.1	23.9	24.2	21.3	
3.30am	22.5	23.2	23.8	24.1	21.3	
4.00am	22.9	22.6	23.7	24.5	21.2	
4.30am	22.5	22.7	23.2	24	21.2	
5.00am	22.5	22.9	23.8	24.1	21.1	
5.30am	22.4	22.8	23.5	24.1	21.1	
6.00am	21.8	22.9	23	23.6	21.0	

12/08/2010

Time	Trad	Tamb	Twater	Troom	T dewp	comment
6.30pm	21.9	22.9	23.5	23	21.9	
7.00pm	21.9	22.9	23.5	23	21.8	
7.30pm	21.9	22.9	23.5	23	21.7	
8.00pm	21.9	22.9	23.5	23	21.7	Rainy and cloudy
8.30pm	21.9	22.9	23.5	23	21.6	weather throughout
9.00pm	21.9	22.9	23.5	23	21.6	the night
9.30pm	21.9	22.9	23.5	23	21.6	
10.00pm	21.9	22.9	23.5	23	21.6	
10.30pm	21.9	22.9	23.5	22.9	21.5	
11.00pm	21.9	22.9	23	22.9	21.5	
11.30pm	21.8	22.9	23	22.9	21.5	
12	21.6	22.9	23	22.9	21.5	
1.00am	21.6	22.9	23	22.9	21.4	
1.30am	21.6	22.9	23	22.9	21.4	
2.00am	21.6	22.9	22.9	22.9	21.4	
2.30am	21.6	22.8	22.9	22.8	21.4	
3.00am	21.6	22.7	22.9	22.3	21.3	
3.30am	21.6	22.6	22.9	22.4	21.3	
4.00am	20.9	22.5	22.9	22.4	21.3	
4.30am	20.9	22.1	22.9	22.4	21.2	
5.00am	20.8	21.9	22.8	22.5	21.2	
5.30am	20.8	21.9	22.7	22.5	21.1	
6.00am	20.7	21.9	22.5	22.4	21.1	
					21.0	

15/08/2010

TIME	Trad	Tamb	Twater	Tdwep	Troom	T dewp		comment
6.00pm	24.5	25.7	23.5	21.9	23	22		
6.30pm	24.5	25.7	23.5	21.8	23	21.8		
7.00pm	24.3	25.7	23.5	21.7	23	21.7		
7.30pm	24.3	24.9	23.5	21.7	23	21.7		
8.00pm	24.3	24.5	23.5	21.6	23	21.6		
8.30pm	23.8	24.2	23.5	21.5	23	21.6		
9.00pm	23.8	24.2	23.5	21.5	23	21.6		
9.30pm	23.8	24.2	23.5	21.5	23	21.6		
10.00pm	23.3	24.2	23.5	21.5	23	21.5		
10.30pm	23.1	24.2	23.5	21.5	22.9	21.5		
11.00pm	22.9	23.4	23	21.4	22.9	21.5		
11.30pm	22.8	23.7	23	21.3	22.9	21.5		
12	22.1	23.5	23	21.3	22.9	21.4		
1.00am	21.6	23.2	23	21.3	22.9	21.4		
1.30am	21.6	23.2	23	21.2	22.9	21.4		
2.00am	21.5	23.2	22.9	21.2	22.9	21.4		
2.30am	21.5	23.2	22.9	21.2	22.8	21.3		
3.00am	21.5	23.2	22.9	21.1	22.3	21.3		
3.30am	21.5	22.8	22.9	21.1	22.4	21.3		
4.00am	21.5	22.8	22.9	21.1	22.4	21.2		
4.30am	21.3	22.8	22.9	21	22.4	21.2		
5.00am	21.2	22.8	22.8	21	22.5	21.1		
5.30am	20.8	21.7	22.7	21	22.5	21.1		
6.00am	20.7	21.9	22.5	20.9	22.4	21.0		

20/08/2010

TIME	Trad	Tamb	Twater	Troom	COMMENT
6.00pm	25.6	26	25.9	27	Clear weather throughout night the radiator surface temperature was constantly lower than that of the ambient
6.30pm	25.3	25	25.9	26.6	
7.00pm	25	24.8	25.9	26.5	
7.30pm	25	24.5	26.7	26.3	
8.00pm	24.9	24.5	26.5	26.5	
8.30pm	24.4	24.4	26.2	26	
9.00pm	24	24.3	26	26.6	
9.30pm	23.3	24.2	25.9	25.9	
10.00pm	23.3	24.1	25.5	25.9	
10.30pm	22.9	23.9	25.5	25.9	
11.00pm	22.8	23.7	25.5	25.5	
11.30pm	22.5	23.6	25.3	25.5	
12	22.5	23.2	25.3	25.5	
1.00am	22.3	23.2	25.3	25.6	
1.30am	22.4	23	25.2	25	
2.00am	22.2	23.1	25.5	25	
2.30am	22.7	23	25.5	25.2	
3.00am	22.8	22.9	25.5	25.2	
3.30am	22.5	22.6	25.5	25.2	
4.00am	22	22.7	25.5	24.9	
4.30am	22.1	22.9	25	24.8	
5.00am	22.1	22.8	25.2	24.3	
5.30am	22	22.6	24.9	24.1	
6.00am	22	22.7	24.9	24	

29/07/10

TIME	Trad	Tamb	Twater	Troom	comment
6.00pm	24	25	25.9	27	The weather condition at
6.30pm	24.4	25	25.9	26.6	the beginning was clear
7.00pm	24.4	24.8	25.9	26.5	with high ambient
7.30pm	24	24.5	26.7	26.3	condition. However,
8.00pm	24.1	24.5	26.5	26.5	towards the midnight, the
8.30pm	23.8	24.4	26.2	26	weather condition
9.00pm	23.4	24.3	26	26.6	changed to a rainy cloudy
9.30pm	23.2	24.2	25.9	25.9	sky.
10.00pm	23	24.1	25.5	25.9	
10.30pm	22.9	23.9	24	24.5	
11.00pm	22.8	23.7	24	24.4	
11.30pm	22.5	23.6	24	24.4	
12	22.1	23.2	23.8	24.6	
1.00am	22.3	23.2	25.3	24.4	
1.30am	22.4	23	25.2	25	
2.00am	22.5	23.1	25.5	25	
2.30am	22.3	23	25.5	24.1	
3.00am	22	22.9	25.5	24	
3.30am	21.8	22.6	25.5	24.3	
4.00am	21.9	22	25.5	24.2	
4.30am	21.3	22	25	24	
5.00am	21.4	21.9	25.2	24.3	
5.30am	20.9	21.3	24.9	24.1	
6.00am	20.9	21.2	24.9	24	

15/07/2010

TIME	Trad	Tamb	Troom	Twater	Comment
6.00pm	24	25	25.9	27	**Rainy/ cloudy weather. Ambient condition very cool temperatures of radiator and ambient air almost the same. This may be attributed to the high moisture content in the atmosphere**
6.30pm	24.4	25	25.9	26.6	
7.00pm	24.4	24.8	25.9	26.5	
7.30pm	24	24.5	26.7	26.3	
8.00pm	24.1	24.5	26.5	26.5	
8.30pm	23.8	24.4	26.2	26	
9.00pm	23.4	24.3	26	26.6	
9.30pm	23.2	24.2	25.9	25.9	
10.00pm	21.9	22	25.5	25.9	
10.30pm	21.9	22	24	24.5	
11.00pm	21.5	21.8	24	24.4	
11.30pm	21.2	21.8	24	24.4	
12	22.1	23.2	23.8	24.6	
1.00am	22.3	23.2	25.3	24.4	
1.30am	22.4	23	25.2	25	
2.00am	22.5	23.1	25.5	25	
2.30am	22.3	23	25.5	24.1	
3.00am	22	22.9	25.5	24	
3.30am	21.8	22.6	25.5	24.3	
4.00am	21.9	22	25.5	24.2	
4.30am	21	21.3	25	24	
5.00am	21	21.9	25.2	24.3	
5.30am	20.9	21.3	24.9	24.1	
6.00am	20.9	21.2	24.9	24	

2/8/10

6.00pm	24.7	25.3	25.9	27	comment
6.30pm	24.4	24.6	25.9	26.6	Clear weather throughout
7.00pm	24.4	24.5	25.9	26.5	
7.30pm	24	24.5	26.7	26.3	
8.00pm	24.1	24.5	26.5	26.5	
8.30pm	23.8	24.4	26.2	26	
9.00pm	23.4	24.3	26	26.6	
9.30pm	23.2	24.2	25.9	25.9	
10.00pm	23	23.9	25.5	25.9	
10.30pm	23.2	23.8	25.3	24.5	
11.00pm	23.1	23.5	25.2	24.4	
11.30pm	22.7	23.6	24.8	24.4	
12	22.5	23.2	23.8	24.6	
1.00am	22.4	22.8	25.3	24.4	
1.30am	22.4	22.7	25.2	25	
2.00am	22.5	22.6	25.5	25	
2.30am	22.3	23	25.5	24.1	
3.00am	22	22.9	25.5	24	
3.30am	21.8	22.6	25.5	24.3	
4.00am	21.9	22.5	25.5	24.2	
4.30am	22.4	22.5	25	24	
5.00am	22	22.3	25.2	24.3	
5.30am	22	22.4	24.9	24.1	
6.00am	22.2	22.5	24.9	24	

27/07/2010

Time	Trad	Tamb	T water	T room	comment
6.00pm	23.1	25.3	25.9	27	At the beginning the sky was overcast. Intermittently, the weather changes from clear to overcast to cloudy. The temperature variation was obvious in all these changes.
6.30pm	23.4	24.6	25.9	26.6	
7.00pm	23.5	24.5	25.9	26.5	
7.30pm	23	24.5	26.7	26.3	
8.00pm	22.9	24.5	26.5	26.5	
8.30pm	22.8	24.4	26.2	26	
9.00pm	22.2	24.3	26	26.6	
9.30pm	22	24.2	25.9	25.9	
10.00pm	22.1	23.9	25.5	25.9	
10.30pm	21.9	23.8	25.3	24.5	
11.00pm	21.9	23.5	25.2	24.4	
11.30pm	21.9	23.6	24.8	24.4	
12	21.8	23.2	23.8	24.6	
1.00am	21.8	22.8	25.3	24.4	
1.30am	21.7	22.7	25.2	25	
2.00am	21.6	22.6	25.5	25	
2.30am	21.6	23	25.5	24.1	
3.00am	21.6	22.9	25.5	24	
3.30am	21.6	22.6	25.5	24.3	
4.00am	21.6	22.5	25.5	24.2	
4.30 am	21.6	22.5	25	24	
5.00 am	21.8	22.3	25.2	24.3	
5.30 am	21.7	22.4	24.9	24.1	
6.00 am	21.7	22.2	24.9	24	

17/07/2010

6.00pm	**23.1**	**25**	**25.4**	**26**
6.30pm	23.4	24.6	25.4	25.9
7.00pm	23.5	24.5	25.2	25.6
7.30pm	23	24.5	25	25.4
8.00pm	22.9	24.5	24.9	25.3
8.30pm	22.8	24.4	24.6	25.2
9.00pm	22.6	24.3	24.6	25
9.30pm	22.5	24.2	24.7	24.9
10.00pm	22.3	23.9	24.5	24.8
10.30pm	22	23.9	24.3	24.5
11.00pm	21.9	23.9	24.2	24.4
11.30pm	21.8	23.9	24	24.4
12	21.7	23.9	24	24.1
1.00am	21.6	23.9	23.9	24
1.30am	21.5	23.9	23.8	24
2.00am	21.6	23.9	23.6	24.1
2.30am	21.6	23.5	23.4	23.9
3.00am	21.6	23.4	23.3	23.9
3.30am	21.6	23.1	23.2	23.9
4.00am	21.6	22.8	23.1	23.7
4.30am	21.6	22.6	22.9	23.6
5.00am	21.8	22.6	22.8	23.5
5.30am	21.7	22.1	22.7	23.4
6.00am	21.7	22.3	22.3	23

Validation and Error Analysis Table

Time (hrs)	Trad Measured	Trad Predicted
6pm	23.1	19.56
7pm	23.5	18.31
8pm	22.9	18.24
9pm	22.6	17.97
10pm	22.3	17.54
11pm	21.9	17.18
12am	21.7	16.91
1am	21.6	16.82
2am	21.6	16.74
3am	21.6	16.7
4am	21.6	16.62
5am	21.8	16.57
6am	21.7	16.54

Time (hrs)	Troom Measured	Troom Predicted
7pm	26.5	24.5
8pm	26.5	24.5
9pm	25.9	24.3
10pm	25.9	23.9
11pm	24.4	23.5
12am	24.6	23.2
1am	24.4	22.8
2am	25	22.6
3am	24	22.9
4am	24.2	22.5
5am	24.3	22.3
6am	24	22.2

Time (hrs)	Twater Measured	Twater Predicted
6pm	25.9	21.46
7pm	25.9	21.47
8pm	26.5	21.48
9pm	26	21.49
10pm	25.5	21.49
11pm	25.2	21.499
12am	23.8	16.91
1am	25.3	16.84
2am	25.5	16.76
3am	25.5	16.72
4am	25.5	16.64
5am	25.2	16.59

6am	24.9	16.56

Time (hrs)	Trad Measured	Trad Predicted
6pm	23.1	19.28
7pm	23.5	18.3
8pm	22.9	18.24
9pm	22.6	17.97
10pm	22.3	17.54
11pm	21.9	17.55
12am	21.7	17.57
1am	21.6	17.53
2am	21.6	17.51
3am	21.6	17.44
4am	21.6	17.3
5am	21.8	17.18
6am	21.7	17.08

Time (hrs)	Twater Measured	Twater Predicted
6pm	25.4	21.9
7pm	25.2	21.91
8pm	24.9	21.92
9pm	24.6	21.922
10pm	24.5	21.93
11pm	24.2	21.94
12am	24	17.57
1am	23.9	17.55
2am	23.6	17.53
3am	23.3	17.45
4am	23.1	17.31
5am	22.8	17.2
6am	22.3	17.1

Time (hrs)	Troom Measured	Troom Predicted
7pm	25.6	24.5
8pm	25.3	24.5
9pm	25	24.3
10pm	24.8	23.9

11pm	24.4	23.9
12am	24.1	23.9
1am	24	23.9
2am	24.1	23.9
3am	23.9	23.4
4am	23.7	22.8
5am	23.5	22.6
6am	23	22.3

Time (hrs)	Trad Measured	Trad Predicted
6pm	24.7	19.56
7pm	24.4	18.31
8pm	24.1	18.24
9pm	23.4	17.97
10pm	23	17.54
11pm	23.1	17.18
12am	22.5	16.91
1am	22.4	16.82
2am	22.5	16.74
3am	22	16.7
4am	21.9	16.62
5am	22	16.57
6am	22.2	16.58

Time (hrs)	Twater Measured	Twater Predicted
6pm	25.9	21.49
7pm	25.9	21.499
8pm	26.5	21.51
9pm	26	21.52
10pm	25.5	21.53
11pm	25.2	21.532
12am	23.8	16.91
1am	25.3	16.84
2am	25.5	16.76
3am	25.5	16.72
4am	25.5	16.64
5am	25.2	16.59
6am	24.9	16.6

Time (hrs)	Troom Measured	Troom Predicted
7pm	26.5	24.5
8pm	26.5	24.5
9pm	26.6	24.3
10pm	25.9	23.9

11pm	24.4	23.5
12am	24.6	23.2
1am	24.4	22.8
2am	25	22.6
3am	24	22.9
4am	24.2	22.5
5am	24.3	22.3
6am	24	22

Time (hrs)	Trad Measured	Trad Predicted
6pm	24	19.28
7pm	24.4	18.59
8pm	24.1	18.24
9pm	23.4	17.97
10pm	21.9	15.76
11pm	21.5	15.59
12am	22.1	16.91
1am	22.3	16.88
2am	22.5	16.85
3am	22	16.8
4am	21.9	16.64
5am	21	16.53
6am	20.9	16.38

Time (hrs)	Troom Measured	Troom Predicted
6pm		
7pm	25.9	24.8
8pm	26.5	24.5
9pm	26	24.3
10pm	25.5	22
11pm	24	21.8
12am	23.8	23.2
1am	25.3	23.2
2am	25.5	23.1
3am	25.5	22.9
4am	25.5	22
5am	25.2	21.9
6am	24.9	21.2

Time (hrs)	Twater Measured	Twater Predicted
7pm	26.5	21.33
8pm	26.5	21.34
9pm	26.6	21.35
10pm	25.9	21.35

11pm	24.4	21.351
12am	24.6	16.913
1am	24.4	16.895
2am	25	16.866
3am	24	16.815
4am	24.2	16.66
5am	24.3	16.548
6am	24	16.39

Time (hrs)	Trad Measured	Trad Predicted
6pm	24	19.28
7pm	24.4	18.59
8pm	24.1	18.24
9pm	23.4	17.97
10pm	23	17.73
11pm	22.8	17.37
12am	22.1	16.91
1am	22.3	16.87
2am	22.5	16.84
3am	22	16.79
4am	21.9	16.64
5am	21.4	16.53
6am	20.9	16.38

Time (hrs)	Twater Measured	Twater Predicted
6pm	25.9	21.32
7pm	25.9	21.33
8pm	26.5	21.34
9pm	26	21.35
10pm	25.5	21.36
11pm	24	21.362
12am	23.8	16.91
1am	25.3	16.89
2am	25.5	16.86
3am	25.5	16.81
4am	25.5	16.66
5am	25.2	16.55
6am	24.9	16.39

Time (hrs)	Troom Measured	Troom Predicted
7pm	26.5	24.8
8pm	26.5	24.5
9pm	26.6	24.3
10pm	25.9	24.1

11pm	24.4	23.7
12am	24.6	23.2
1am	24.4	23.2
2am	25	23.1
3am	24	22.9
4am	24.2	22
5am	24.3	21.9
6am	24	21.2

Time (hrs)	Trad Measured	Trad Predicted
6pm	25.6	20.22
7pm	25	18.59
8pm	24.9	18.24
9pm	24	17.97
10pm	23.3	17.73
11pm	22.8	17.37
12am	22.5	16.91
1am	22.3	16.87
2am	22.2	16.84
3am	22.8	16.79
4am	22	16.73
5am	22.1	16.72
6am	22	16.74

Time (hrs)	Twater Measured	Twater Predicted
6pm	25.9	21.63
7pm	25.9	21.64
8pm	26.5	21.65
9pm	26	21.652
10pm	25.5	21.66
11pm	25.5	21.67
12am	25.3	16.91
1am	25.3	16.89
2am	25.5	16.86
3am	25.5	16.81
4am	25.5	16.75
5am	25.2	16.74
6am	24.9	16.76

Time (hrs)	Troom Measured	Troom Predicted
7pm	26.5	24.8
8pm	26.5	24.5
9pm	26.6	24.3
10pm	25.9	24.1

11pm	25.5	23.7
12am	25.5	23.2
1am	25.6	23.2
2am	25	23.1
3am	25.2	22.9
4am	24.9	22.7
5am	24.3	22.8
6am	24	22.7

Time (hrs)	Trad Measured	Trad Predicted
6pm	24.5	19.94
7pm	24.3	19.43
8pm	24.3	18.24
9pm	23.8	17.88
10pm	23.3	17.82
11pm	22.9	17.09
12am	22.1	17.19
1am	21.6	17.12
2am	21.5	17.07
3am	21.5	17.03
4am	21.5	16.94
5am	21.2	16.91
6am	20.7	16.79

Time (hrs)	Twater Measured	Twater Predicted
6pm	23.5	21.66
7pm	23.5	21.67
8pm	23.5	21.68
9pm	23.5	21.69
10pm	23.5	21.7
11pm	23	21.704
12am	23	17.19
1am	23	17.14
2am	22.9	17.09
3am	22.9	17.04
4am	22.9	16.96
5am	22.8	16.92
6am	22.5	16.81

Time (hrs)	Troom Measured	Troom Predicted
7pm	23	25.7
8pm	23	24.5
9pm	23	24.2
10pm	23	24.2

11pm	22.9	23.4
12am	22.9	23.5
1am	22.9	23.2
2am	22.9	23.2
3am	22.3	23.2
4am	22.4	22.8
5am	22.5	22.8
6am	22.4	21.9

Time (hrs)	Trad Measured	Trad Predicted
6pm	21.9	17.3
7pm	21.9	16.81
8pm	21.9	16.74
9pm	21.9	16.67
10pm	21.9	16.61
11pm	21.9	16.62
12am	21.6	16.63
1am	21.6	16.59
2am	21.6	16.58
3am	21.6	16.54
4am	20.9	16.48
5am	20.8	16.39
6am	20.7	16.35

Time (hrs)	Twater Measured	Twater Predicted
6pm	23.5	21.29
7pm	23.5	21.298
8pm	23.5	21.3
9pm	23.5	21.31
10pm	23.5	21.313
11pm	23	21.318
12am	23	16.63
1am	23	16.61
2am	22.9	16.6
3am	22.9	16.56
4am	22.9	16.5
5am	22.8	16.41
6am	22.5	16.37

Time (hrs)	Troom Measured	Troom Predicted
7pm	23	22.9
8pm	23	22.9
9pm	23	22.9
10pm	23	22.9

11pm	22.9	22.9
12am	22.9	22.9
1am	22.9	22.9
2am	22.9	22.9
3am	22.3	22.7
4am	22.4	22.5
5am	22.5	21.9
6am	22.4	21.9

Time (hrs)	Trad Measured	Trad Predicted
6pm	24.1	19.56
7pm	24.4	18.59
8pm	24.2	17.95
9pm	24.4	17.69
10pm	24.1	17.82
11pm	23.5	17.37
12am	23.2	16.82
1am	22.7	16.85
2am	23.1	16.92
3am	22.8	16.88
4am	22.9	16.79
5am	22.5	16.79
6am	21.8	16.83

Time (hrs)	Troom Measured	Troom Predicted
6pm		
7pm	26.7	24.8
8pm	26.8	24.2
9pm	25.6	24
10pm	24.7	24.2
11pm	24.3	23.7
12am	24.6	23.1
1am	24.5	23.7
2am	24.4	23.8
3am	23.9	23.1
4am	23.7	22.6
5am	23.8	22.9
6am	23	22.9

Time (hrs)	Twater Measured	Twater Predicted
7pm	25.5	21.7
8pm	25.6	21.71
9pm	26	21.72
10pm	24.5	21.73

11pm	24.5	21.732
12am	24.5	16.82
1am	24.5	16.88
2am	24.5	16.94
3am	24.2	16.9
4am	24.5	16.81
5am	24.1	16.81
6am	23.6	16.85